

Non-coding RNA analysis of iPSCs-derived hepatocyte-like cells

Dissertation
zur Erlangung des akademischen Grades
DOCTOR RERUM NATURALIUM
(Dr. rer. nat.)

an der Medizinischen Fakultät
der Universität Leipzig

eingereicht von:

MSc Aniela Skrzypczyk

geboren am 02. Oktober 1988 in Siemianowice Slaskie (Polen)

angefertigt an / in:

Universität Leipzig

Biotechnologisch-Biomedizinisches Zentrum

Zelltechniken und Angewandte Stammzellbiologie

Betreuer:

Univ.-Prof. Dr. med. Augustinus Bader

Prof. Peter F. Stadler

Ko-Betreuer:

Dr. Shibashish Giri

Beschluss über die Verleihung des Doktorgrades vom: 17.12.2019

BIBLIOGRAPHIC DESCRIPTION

Skrzypczyk Aniela

Non-coding RNA analysis of iPSCs-derived hepatocyte-like cells

University of Leipzig, Medical Faculty, Dissertation

Liver diseases are associated with hepatocytes damage. Currently, liver transplant is the only treatment for liver failure. A shortage of donors has forced extensive research for alternative treatments. The most promising hepatocyte source could be obtained from the differentiation of induced pluripotent stem cells (iPSCs). This technology can give us great amounts of pluripotent cells without any ethical restrictions which could be available in variety of haplotypes to minimize the possibility of rejection. From those stem cells, it is possible to obtain hepatic-like cells (HLCs). However, they show fetal liver identity. Varieties of hepatic differentiation protocols were described, although the process of hepatic differentiation still needs to be improved. Along with genes, microRNA (miRNA) is the well-known controller of cell fate. In contrast to genes, many miRNAs can affect up to thousands of genes simultaneously. Another group of non-coding RNA (ncRNA) that is a subject to potential differences are small nucleolar RNA (snoRNA). SnoRNA are involved in RNA chemical modifications by acting as a guide, mostly for ribosomal RNA (rRNA).

In this study, a new iPSCs line was generated from skin fibroblasts and characterized. Next, HLCs were derived from those iPSCs using a four-stage hepatic differentiation protocol, and ncRNA sequencing was performed to compare the expression profiles of HLCs at two stages of differentiation (day 20 and 24) with mature hepatocytes. The involvement of miRNAs and snoRNAs in the dynamics of hepatic differentiation was explored in order to shed light on the molecular and regulatory mechanisms that underlie this complex process. Obtained HLCs maintain an epithelial characteristic and express miRNA, which can block maturation by inhibiting Epithelial-Mesenchymal Transition (EMT). In addition, differentially expressed snoRNA were identified and novel snoRNA genes were discovered.

Abbreviations

A1AT – Human Serpin peptidase inhibitor

AFP – α -fetoprotein

ALB – Albumin

BMP4 – bone morphogenetic protein 4

DAPI – 4',6-Diamidino-2-Phenylindole, Dilactate

E-cadherin – epithelial cadherin

ECM – extracellular matrix

EMT – Epithelial to mesenchymal transition

ESCs – embryonic stem cells

FDA – The Food and Drug Administration

FDR – False Discovery Rate (adjusted p-value)

GFP – Green fluorescent protein

HLCs – Hepatocyte like cells

HNF4a – Hepatic nuclear factor 4 α

ICG – Indocyanine green

iPSCs – Induced pluripotent stem cells

KEGG - Kyoto Encyclopedia of Genes and Genomes

Klf4 – Kruppel-like factor 4

linkRNA – long intergenic noncoding RNA

MET – mesenchymal to epithelial transition

miRNA – Micro RNA, plural miRNAs

miscRNA – miscellaneous RNA

mRNA – Messenger RNA

MRR2 – multidrug resistance protein 2

MSCs – mesenchymal stem cells

N-cadherin – neural cadherin

ncRNA – non-coding RNA

Oct4 – Octamer-binding transcription factor 4 (POU5F1)

PAS – Periodic acid shift

PP1 – Protein phosphatase 1

PSCs – pluripotent stem cells

q-PCR – quantitative PCR

Snail – Zinc finger protein SNAI1

snoRNA – Small nucleolar RNA, plural snoRNAs

snRNA – small nuclear RNA

Sox2 – SRY (sex determining region Y)-box 2

WGA – Wheat Germ Agglutinin

ZEB1 – Zinc finger E-box-binding homeobox 1

ZEB2 – Zinc finger E-box-binding homeobox 2

CONTENTS

1. INTRODUCTION.....	11
1.1. PLURIPOTENT STEM CELLS	11
1.1.1. Pluripotency	11
1.1.2. iPSCs.....	13
1.1.3. Reprogramming methods	14
1.1.4. iPSCs as an alternative cell source for disease modelling and regenerative medicine 16	
1.2. LIVER	18
1.2.1. Liver anatomy and function	18
1.2.2. Liver embryonal development	20
1.3. HEPATIC DIFFERENTIATION OF iPSCs IN VITRO	22
1.3.1. HLCs	22
1.3.2. Differentiation protocols into hepatocytes	24
1.4. NCRNA	25
1.4.1. MiRNA.....	26
1.4.2. SnoRNA	28
2. AIMS	31
3. MATERIALS.....	32
3.1. EQUIPMENT	32
3.2. SOFTWARE	32
3.3. ENZYMES, KITS AND TRANSFECTION REAGENTS	33
3.4. SOLUTIONS AND REAGENTS	33
3.5. CELL LINES.....	34
3.6. CELL CULTURE MEDIA AND CYTOKINES	34
3.7. PLASMIDS.....	35
3.8. PCR REAGENTS AND PRIMERS	35
3.8.1. PCR reagents	35
3.8.2. PCR primers	35
3.9. ANTIBODIES	36
4. METHODS	37

4.1.	CELL BIOLOGY	37
4.1.1.	Derivation and culture of primary human foreskin fibroblasts	37
4.1.2.	Counting cells.....	37
4.1.3.	Cryo-preservation of cells	37
4.1.4.	Thawing of cryo-preserved cells	38
4.1.5.	Cell reprogramming	38
4.1.6.	Cultivation and expansion of iPSCs.....	39
4.2.	IMMUNOCYTOCHEMISTRY	39
4.3.	IN VITRO SPONTANEOUS DIFFERENTIATION	39
4.4.	KARYOTYPE ANALYSIS.....	40
4.5.	RNA ISOLATION.....	40
4.6.	QUANTITATIVE PCR	40
4.7.	PERIODIC ACID-SCHIFF (PAS) STAINING.....	41
4.8.	INDOCYANINE GREEN UPTAKE AND RELEASE.....	41
4.9.	PLASMID TRANSFECTION	42
4.10.	HEPATIC DIFFERENTIATION	42
4.11.	WHEAT GERM AGGLUTININ STAINING	42
4.12.	VALIDATION OF HEPATIC DIFFERENTIATION EFFICIENCY	43
4.13.	RNA ISOLATION AND SEQUENCING	43
4.14.	BIOINFORMATIC ANALYSIS	44
4.14.1.	Sequencing quality and mapping	44
4.14.2.	Analysis of differential expressed ncRNAs	44
4.14.3.	Target pathways prediction of differentially expressed miRNAs.....	44
4.14.4.	Identification of novel ncRNAs candidates	45
5.	RESULTS.....	46
5.1.	GENERATION OF iPSCs USING EPISOMAL VECTORS	46
5.1.1.	Cell transfection	46
5.1.2.	Establishment of iPSCs line	48
5.2.	PLURIPOTENCY CHARACTERISATION OF THE iPSCs.....	49
5.2.1.	Pluripotency markers.....	49
5.2.2.	Spontaneous differentiation assay	50
5.2.3.	Karyotype.....	52
5.3.	HEPATIC DIFFERENTIATION OF iPSCs AND HLCs CHARACTERISATION.....	53

5.3.1.	iPSCs hepatic differentiation.....	53
5.3.2.	Expression of hepatic markers	54
5.3.3.	Hepatic gene expression in HLCs	56
5.3.4.	Hepatic functions in HLCs.....	58
5.4.	HNF4A OVEREXPRESSION DURING DIFFERENTIATION	59
5.4.1.	Cell transfection during differentiation	59
5.4.2.	Comparison of hepatic differentiation efficiency.....	60
5.4.3.	Whole slide scanning	62
5.5.	NON-CODING RNA ANALYSIS	64
5.5.1.	Non-coding RNA sequencing quality	64
5.5.2.	MicroRNA analysis.....	68
5.5.3.	SnoRNA analysis	79
5.5.4.	Short reads snoRNA analysis.....	84
5.5.5.	New gene candidates	85
6.	DISCUSSION	88
6.1.	METHODICAL STRATEGY	88
6.2.	CHARACTERISATION OF GENERATED IPSCS	89
6.3.	HEPATIC DIFFERENTIATION OF IPSCS.....	89
6.3.1.	Characterisation of HLCs.....	89
6.3.2.	Protocol with HNF4a overexpression	90
6.3.3.	Differentially expressed miRNA.....	90
6.3.4.	Differentially expressed snoRNA	93
6.4.	NOVEL SNORNA GENES	95
7.	SUMMARY.....	96
8.	REFERENCES.....	99
9.	APPENDIX	118
	ERKLÄRUNG ÜBER DIE EIGENSTÄNDIGE ABFASSUNG DER ARBEIT	122
	CURRICULUM VITAE	BŁĄD! NIE ZDEFINIOWANO ZAKŁADKI.
	PUBLICATIONS:.....	BŁĄD! NIE ZDEFINIOWANO ZAKŁADKI.
	PRESENTATIONS	BŁĄD! NIE ZDEFINIOWANO ZAKŁADKI.
	ACKNOWLEDGEMENTS.....	123

LIST OF FIGURES

FIGURE 1 ORIGIN AND BIOLOGICAL PROPERTIES OF PSCs.	12
FIGURE 2 GENE DELIVERY SYSTEMS FOR CELL REPROGRAMMING.	16
FIGURE 3 LIVER STRUCTURE AND CELL TYPES. (A) ORGANISATION OF HEPATIC LOBULE, HEPATOCTE CORDS RADIATE FROM THE CENTRAL VEIN (CV). (B) CELL TYPES IN THE LIVER.....	19
FIGURE 4 EXTRA- AND INTRACELLULAR MOLECULES INVOLVED IN DEVELOPMENT OF LIVER IN DIFFERENT STAGES.	22
FIGURE 5 STRUCTURE OF BOX C/D AND BOX H/ACA SNORNAs.	29
FIGURE 6 MORPHOLOGY OF FIBROBLASTS ON DAY 0 OF REPROGRAMMING.	47
FIGURE 7 TRANSFECTION OF FIBROBLASTS WITH EPISOMAL VECTORS – EFFICIENCY ON DAY A) 7 AND B) 14.	47
FIGURE 8 iPSCs APPEARING COLONIES ON DAY 21 (LEFT) AND 23 (RIGHT).	48
FIGURE 9 iPSCs COLONY CHOSEN FOR FUTURE EXPANSION.	49
FIGURE 10 MORPHOLOGY OF iPSCs IN THE CULTURE AFTER CRYOPRESERVATION.	49
FIGURE 11 IMMUNOSTAINING OF iPSCs SHOWING EXPRESSION OF PLURIPOTENCY MARKERS: OCT4, SOX2, NANOG, SSEA4 AND CLAUDIN6 (SKRZYPCZYK ET AL., 2016).....	50
FIGURE 12 EMBRYOID BODIES; LEFT IMAGE 2 DAYS AND RIGHT IMAGE 4 DAYS IN SUSPENSION CULTURE.	51
FIGURE 13 DIFFERENTIATION POTENTIAL OF iPSCs (SKRZYPCZYK ET AL., 2016).....	51
FIGURE 14 KARYOGRAM OF THE iPSCs PASSAGE NUMBER 20 (SKRZYPCZYK ET AL., 2016).	52
FIGURE 15 MORPHOLOGY OF HLCs OBTAINED FROM DIFFERENTIATION OF NEW iPSCs.	53
FIGURE 16 VEGEA CONFOCAL STAINING OF HLCs SHAPE.	54
FIGURE 17 EXPRESSION OF HEPATIC MARKERS IN NEW iPSCs-DERIVED HLC: HNF4A, ALB, AFP, MRP2 AND CK18.	55
FIGURE 18 QUANTITATION OF HEPATIC GENES: AFP, A1AT, HNF4A, ALBUMIN mRNA LEVELS BY QPCR ANALYSIS IN HLCs, HEPG2, HEPATOCTES AND iPSCs.....	57
FIGURE 19 REPRESENTATIVE IMAGES OF PAS STAINING TO DETECT GLYCOGEN STORAGE IN HLCs.	58
FIGURE 20 REPRESENTATIVE IMAGES OF ICG ASSAY.	59
FIGURE 21 OVEREXPRESSION OF HNF4A AFTER TRANSFECTION IN CELLS DURING DIFFERENTIATION.	60

FIGURE 22 EXPRESSION OF HEPATIC MARKERS IN HLCs OBTAINED WITH HNF4A OVEREXPRESSION.	61
FIGURE 23 REPRESENTATIVE IMAGES OF HEPATIC FUNCTIONS IN HLCs OBTAINED WITH OVEREXPRESSION OF HNF4A; A) PAS STAINING, B) ICG UPTAKE; C) ICG RELEASE AFTER 6H.....	61
FIGURE 24 COMPARISON OF THE HEPATIC DIFFERENTIATION PROTOCOLS BY QPCR RESULTS...	62
FIGURE 25 REPRESENTATIVE VIRTUAL SLIDE.	63
FIGURE 26 IMAGE ANALYSIS OF SLIDES AFTER SCANNING.	63
FIGURE 27 TOTAL NUMBER OF SEQUENCED READS, READS AFTER CLIPPING AND MAPPED READS.	65
FIGURE 28 PERCENTAGE OF MAPPED READS WITH AN ADAPTER.	66
FIGURE 29 PERCENTAGE OF DIFFERENT TRANSCRIPT TYPES IN THE SEQUENCING.	67
FIGURE 30 CLUSTER HEAT MAP OF GENE EXPRESSION DATA.	68
FIGURE 31 EXPRESSION OF HEPATIC SPECIFIC MIRNAS.....	69
FIGURE 32 EXPRESSION OF FETAL LIVER MIRNAS.	70
FIGURE 33 EXPRESSION OF MIRNAS RELATED TO MET.....	71
FIGURE 34 EXPRESSION OF PI3K RELATED MIRNAS SHOWN TO BE UPREGULATED DURING HEPATIC DIFFERENTIATION.....	72
FIGURE 35 THE VOLCANO PLOT OF DIFFERENTIALLY EXPRESSED MIRNAS BETWEEN HLCs DAY 20 AND HLCs DAY 24.	73
FIGURE 36 THE VOLCANO PLOT OF DIFFERENTIALLY EXPRESSED MIRNAS BETWEEN HLCs DAY 20 AND HEPATOCYTES.	74
FIGURE 37 THE VOLCANO PLOT OF DIFFERENTIALLY EXPRESSED MIRNAS BETWEEN HLCs DAY 24 AND HEPATOCYTES.	75
FIGURE 38 HEATMAP SHOWING THE DIFFERENTIALLY EXPRESSED MIRNAS.	76
FIGURE 39 THE VOLCANO PLOT OF DIFFERENTIALLY EXPRESSED SNORNAs BETWEEN HLCs DAY 20 AND HLCs DAY 24.....	80
FIGURE 40 THE VOLCANO PLOT OF DIFFERENTIALLY EXPRESSED SNORNAs BETWEEN HLCs DAY 20 AND HEPATOCYTES.....	81
FIGURE 41 THE VOLCANO PLOT OF DIFFERENTIALLY EXPRESSED SNORNAs BETWEEN HLCs DAY 24 AND HEPATOCYTES.....	82
FIGURE 42 HEATMAP SHOWING THE DIFFERENTIALLY EXPRESSED SNORNAs.....	83
FIGURE 43 CORRELATION OF FOLD CHANGES BETWEEN SHORT READS AND ALL READS MAPPING SNORNA GENES.	85

LIST OF TABLES

TABLE 1 DESCRIPTION OF THE PLASMIDS USED.	35
TABLE 2 THE PRIMER SEQUENCES FOR QRT-PCR	36
TABLE 3 ANTIBODIES USED FOR IMMUNOSTAINING.....	36
TABLE 4 GENE ONTOLOGY CATEGORIES OF DIFFERENTIALLY EXPRESSED MIRNAS TARGETS (PATHWAY UNION).	77
TABLE 5 CONSERVATION OF NOVEL RNA CANDIDATES.....	86
TABLE 6 LIST OF NOVEL NCRNAS.....	86
TABLE 7 LIST OF DIFFERENTIALLY EXPRESSED MIRNA.....	118
TABLE 8 LIST OF DIFFERENTIALLY EXPRESSED SNORNA	120

1. Introduction

1.1. Pluripotent stem cells

1.1.1. Pluripotency

The pluripotency of the cells is defined as a capability to self-renewal and differentiation into all body cells. Two types of the pluripotent stem cells (PSCs) can be distinguished: naturally occurring embryonic stem cells (ESCs) and generated in vitro induced pluripotent stem cells (iPSCs) (Laustriat, Gide, & Peschanski, 2010). The ESCs can be derived from the inner cell mass of a blastocyst. The first mouse ESCs were isolated independently by Evans and Kaufman and as well by Martin in 1981 (Evans & Kaufman, 1981; Martin, 1981). This discovery sparked hopes that those cells may be useful to treat many degenerative diseases as a source of cells for transplantation or tissue engineering. However, human cells originating from an early-stage preimplantation embryo create many controversies. Despite this, in 1998 human ESCs were isolated from in vitro fertilized embryos donated for scientific purposes (Thomson et al., 1998). One of the obstacles to use those ESCs in clinics was an incompatibility with a broad number of patients. There were many attempts to obtain embryonic cells which genetically match the patient. The first successful somatic cell nuclear transfer (SCNT) was performed on the sheep embryo and later another mammal and human embryos were used (Campbell, McWhir, Ritchie, & Wilmut, 1996; Polejaeva et al., 2000; Tachibana et al., 2013). The essence of this process is to transfer a differentiated cell nucleus into the oocyte from which the nucleus has been previously removed. This process is very inefficient and requires usage of hundreds of oocytes to obtain one of the modified embryo. Nevertheless, this experiment demonstrated that some unknown factors present in the cytoplasm of the egg cells cause changes in the nuclei of somatic cells and revert them to the embryo. Pluripotent cells can be obtained also by fusion of the undifferentiated cells with mature ones (Miller & Ruddle, 1976). This was achieved already in 1976 when Miller and Ruddle showed that thymocytes fuse with cancer embryonic stem cells. Similar results have been obtained by electrofusion of mature cells with embryonic stem cells of mice and humans (Flasza et al., 2003). However, chimeric cells are not suitable for the medical purpose. Based on the hypothesis that the ESCs contain factors that keeps them pluripotent Takahashi and Yamanaka have selected 24 proteins which were tested for the ability to restore pluripotent

phenotype in somatic cells. In 2006, they discovered that overexpression of four transcription factors: Oct4, Sox2, Klf4, and c-Myc induces pluripotency in mature cells (Takahashi et al., 2007; Takahashi & Yamanaka, 2006). This led to emergence of new kind of stem cells called induced pluripotent stem cells, and the process of their formation – cell reprogramming (Yamanaka, 2007).

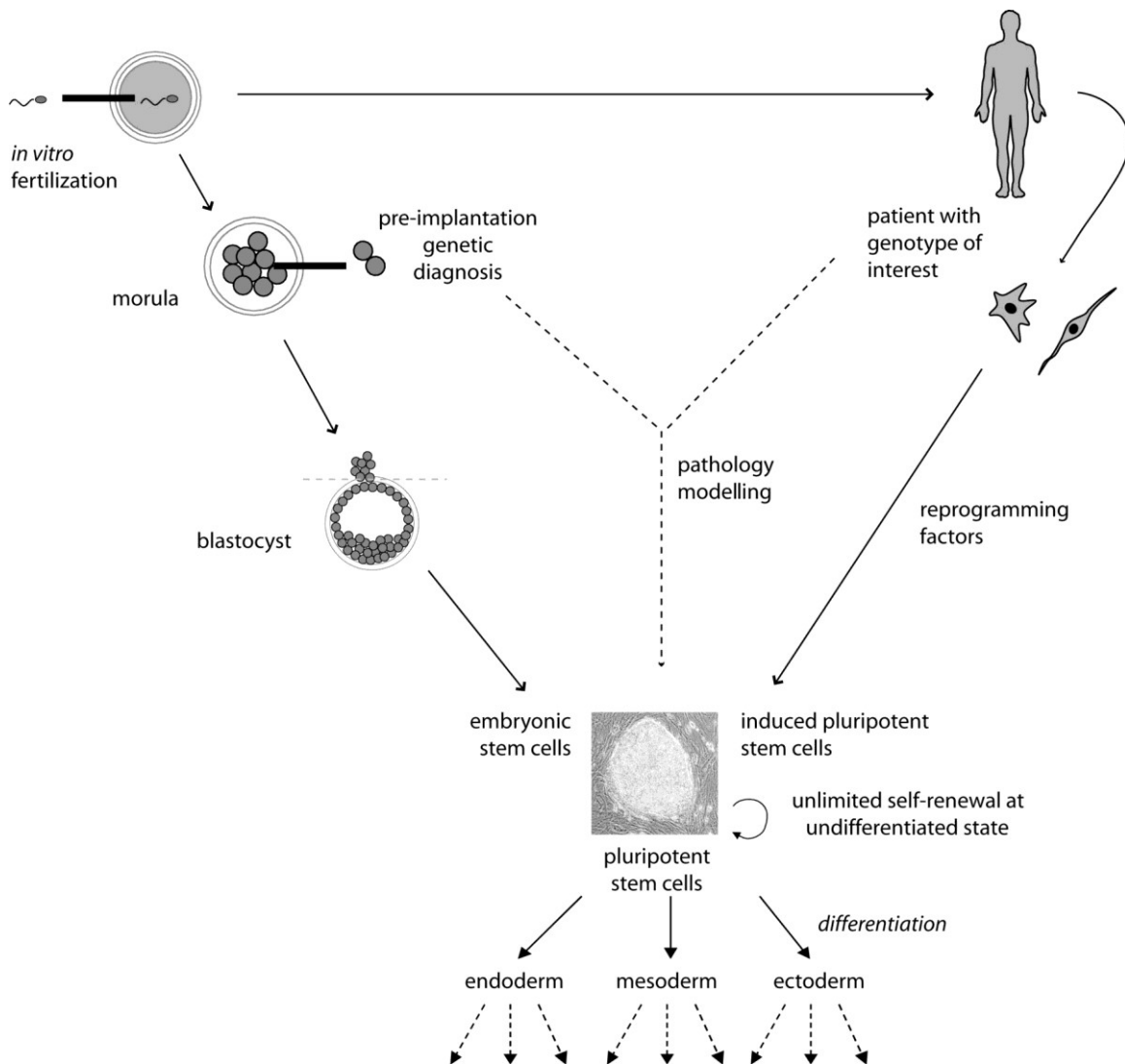


Figure 1 Origin and biological properties of PSCs.

Source: (Laustriat et al., 2010).

Morphologically, pluripotent stem cells can be described as small, round cells with a large nucleus. PSCs grow in colonies with the support of feeder layer or extracellular matrix.

During standard culture, a small fraction of the cells undergoes spontaneous differentiation. Determination of the phenotype of cells is extremely important for the usage of those cells in the clinic (Adewumi et al., 2007). The pluripotent cells when deprived of factors maintaining their undifferentiated phenotype, form embryoid bodies, which is an intermediate step in the differentiation into all types of cells. Among the pluripotency gene expression analysis, scientist developed methods of testing functionally newly derived iPSCs. One of those tests is teratoma formation assay. It is performed by injection of iPSCs into nude mice strain which exhibits impaired immune response. Teratomas composed of cells derived from all three germ layers proves the differentiation potential of the injected cells. Two more methods confirming differentiation in vivo are not performed on human cells for ethical reasons. The injection of iPSCs into developing blastocyst and observation of their integration during embryonic development is called a blastocyst complementation assay. It is convenient to observe incorporation of the cells expressing reporter gene for example GFP. Developed chimera should show the presence of the reporter gene in the tissues from different germ layers (Tam & Rossant, 2003). The second method called tetraploid blastocyst complementation assay uses a tetraploid embryo, usually tetraploid morula, formed by electrofusion of two blastomeres. The created tetraploid cells are mixed with diploid iPSCs, and then the newly created embryo is implanted into the uterus of the animal. Tetraploid cells can produce only extraembryonic tissue, and if the diploid cells are pluripotent, the whole organism will develop normally (Kang, Wang, Zhang, Kou, & Gao, 2009). The latest method is based on microarray analysis of iPSCs and comparison to the created database as an alternative to high expensive teratoma assays (Müller et al., 2011).

1.1.2. iPSCs

The first reprogramming of somatic cells was preceded by selecting factors that may restore the pluripotent nature of somatic cells. For this purpose, Takahashi and Yamanaka created mouse line "Fbx β geo/ β geo" by homologous recombination of the Fbx15 gene substituting gene β -geo which codes among others, neomycin resistance gene (G418). The Fbx15 gene encodes a protein that is expressed only in embryonic stem cells, however, lack of its expression does not interfere with the embryonic development of mice. 24 transcription factors were chosen for testing and introduced by retroviral vectors to embryonic fibroblasts isolated from mouse Fbx β geo/ β geo. The cells with gene overexpression were then checked

for resistance to G418. Individually none of the factors caused such resistance appearing together enable the induce antibiotic resistant colonies. During further analysis, 4 transcription factors were selected: Oct4, Sox2, Klf4, and c-Myc which induce pluripotency effectively. The reprogrammed cells express pluripotent markers and genes. They could also create teratomas consisting of tissues derived from the three germ layers and form in vitro embryoid bodies. Injected into the mouse blastocyst, could create the chimeric organism proving definitively the pluripotent character (Takahashi & Yamanaka, 2006).

1.1.3. Reprogramming methods

Starting from reprogramming breakthrough, many scientists sought to improve the process to make it safer and more efficient. A year after the first pluripotency induction in mouse fibroblasts, reprogramming of human somatic cells was achieved. Skin fibroblasts from the 36-year-old woman were transduced with retroviral vectors containing “four Yamanaka’s factors”. The process of reprogramming human cells was twice as long because of the slower proliferation of human cells. It has been shown that obtained iPSCs resemble human ESCs (Takahashi et al., 2007). Two reprogramming factors: c-Myc and Klf4 are well-known oncogenes which overexpression can lead to the formation of cancer. A group of American scientists proved the possibility of using some other factors in the reprogramming process identified by comparing gene expression of ESCs and bone marrow-derived stem cell line. Using a set of four genes: Oct4, Sox2, NANOG and LIN28 they demonstrated that human foreskin fibroblasts can be successfully reprogrammed into iPSCs (Yu et al., 2007). The next step in the process of improving the technique of cell reprogramming was to use a single polycistronic vector including four factors in one expression cassette. This approach reduced the amount of integration of exogenous genes into the cellular genome which may cause mutations (Sommer et al., 2009). Lentiviral vectors find to be more effective tools than retroviral vectors, but the efficiency of reprogramming with them was still low (0.1%) (Stadtfield, Maherali, Breault, & Hochedlinger, 2008). Adding small molecule compounds, which activate reprogramming, was one of the attempts to increase the efficiency of the process. One of such compounds is valproic acid which allowed reprogramming of human cells with only two genes: Oct4 and Sox2 (Huangfu et al., 2008). Nevertheless, integration of the introduced genes into the genome of the transduced cells involves a high risk of mutations and reduces the possibility of using such modified cells in regenerative medicine. Therefore,

alternative methods for cell reprogramming were investigated. Okita et al. showed that plasmid vectors in combination with electroporation are sufficient, while the team of Konrad Hochedlinger managed to obtain iPSCs using adenoviral vectors (Okita, Hong, Takahashi, & Yamanaka, 2010; Stadtfeld, Nagaya, Utikal, Weir, & Hochedlinger, 2008). In both cases, the introduced exogenes did not integrate into the cellular genome, but these methods have low efficiency (Oh et al., 2012). Higher efficiency can be obtained by using transposons, but this method requires an additional step of selecting cells which significantly complicates and prolongs the reprogramming process (Yusa, Rad, Takeda, & Bradley, 2009). The transfection of somatic cells with synthetic mRNA molecules was one of the latest developed approaches which eliminate the risk of integration of the inserted sequences (Warren et al., 2010; Yakubov, Rechavi, Rozenblatt, & Givol, 2010). The very high efficiency of reprogramming human cells isolated from different tissues was an additional advantage of this approach. Zhou et al. went even further and showed that it is possible to obtain iPSCs using transcription factors in the form of recombinant proteins (Zhou et al., 2009). Such modified proteins had linked polyarginine anchor to the C-end and could migrate to the cell nuclei where they remain for 48 hours. The resulting iPSCs exhibit markers and morphology of human embryonic stem cells. The possibility of obtaining iPSCs by transduction with a lentiviral vector containing a single cluster microRNA demonstrated by Anokye-Danso et al. was another breakthrough in the development of new methods for reprogramming (Anokye-Danso et al., 2011). Overexpression of Mir-302/367 cluster induced pluripotency in mouse and human fibroblasts. Moreover, this process was two times more efficient than a standard method of gene transduction, but valproic acid was required. Valproic acid inhibits histone deacetylase 2 (HDAC2) activity which is responsible for chromatin condensation. Cells quickly respond to the miRNAs because one miRNA can act on multiple target mRNA and its action does not involve the production of proteins. Miyoshi et al. connected the two latest methods of obtaining iPSCs by the transfection of cells with mature, synthetic miRNAs. Multiple transfections with three produced miRNAs (mir-200c, mir-302, and mir-369) effectively reprogrammed mouse and human fibroblasts (Miyoshi et al., 2011). For more than 10 years, the process of cell reprogramming has been carefully investigated. Many other genes were discovered to influence the process. For example, inhibition of the Mbd3, a core member of the Mbd3/NuRD (nucleosome remodelling and deacetylation) repressor complex, together with Yamanaka's factors (OSKM) transduction give almost 100% of reprogramming efficiency in mouse and human cells (Rais et al., 2013). Within the next few years,

reprogramming for clinical approach will likely become a fully standardized method without genome modification.

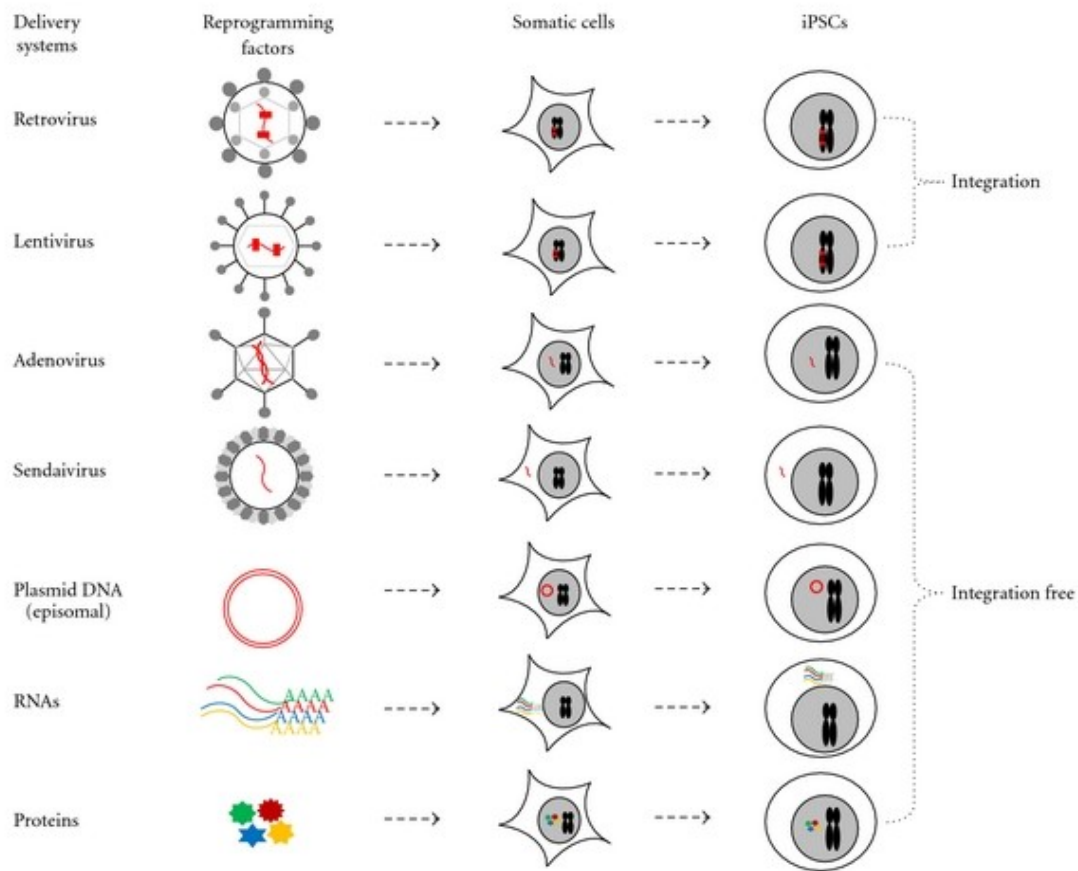


Figure 2 Gene delivery systems for cell reprogramming.

Source: (Oh et al., 2012).

1.1.4. iPSCs as an alternative cell source for disease modelling and regenerative medicine

The PSCs can be an unlimited source of cells for medical purpose as a consequence of their self-renewal and differentiation potential. The biggest concern is to prove that transplanted cells integrate and do not create teratomas. A clinical approval of the PSCs derivatives requires a full multi-phase drug pipeline process, which is long and expensive, but already in progress. The ESCs are now in clinical trials for eye diseases, spinal cord injury, myocardial infarct, Parkinson disease and diabetes (Chapman & Scala, 2012; Fields, Cai, Gong, & Del Priore, 2016; Menasché et al., 2015; Schulz, 2015; Schwartz et al., 2015). Many other

potential applications are registered and waiting for approval to start the trials. Those experimental procedures are in the first phase of the clinical trials which were designed to prove their safety. So far, there have been no reports of adverse effects (Trounson & DeWitt, 2016). The iPSCs derivatives have been used once on an individual to treat age-related macular degeneration in Japanese clinical trial (Fields et al., 2016). Improvements in vision were observed and more patients were included in the trial, however, one of the autologous iPSCs lines developed mutation during in vitro culture. The clinical trial was stopped. In the near future, it is planned for patients to obtain allogenic iPSCs with proven genetic stability.

A cell transplantation is an essential objective in the iPSCs research, however, those cells also revolutionised the field of diseases modelling and toxicology. The possibility to culture patient-derived iPSCs is beneficial for studying disease aetiologies and to develop new treatments (Burkhardt et al., 2013; Ren et al., 2015). It is possible to recapitulate differentiation process and obtain large amounts of cells for drugs testing (Young et al., 2015). As an outcome, personalized medicine can arise with the aim of identifying the most potent therapy for patients with diverse genetic backgrounds (Avior, Sagi, & Benvenisty, 2016). To improve safety and standardisation of iPSCs production stem cell banks were initiated. In those facilities, iPSCs are generated under good manufacturing practice (GMP) conditions and stored. Cells will be there carefully monitored and characterised for medical purpose. As an alternative to autologous iPSCs, human leukocyte antigen (HLA) homozygous cells will be reprogrammed to reduce the possibility of cells rejection for many patients worldwide (Taylor, Peacock, Chaudhry, Bradley, & Bolton, 2012; Zimmermann, Preynat-Seauve, Tiercy, Krause, & Villard, 2012) This step will be necessary for future safe use of those cells. Now, commercially available GMP-qualified iPSCs produced by Lonza could be an alternative for clinicians (Baghbaderani et al., 2015). Although iPSCs clinical potential is now broadly explored, many years will pass before new treatments will be available for patients.

1.2. Liver

1.2.1. Liver anatomy and function

A human liver is located in the upper right quadrant of the abdomen and can be divided into a right and a left lobe. Histologically, a liver structure is complex and highly organized. The liver functional unit called lobule consist of plates of hepatocytes radiating from a central vein and portal triads located on the periphery (Fig. 3) (Saxena, Theise, & Crawford, 1999). The portal triad is composed of the portal vein, bile duct, and hepatic artery in the sinuous. The liver tissue is built in 80% by hepatocytes and consists also other cell types (Kmiec, 2001). Bile ducts are made up from cholangiocytes which can resorb water from bile salts. The endothelial cells, stellate cells, and Kupffer cells are nonparenchymal liver cells which supports liver functions but are of mesodermal origin. The stellate cells also known as Ito cells, lipocytes, perisinusoidal cells, or vitamin A-rich cells is the major cell type involved in liver fibrosis (Hautekeete & Geerts, 1997), whereas Kupffer cells are resident macrophage population in the liver (Dixon, Barnes, Tang, Pritchard, & Nagy, 2013). The liver receives venous blood directly from the intestine, spleen, and pancreas by hepatic portal vein which covers approximately 75% of the livers blood supply. The remaining one quarter is delivered by hepatic arteries. Receiving nutrients, hormones and toxins as the first organ, uncover complex functions which liver performs. The liver filters certain substances from the blood and metabolises them. Components of the body like hormones, such as estrogen, aldosterone and anti-diuretic hormone are metabolised as well as potential exotoxins: alcohol and other drugs. The liver stores vitamins (A, D, E, K, B12), copper and iron. Bilirubin released after red blood cells break down is metabolised into ferritin. The hepatocytes are also involved in protein degradation which produces urea and regulation of carbohydrates metabolism by storing glycogen. The liver produces components of the blood: albumin, prothrombin, fibrinogen and some globulin. Additionally, the liver is an accessory digestive gland and produces bile salts which help to digest lipids by emulsification (Laker, 1990; Malarkey, Johnson, Ryan, Boorman, & Maronpot, 2005).

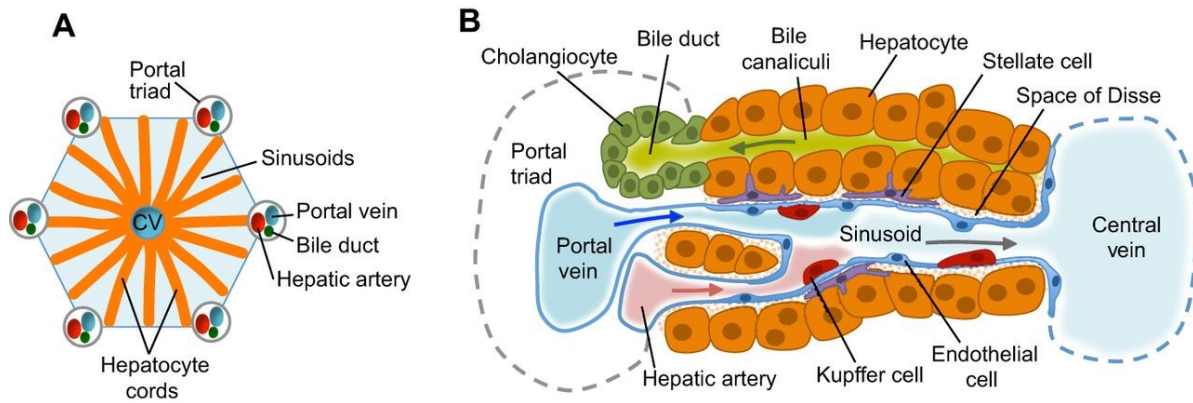


Figure 3 Liver structure and cell types. (A) Organisation of hepatic lobule, hepatocyte cords radiate from the central vein (CV). (B) Cell types in the liver.

Source: (Gordillo, Evans, & Gouon-Evans, 2015).

In the liver hepatocytes form a cell layer that separates blood from the canalicular bile. Unlike the other epithelial cells which are polarized in the plane of the tissue, hepatocytes contribute to creating capillary-like structures, the bile canaliculus. Apical and basolateral plasma membrane differ in cell adhesion molecules, cell junctions, membrane transporters and extracellular matrix (Gissen & Arias, 2015). On the apical side, membrane creates microvilli. These structures increase the surface area of the canalicular membrane and facilitate secretion of bile. In culture, primary hepatocytes and cell lines have significant limitations to create bile canaliculi and only collagen sandwich cultures allow recreating cell polarity so far (Knop, Bader, Böker, Pichlmayr, & Sewing, 1995; Müsch, 2014). Another type of polarisation occurs in hepatic lobule. This phenomenon is called metabolic zonation (Gebhardt, 1992; Jungermann & Kietzmann, 2000). A heterogeneous population of hepatocytes can be distinguished in the axis between hepatic vein and veins leaving the liver. Close to the portal vein, which is in contact with hepatic artery and the bile ducts, there are situated periportal hepatocytes. These cells receive blood rich in oxygen and nutrients, but also are exposed to contact with toxins. On the opposite side, around a hepatic centrilobular vein, there are located perivenous hepatocytes. Those cells are major protein producers in the liver. Hepatocytes form different compartments, vary in expression of enzymes and membrane transporters.

The liver has great regeneration potential, however, under pathological conditions it can suffer many diseases (Taub, 2004). Hepatitis is a liver inflammation, mostly caused by virus

infection or heavy alcohol abuse. Chronic hepatitis can be a cause of liver failure or cancer. Excessive alcohol consumption can be a starting point for other liver diseases: fatty liver disease and cirrhosis. Large vacuoles filled with triglycerides appear in hepatocytes during fatty liver disease (Cohen, Horton, & Hobbs, 2011). A nonalcoholic fatty liver disease is linked to obesity and insulin resistance. Fatty liver is sometimes accompanied by inflammation which can progress to more severe forms of the disease. Hepatocyte damage and activation of stellate cells lead to fibrosis and consequently to cirrhosis when liver tissue is replaced by scar tissue. Typically, this condition develops slowly over the years and is not reversible (Schuppan & Afdhal, 2008). Liver injury can also be caused by drugs and toxins. Several inherited liver diseases can be distinguished: Wilson's disease, hemochromatosis, alpha 1-antitrypsin deficiency. Those diseases affect also other organs and often are recognized in adult patients (Kumar & Riely, 1995; Morrison & Kowdley, 2000).

1.2.2. Liver embryonal development

The liver embryonic development is a strictly regulated process. Over the last two decades, significant progress has been made in the understanding of the molecular mechanisms underlying this process. By studying a mice tissue explant cultures, and by using molecular biology techniques, it was possible to identify key factors orchestrating hepatogenesis. Despite this interest, no one has studied liver development in humans thoroughly before iPSCs techniques allowed researchers to recapitulate hepatogenesis in vitro.

The liver development starts when outgrowing bud forms on the foregut endoderm. Then the basal membrane of the bud delaminates, and cells migrate into surrounding mesenchymal septum transversum. During and after migration, the primitive sinusoidal endothelial cells form capillary-like structures between hepatic cords. At this stage, hepatoblast which can give rise to hepatocytes and cholangiocytes can be distinguished. The hepatic maturation is a gradual process which takes place even after birth (Zaret, 2002; Duncan, 2003; Zhao & Duncan, 2005; Gordillo et al., 2015). A fetal liver participates in hematopoiesis during embryonic development. Determination of the hepatic lineage is therefore strongly influenced by mesodermal cells. First, by close contact of the ventral endoderm with the precardiac splanchnic mesoderm and second, by the septum transversum mesenchyme. These two events are necessary for a complete differentiation of liver. It was shown that without FGF-2 secreted

by cardiac mesoderm, the liver formation is repressed, and pancreas develops instead (Deutsch, Jung, Zheng, Lórá, & Zaret, 2001). Secretion of bone morphogenetic proteins by the septum transversum mesenchyme is critical for hepatoblasts expansion (Rossi, Dunn, Hogan, & Zaret, 2001). Additionally, septum transversum is a producer of extracellular matrix (ECM). Integrins are receptors to ECM components, built of different combinations of α and β subunits. Interestingly, $\beta 1$ integrin knockout mice die early. Experiments on chimeras showed that $\beta 1$ integrin-deficient cells failed to colonize liver and spleen (Fässler & Meyer, 1995). It is also believed that endothelial cells support liver development. Inhibition of vascular growth during hepatoblast expansion can reverse liver formation (Matsumoto, Yoshitomi, Rossant, & Zaret, 2001). Specification of hepatocytes is driven later by the hepatic nuclear factor (HNF) and Oncostatin M (Schmidt, Bladt, Goedecke, & Brinkmann, 1995; Kamiya et al., 1999).

During the liver development, several transcriptional factors are sequentially involved in the hepatic differentiation as shown in the figure (Kinoshita & Miyajima, 2002). It is worth mentioning that Hnf3 and Gata4 were shown to have the ability to open chromatin which makes them master transcription regulators of early hepatic lineage commitment (Cirillo et al., 2002). Additionally, this transcription factor can directly enhance albumin expression. Studies on knockout mice generated for all of the genes expressed during differentiation reveals that factors Hex and Hnf4 α are crucial for developing a liver. Embryos lacking those factors die early due to impaired hepatogenesis (Costa, Kalinichenko, Holterman, & Wang, 2003; Parviz et al., 2003).

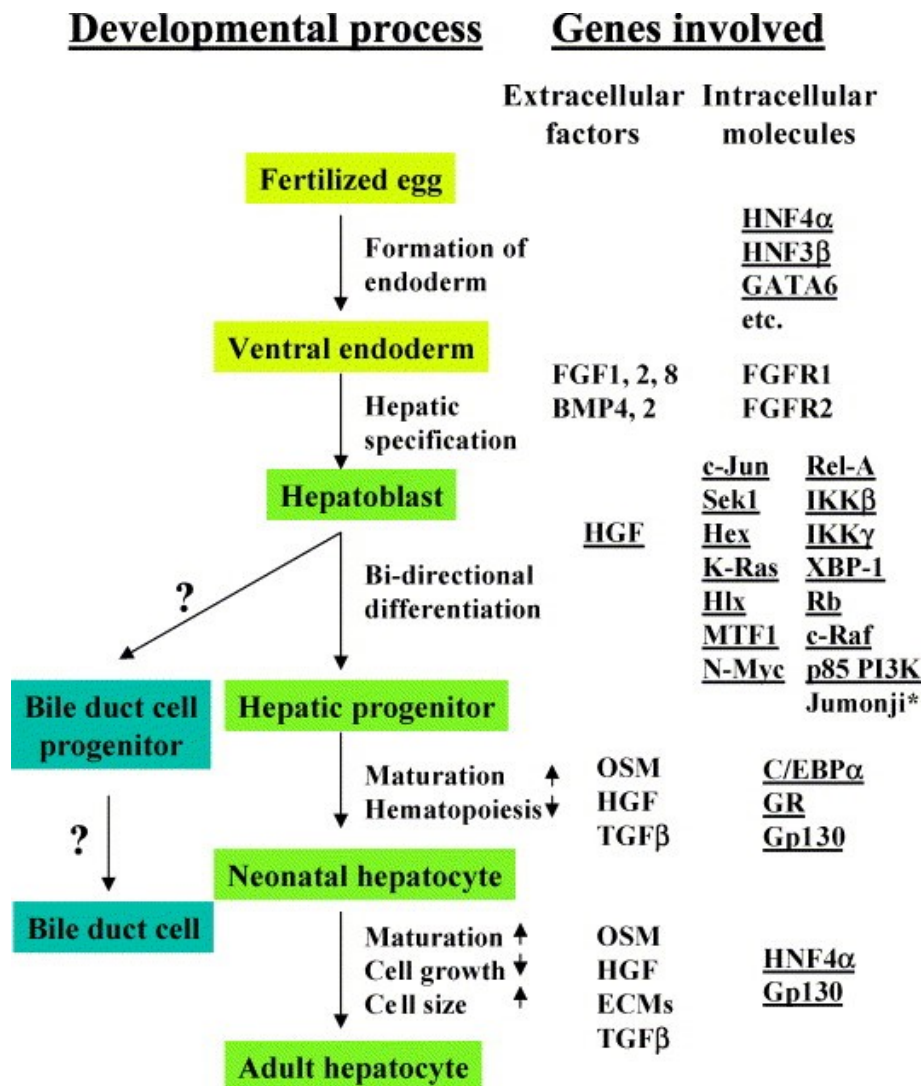


Figure 4 Extra- and intracellular molecules involved in development of liver in different stages.

Underlined molecules were identified from studies of knockout mice. Source: (Kinoshita & Miyajima, 2002).

1.3. Hepatic differentiation of iPSCs in vitro

1.3.1. HLCs

According to the European Liver Transplant Registry, the number of liver transplants is plateauing due to a lack of organs (Adam et al., 2003). This leads to the deaths of many patients with end-stage liver diseases. Transplantations of human hepatocytes could give hope

to people waiting for an organ transplant. Unfortunately, isolated human hepatocytes are restricted in number. During the *in vitro* culture of isolated hepatocytes, cells gradually lose their functions. To overcome those limitations, alternative sources of hepatocytes are proposed. Porcine hepatocytes were clinically tested for their function as a component of extracorporeal hybrid liver support. Despite promising results, this device failed to be available for patients after FDA restrictions that prohibit xenogenous cell usage in medicine (Im Sauer et al., 2003). Immortalized hepatocyte cell lines, as well as cancer-derived cell lines, exhibit some hepatic functions, but due to dedifferentiation and the accumulation of mutations in culture, they are not considered as a source of cells for medical purposes (Dhawan, Puppi, Hughes, & Mitry, 2010). The isolation of human ESC allows *in vitro* hepatic differentiation to be studied. Despite the challenges and ethical issues, the first hepatic differentiation protocols were proposed. Later, after Yamanaka's discovery of iPSCs, the possibility to obtain autologous cell lines gave rise to personalised medicine and pushed studies in this field forward. Significant progress has been made in the derivation of HLCs, however, recapitulating hepatic functions *in vitro* is still arduous (Schwartz, Fleming, Khetani, & Bhatia, 2014). Obtained HLCs resemble a fetal hepatic characteristic (Baxter et al., 2015). Many researchers tried to obtain more mature HLCs using different methods. Unfortunately, the comparison of protocols can be difficult due to a lack of standardised characterisation methods. Detailed tests should be performed in order to characterise an obtained cell identity. Confirming a hepatic lineage commitment can be based on genes and proteins expression. HLCs should be of a polygonal or cuboidal shape with large nucleoli. In electron microscopy studies, the presence of abundant mitochondria, peroxisomes, and lipid bodies should be tested, as well as the presence of microvilli and the bile canalicular network. Cell polarisation is a feature of mature hepatocytes. It can be detected by the presence of several basal or apical proteins (e.g. MRP-2, CD26). Finally, HLCs should exhibit typical hepatic functions. The most popular among characterisation tests are glycogen production, albumin production, urea production, and the activity of detoxification enzymes. To test the liver replacement of hepatocytes and functional engraftment, several mice models were used; nevertheless, they showed a low level of engraftment capacity (Schwartz et al., 2014). Infection by the hepatitis C virus is also considered as a proof for hepatic identity (Si-Tayeb, Duclos-Vallée, & Petit, 2012; Schwartz et al., 2012). The necessity to perform such an enormous work to characterise HLCs makes those cells exceptional. Many laboratories collaborate in order to fully characterise and compare obtained cells with isolated hepatocytes (Godoy et al., 2015). Recently, commercial HLCs called iCell Hepatocytes from Cellular

Dynamics became available for hepatotoxicity test and drug discovery. By using this technology, the first attempts to screen new drugs for the treatment of heritable metabolic liver diseases, like familial hypercholesterolemia, became possible (Cayo et al., 2017).

1.3.2. Differentiation protocols into hepatocytes

As mentioned before, first attempts to obtain hepatocytes from pluripotent stem cells begin after ESC isolation. It was shown that by cell aggregation and the generation of embryoid bodies (EB), it was possible to obtain cells from three germ layers, including hepatic progenitors (Hamazaki et al., 2001). Later, the mouse ESCs were directly differentiated into HLCs (Jones, Tosh, Wilson, Lindsay, & Forrester, 2002). Using a similar approach, human HLCs were derived (Rambhatla, Chiu, Kundu, Peng, & Carpenter, 2003). By mimicking signals observed during embryonic liver development, protocols from spontaneous differentiation events were changed into direct hepatic differentiation with specific cytokine cocktails and defined extracellular matrix. In the case of iPSCs, to prove their differentiation potential, Yamanaka showed endoderm lineage commitment right after their discovery (Takahashi et al., 2007). Later, a group from China applied a modified differentiation protocol and successfully obtained HLCs from iPSCs (Song et al., 2009). All existing direct differentiation protocols can be divided into four parts. First, endoderm induction is an essential step for efficient HLCs formation. It can be done by using Activin A supplementation combined with the activation of Wnt3a signalling or FGF addition (Hay et al., 2008). Many groups, in order to improve efficiency, sorted the cells according to their extracellular markers. Recently, the GSK-3 inhibitor - CHIR99021 has been used as an alternative in defined differentiation conditions (Mathapati et al., 2016). It was also shown that a 24-hour cell exposition to CHIR99021 produces a more homogenous definitive endoderm. A hepatic specification with the addition of BMP4 and FGF2 occurs in the second phase. Then, there is a hepatoblast expansion phase with HGF supplementation, and finally a hepatic maturation with Oncostatin M (Han et al., 2012; Schwartz et al., 2014). Some protocols contain DMSO to improve hepatic differentiation (Czysz, Minger, & Thomas, 2015). However, the usage of DMSO is controversial and some reports show an inhibition of differentiation (Pal, Mamidi, Das, & Bhonde, 2012). An extracellular matrix used for supporting the cells also can influence hepatic differentiation. Commonly used Matrigel and

their derivatives are not suitable for defined culture conditions. Recently shown differentiation of iPSCs on recombinant laminins can be a step forward for the medical usage of those cells (Cameron et al., 2015). Attempts to generate HLCs in defined conditions gave rise to the protocol using only small molecules (Siller, Greenhough, Naumovska, & Sullivan, 2015). Another direction is to use 3D culture and bioreactors to improve differentiation efficiency (Sivertsson, Synnergren, Jensen, Björquist, & Ingelman-Sundberg, 2012; Takayama et al., 2013). Perfused systems allow for the constant control of culture conditions, and when compared to standard 2D culture, they produce more mature HLCs (Freyer et al., 2016). Innovative organs on the chip which are miniature complex bioreactors designed to mimic a liver microenvironment in vitro. The hepatic differentiation of iPSCs in those devices confirmed that functionality of the HLCs can be elaborated (Caralt, Velasco, Lanas, & Baptista, 2014a). To imitate whole hepatocyte niche, a decellularized liver scaffold can be used (Caralt, Velasco, Lanas, & Baptista, 2014b). By using this technique, bioengineered tissue mimics a natural liver structure. However, there is a necessity for the implementation of endothelial progenitors to fill the vascular network (Baptista et al., 2011). Co-culture methods demonstrated great potential for liver tissue engineering. A combination of hepatic, endothelial, and mesenchymal progenitors spontaneously produces 3D organoids (Shinozawa, Yoshikawa, & Takebe, 2016). The self-organizing approach coupled with iPSCs technology is the most advanced and complex organoid model (Takebe, Zhang et al., 2014). Nevertheless, the acquisition of hepatic functions occurs after transplantation and vascularisation of the liver bud (Takebe, Koike et al., 2014). Recently, a similar effort has been made to obtain cholangiocyte-like cells from iPSCs (Dianat et al., 2014). Generated organ models are useful for studying the molecular mechanism underlying liver development and pathogenicity. In the future, these examples will hopefully be the base for developing therapeutic strategies for bioengineered liver transplants.

1.4.NcRNA

In contrast to genes coding messenger RNA (mRNA), ncRNAs participate mostly in regulating gene expression and gene translation. There are many types of ncRNAs that differ in structure and function. The ribosomal RNAs (rRNAs), and transfer RNA (tRNAs) are involved in mRNA translation. The micro RNA (miRNAs) function as gene silencers. The

small nucleolar RNAs (snoRNAs) are involved mostly in the modification of other rRNAs. The Small Cajal body RNA (scaRNAs) and related small nuclear RNAs (snRNAs) are snoRNAs which are taking part in splicing (Abbas, Raza, Biyabani, & Jaffar, 2016; Isakov et al., 2012). The liver miRNAs and snoRNAs will be described here in detail since they are the main objectives of this study.

1.4.1. MiRNA

MiRNAs are post-transcriptional gene expression regulators. These 21-22 nucleotide long molecules can affect the expression of multiple genes simultaneously by binding to the complementary regions of a messenger RNA (mRNA). A large number of miRNA are highly conserved in sequences among different organisms (Cai, Yu, Hu, & Yu, 2009; Chen & Verfaillie, 2014). MiRNA serve as potential diagnostic and therapeutic targets. The human miRNAs are initially transcribed by RNA polymerase II as several hundred-nucleotide long miRNA precursors, termed a primary miRNA (pri-miRNA), which contain RNA stem-loop. In canonical processing, pri-miRNA is cleaved by Drosha. A shorter hairpin termed a pre-miRNA that contains a 2 nt 3' overhang, is the resultant of the cleavage. Then, the pre-miRNA is exported to the cytoplasm by nuclear Exportin 5 for another cleavage. Enzyme Dicer cuts the loop of pre-miRNA leaving 22 base pairs RNA duplexes bearing 2 nt 3' overhangs. One strand of the duplex stays associated with Dicer and is then incorporated into the RNA induced silencing complex (RISC). This complex includes protein Argonaute which leads the interaction with target mRNA and has nuclease activity. There are also other pathways of RISC preventing translation (Cullen, 2004; Winter, Jung, Keller, Gregory, & Diederichs, 2009; Inui, Martello, & Piccolo, 2010). Deletion of Dicer is lethal in a mouse. Further, it was shown that hepatocytes of recombinant Dicer negative mouse liver (AlbCre; Dicer flox/flox), undergo activation of proliferation and apoptosis. Recombinant mouse had lack of liver zonation and developed lethal hepatocarcinomas (Sekine, Ogawa, Mcmanus, Kanai, & Hebrok, 2009).

In the liver, the most abundant miR-122 is involved in the metabolism of lipids, glucose, and iron as well as in hepatocyte differentiation (Lewis & Jopling, 2010; Hu et al., 2012; Wen & Friedman, 2012). It was shown that overexpression of miR-122 enhances expression of HNF6, FOXA1, and HNF4a which are the master transcription factors during liver

development (Laudadio et al., 2012; Deng et al., 2014). Overexpression of miR-122 can enhance hepatic maturation of fetal liver progenitors (Doddapaneni et al., 2013). The miR-122 can suppress cell proliferation and tumor metastasis by down-regulating the protein levels of Wnt1 (Wnt signaling is an inducer of EMT) (Girard, Jacquemin, Munnich, Lyonnet, & Henrion-Caude, 2008; Coulouarn, Factor, Andersen, Durkin, & Thorgeirsson, 2009; Xu et al., 2012). Additionally, its expression enhances replication of the Hepatitis C virus (HCV) (Lanford et al., 2010). Another miRNA which is highly expressed in the liver is miR-148. It promotes hepatic maturation by targeting DNA methyltransferase 1 (DNMT, dominant de-novo DNA cytosine methyltransferase in human, responsible for epigenetic silencing) and is a tumor suppressor (Gailhouste et al., 2013). Studies on mouse hepatic stem cell line HBC-3 demonstrated the importance of the miR-23b cluster, which contains miR-23b, miR-27b, miR-24-1, miR-10a, miR-26a, and miR-30a in regulating hepatic specification (Rogler et al., 2009). The miR-23b cluster members repress bile duct gene expression in fetal hepatocytes by down-regulating Smads 3, 4, and 5 and as a result of TGF β signalling. The miR-194 is responsible for the preservation of hepatocyte epithelial phenotype by inhibition of N-cadherin expression and other known prometastatic genes (HBEGF, RAC1, PTPN12, ITGA9, SOCS2) (Meng et al., 2010). Moreover, expression of the miR-194 together with miR-192 and miR-215 is regulated by HNF1a and it was shown that they can inhibit EMT (Krützfeldt et al., 2012; Khella et al., 2013).

In comparison to mature liver, several miRNAs have been found to be highly expressed in fetal liver (Fu et al., 2005; Liu et al., 2010; Tang, Liu, Zhang, Ingvarsson, & Chen, 2011). Studies on mice have discovered functions of some of those miRNAs. The miR-92b is important for hepatic progenitors to proliferate and by targeting CCAAT/enhancer binding protein beta (C/EBP β) gene, it can block maturation (Qian et al., 2013). The miR-483, another upregulated gene during liver development promotes proliferation in a prooncogenic manner, but can inhibit fibrosis by targeting platelet-derived growth factor- β (PDGF- β) and tissue inhibitor of metalloproteinase 2 (TIMP2) (Li et al., 2014; Ma et al., 2012). It is important to mention that it was possible to initiate hepatic differentiation by overexpression of the seven miRNAs (miR-1246, miR-1290, miR-148a, miR-30a, miR-424, miR-542-5p, and miR-122) in differentiating human umbilical cord lining-derived mesenchymal stem cells (Cui et al., 2013). Additionally, when expression of any of these miRNAs was inhibited, the hepatic differentiation was blocked.

1.4.2. SnoRNA

SnoRNAs act as guides for chemical modifications of other RNAs, mainly rRNAs. In the humans, snoRNAs are encoded in introns of the host genes. Based on different sequence motifs and secondary structures, snoRNAs are divided into two types: box C/D snoRNAs, that guide ribose methylation and box H/ACA snoRNAs which guide pseudouridylation (Dupuis-Sandoval, Poirier, & Scott, 2015; Kiss, 2002). Typical box C/D snoRNAs have conserved boxes C (consensus sequence RUGAUGA) near their 5' and D (consensus sequence CUGA) at 3' termini. Usually, they are between 60 and 90 nucleotides long. The box C base pairs with D and creates a k-turn which is a binding site for a set of core proteins forming a box C/D snoRNP. In the loop region there are additional motifs, boxes C' and D'. Their sequences have the same consensus as the boxes C and D, respectively, but are typically less conserved. The target RNA is complementary to the regions upstream of the boxes D' and/or D. The modified nucleotide in the target RNA is the fifth residue upstream of the box. Whereas box H/ACA snoRNAs secondary structure consists of two hairpins. They are also longer, up to 140 nucleotides. In between the hairpin structures, there is an unpaired region that contains conserved motive H box (ANANNA where N can be any nucleotide) called hinge. After the second hairpin, upstream of the 3' end of the molecule in the tail, another conserved box called ACA is located. The name reflects the consensus sequence. Targets bind complementarily into the pseudouridylation pockets forming small duplexes with the target RNA, allowing only few mismatches in the middle of hairpins. The modified uridine is typically located 14–16 nucleotides upstream from the conserved boxes where bulges are created (Reichow, Hamma, Ferré-D'Amaré, & Varani, 2007). To form functional complexes, snoRNAs associate with specific protein components such as GAR-1 (Box H/ACA) or fibrillarin (Box C/D).

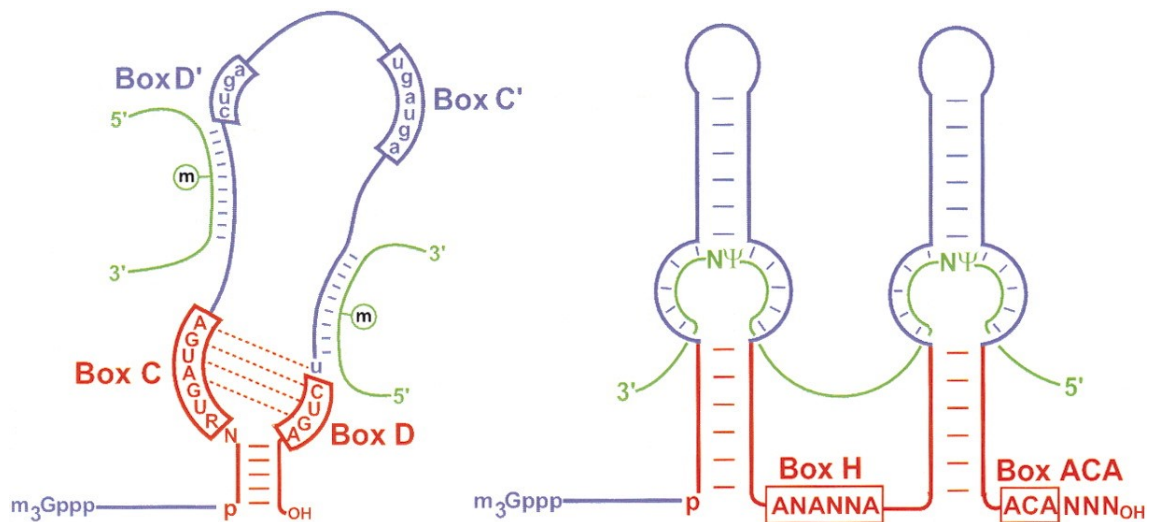


Figure 5 Structure of Box C/D and Box H/ACA snoRNAs.

m₃Gppp – trimethylguanosine cap structure on 5' end. In green highlighted substrate RNAs and in red – snoRNAs core motifs. Pseudouridylation (Ψ) and 2'-O-methylation (circled m) of the nucleotides are marked. Source: (Kiss, 2002).

ScaRNAs unlike typical snoRNAs, are accumulated and possess additional localization motifs. ScaRNAs can have typical box C/D or H/ACA structure, single or tandem or can be a hybrid of box C/D and box H/ACA snoRNAs. They target snRNAs (U1, U2, U4, U5, U11, U12, U6) (Hebert, 2013). Apart from the canonical function in guiding nucleotide modifications, further snoRNA functions have been discovered. SNORD3, SNORD14, SNORD22, SNORA63, SNORA73, and SNORD118 are involved in the cleavage of the rRNA operon. Several box H/ACA snoRNAs are found to be enriched in chromatin-associated RNA (caRNA) which are responsible for chromatin decondensation. SCARNA19 is a telomerase RNA component (TERC) (Dupuis-Sandoval et al., 2015). Bioinformatic methods allow to predict targets for some of snoRNAs guided modifications. SnoRNAs without predicted targets are called 'orphan snoRNA' and some of them play a role in the regulation of alternative splicing (Bazeley et al., 2008). Some specific snoRNAs are known to act in a miRNA-like fashion and there are examples of their association with the Argonaute protein (Ender et al., 2008; Brameier, Herwig, Reinhardt, Walter, & Gruber, 2011; Burroughs et al., 2011). The region SNURF-SNRPN is one of two imprinted regions coding snoRNA. It contains five box C/D snoRNA: SNORD64, SNORD107, SNORD108, SNORD109 (two copies) and the tandem repeats of SNORD116 and SNORD115 (Runte et al., 2001). An

inheritance of deletion in this locus of paternal chromosome causes Prader-Willi syndrome (Bieth et al., 2015). Numbers of snoRNAs were recently proposed to be massively processed into shorter RNA species, called processed snoRNA (psnoRNA) or sno-derived RNA (sdRNA) (Falaleeva & Stamm, 2013a). It was shown that SNORD115-derived short RNA regulates alternative splicing of serotonin 2C receptor mRNA (Kishore et al., 2010). In the human tissues snoRNAs have been observed to be differentially expressed and have recently attracted attention as biomarkers (Castle et al., 2010; Ho et al., 2014; Su et al., 2016).

2. Aims

Induced pluripotent stem cells revolutionised developmental biology. Now, by using those cells, it is possible to follow their natural embryonal development to generate tissues in vitro. There are many problems to overcome before the use of iPSCs in medicine can be possible. The biggest challenge is to obtain genetically stable pluripotent cell lines with high efficiency. Transfection with episomal vectors is currently the most popular method of generating iPSCs. However, this method is limited by transfection efficiency. The present thesis aims to generate stable iPSCs by overcoming those limitations in order to enable the wide use of cellular reprogramming.

The first aims of the current thesis are:

- Generation of stable iPSCs through episomal vector transfection,
- Pluripotency characterization of the generated iPSCs.

Liver failure is an untreatable disease which causes millions of deaths every year. Liver tissue is also very important for the toxicological testing of new drugs. iPSCs which have unlimited differentiation potential, can be applied in order to overcome current limitations with accessing hepatocytes. Although many hepatic differentiation protocols exist, there is still a room for improvement. Obtained hepatic-like cells resemble a fetal liver and thus, their functions are impaired. The current thesis will compare HLCs and hepatocytes, with focus on the ncRNA, to study the potential inhibitors of hepatic maturation.

The second aims of the current thesis are:

- Hepatic differentiation of obtained iPSCs,
- Characterisation of HLCs
- Non-coding RNA analysis.

In summary, the aims of the current study are first, the generation of stable, footprint-free iPSCs which can be used for hepatic differentiation, and second, an analysis of the obtained iPSCs-derived hepatic-like cells non-coding RNA profiles in order to improve hepatic differentiation.

3. Materials

3.1. Equipment

- Milli-Q (Millipore)
- Microscope Olympus IX 51
- Microscope Nikon eclipse TE2000-S
- Fluorescence microscope (Zeiss and CTR600 Leica)
- ND1000 Spectrophotometer (NanoDrop Technologies)
- Thermocycler Primus 96 plus (MWG AG Biotech)
- Biosafety cabinet (Heraeus)
- Applied Biosystems 7500 Real-Time PCR System (Thermo Fisher Scientific)
- Confocal microscope (Leica Microsystems)
- Labofuge 400R (Heraeus)
- Minishaker MS 2 (IKA)
- Incubator Cytoperm 2(Heraeus)
- -86°C ULT Freezer (Thermo Forma)
- Biofuge pico (Heraeus)

3.2. Software

- MS-Office 2007 SP2 (Microsoft)
- Leica Software v. 1.4.0 (Leica)
- Cell^A (Olympus)
- AxioVision (Zeiss)
- ImageJ (image analysis)
- FastQC (sequencing quality)
- Segemehl (mapping to the genome, Bioinformatics Leipzig)
- R (The R Foundation)

- R Studio (FOAS)
- Bioconductor package
- EdgeR package
- Rnacounter (counting the reads)
- Bedtools (analysis of the reads)
- DIANA mirPath V. 3.0

3.3. Enzymes, Kits and Transfection Reagents

- Lipofectamine 3000 transfection reagent (Life Technologies)
- Trypsin/EDTA (Life Technologies)
- RNeasy Mini Kit (Qiagen)
- miRNeasy Micro Kit (Qiagen)
- Periodic Acid-Schiff (PAS) staining system (Sigma-Aldrich)
- Superscript III Reverse Transcriptase (Thermo Fisher Scientific)
- CYBR Green PCR master mix (Thermo Fisher Scientific)

3.4. Solutions and reagents

- PBS (Life Technologies)
- 4% paraformaldehyde Roti-Histofix (Carl Roth GmbH)
- Versene (Life Technologies)
- 4,6-diamidino-2-phenylindole dilactate (DAPI) (Sigma)
- BSA powder (PPA)
- Dimethyl Sulfoxide (DMSO) (Sigma-Aldrich)
- Dimethyl Sulfoxide (DMSO) Cell culture grade (AppliChem)
- Opti-MEM® I Reduced Serum Medium (Life Technologies)
- Penicillin/streptomycin (Life Technologies)
- Cardiogreen (Sigma-Aldrich)
- Saponin powder (Sigma-Aldrich)

- Nuclease-Free Water (Qiagen)
- Geltrex ESC qualified (Thermo Fisher Scientific)
- Wheat Germ Agglutinin, Alexa Fluor® 488 Conjugate (Thermo Fisher Scientific)
- DAPI (Sigma)
- Chloroform (Roth)
- Ethanol (Roth, Sigma)
- TE Buffer (AppliChem)

3.5. Cell lines

- Gibco Episomal hiPSC line (A18945, Life Technologies)
- HepG2 cell line (ATCC)
- Primary cells: isolated human foreskin fibroblasts (HIV, HBV, HCV negative cells obtained from 6 years old, healthy boy)
- Generated cells: iPS cell line (ULEi001-A)
- Frozen hepatocytes pooled 10 donors (HMCS10, GIBCO)

3.6. Cell culture media and cytokines

- DMEM low glucose (Thermo Fisher Scientific)
- Essential 8 (Thermo Fisher Scientific)
- ESC qualified FBS
- RPMI1640 medium (Thermo Fisher Scientific)
- B27 Supplement Minus Insulin (ThermoFisher Scientific)
- B27 Supplement (ThermoFisher Scientific)
- Activin A (R&D Systems)
- Fibroblast growth factor 2 (FGF2, R&D Systems)
- Bone morphogenetic protein 4 (BMP4, Peprotech)
- Hepatocyte growth factor (HGF, Peprotech)
- HCM™ hepatocyte culture medium (Lonza)

- Oncostatin M (R&D Systems)

3.7.Plasmids

Table 1 Description of the plasmids used.

Plasmid	Expressed genes	Supplier	Cells transfected
TrueClone Human cDNA clone (SC123863)	Human Hepatocyte Nuclear Factor 4	Origene	Gibco Episomal hiPSCs
Episomal iPSCs Reprogramming Plasmids with GFP reporter gene (SC900A)	Oct4, Sox2, L-Myc, Klf4, Nanog, Lin28, shRNA-p53, miR302/367, GFP	System Biosciences	Isolated human foreskin fibroblasts

3.8.PCR reagents and primers

3.8.1. PCR reagents

- Deoxynucleotide triphosphates (dNTPs) (Thermo Fisher Scientific)
- Oligo(dT)18-Primer (Thermo Fisher Scientific)
- RNase-Free DNase I (Thermo Fisher Scientific)
- Superscript III Reverse Transcriptase (Thermo Fisher Scientific)
- CYBR Green PCR master mix (Thermo Fisher Scientific)

3.8.2. PCR primers

Table 2 The primer sequences for qRT-PCR

Gene	Primer forward	Primer reverse	Product size	Tm °C
Human Hepatocyte Nuclear Factor 4	5`-ATG GCT CTC CTG AGA GTG GA-3`	5`-CAG CGC AAG ACC TAA TGA CA – 3`	223 bp	60
Albumin	5`-GAA ACA TTC ACC TTC CAT GC-3`	5`-ACA AAA GCT GCG AAA TCA TC-3`	152 bp	60
Alpha-fetoprotein	5`-CAT ATG TCC CTC CTG CAT TC-3`	5`-TTA AAC TCC CAA AGC AGC AC-3`	272 bp	60
Human Serpin peptidase inhibitor	5`-ATG ATC TGA AGA GCG TCC TG-3`	5`-AGC TTC AGT CCC TTT CTC GT-3`	152 bp	60
Peptidylprolyl isomerase A (PPIA)	5`-TTC ATC TGC ACT GCC AAG AC-3`	5`-TCG AGT TGT CCA CAG TCA GC-3`	158 bp	60

3.9. Antibodies

Table 3 Antibodies used for immunostaining.

Antibody	I/II	Dilution	Host and type	Supplier
Albumin	Primary	1:200	Mouse monoclonal	R&D Systems
α fetoprotein	Primary	1:200	Rabbit polyclonal	DAKO
α1- antitrypsin	Primary	1:200	Mouse monoclonal	Novus Biologicals
Hepatocyte nuclear factor 4α	Primary	1:200	Rabbit monoclonal	Abcam
Cytokeratin 18	Primary	1:100	Mouse monoclonal	Abcam
MRP2	Primary	1:100	Rabbit monoclonal	Abcam
Goat anti-mouse conjugated with Alexa Fluor 568	Secondary	1:1000	Goat polyclonal	ThermoFisher Scientific
Goat anti-rabbit conjugated with Alexa Fluor 488	Secondary	1:1000	Goat polyclonal	ThermoFisher Scientific

4. Methods

4.1. Cell biology

4.1.1. Derivation and culture of primary human foreskin fibroblasts

The foreskin samples were obtained from the private clinic (Pediatric and Ambulatory Surgery, Elster Passage, Zschochersche Straße 48, 04229 Leipzig). The donor was a healthy 6-year-old boy. The tissue was removed according to conventional aseptic techniques. The dissected skin was washed and disinfected. After overnight incubation in Diaspase II (Sigma-Aldrich) 4 °C, the epidermis was removed. The remaining skin was cut with a scalpel to micrometers pieces. Skin pieces were then plated on culture dish and explant fibroblast cultures were maintained at 37 °C in 5% CO₂ in Dulbecco's Modified Eagle's Medium (DMEM, LifeTechnologies) low glucose, supplemented with 20% fetal bovine serum (FBS, LifeTechnologies) and penicillin (100 U/mL)-streptomycin (100 µg/mL).

4.1.2. Counting cells

The cells were counted using Neubauer chamber. To loading groove, 10µl of sample diluted with trypan blue dye was added. The counting was performed using 10x objective. Cells which were not blue were counted in the few squares. The concentration was calculated using this formula:

Concentration = (Number of Cells x 10.000)/ (Number of square x dilution).

4.1.3. Cryo-preservation of cells

To prepare cells for cryostorage, confluent cultures were detached using Versene (iPSCs) or trypsin/EDTA solution and centrifuged at 900g for a period of 5 minutes. The supernatant was

aspirated, and cells were re-suspended in the cryogenic medium. For fibroblast, cryogenic medium contained 45% DMEM, 45%FBS and 10 % dimethyl sulfoxide (DMSO). Pluripotent stem cells were cryopreserved in 90% of Essential 8 medium containing 10% of DMSO. Cell suspensions transferred to cryogenic vials were prepared for liquid nitrogen storage by incubation in -80°C freezer overnight in Mr. Frosty™ freezing container.

4.1.4. Thawing of cryo-preserved cells

The cryostored cells were recovered from storage by thawing in a 37°C for 5 min. To remove residual cryogenic medium prior to culture, the contents of each vial were transferred to 15 mL Falcon® tubes containing culture medium and centrifuged at 900g for 5 minutes. The cell viability was measured after thawing using the Trypan blue exclusion assay and cells were seeded into culture vessels or flasks in adequate density.

4.1.5. Cell reprogramming

The foreskin fibroblasts were thawed and expanded in DMEM medium low glucose with 10% ESC qualified FBS (Life Technologies). The cells were transfected with episomal vectors containing reprogramming factors: human Oct4, Sox2, Klf4, L-myc, Lin28, shRNA-p53, miR302/367 cluster and GFP (System Biosciences). For transfections, Lipofectamine 3000 (Life Technologies) was used according to manufacturer's protocol. The cells in passage number 4 were seeded into the Geltrex-coated 6-well plate (Life Technologies) one day before transfection. The plasmids DNA-lipid complexes were prepared in OptiMEM medium (Thermo Fisher Scientific) and added dropwise to the cells. On the following day, the medium was changed and on the third day the second transfection was performed. The medium was changed daily. The fibroblast medium was changed to Essential 8 (E8, Life Technologies) 15 days after transfection. Colonies were picked up mechanically on day 24 and plated in separate wells on Geltrex-coated 24-well plate. After 5 days, the best iPS cell line was chosen for future expansion. There was no GFP expression in the cells 30 days after plasmid transfection. The cells were routinely split using Versene (LifeTechnologies) in feeder-free conditions in the presence of Essential 8 medium.

4.1.6. Cultivation and expansion of iPSCs

The induced pluripotent stem cells were cultured in Essential 8 medium (ThermoFisher Scientific) on the 6-well plates coated with Geltrex (ThermoFisher Scientific) at the concentration of 0,12–0,18 mg/mL. Every 4-5 days cells were split using Versene (ThermoFisher Scientific) usually in a ratio 1:4.

4.2. Immunocytochemistry

For immunostaining, cells were fixed for 15 min at room temperature (RT) in 4% Paraformaldehyde solution Roti-Histofi (Carl Roth GmbH + Co. KG), then washed three times in PBS (LifeTechnologies), and blocked and permeabilized for 1 h in PBS with 1% Fetal Bovine Serum (Sigma-Aldrich) and 0,1% of Saponin (Sigma-Aldrich). Cells were then incubated with primary antibodies overnight at 4 °C, rinsed three times with PBS, and incubated with secondary antibodies for 1 hour at RT. DAPI was used as a nuclear counterstain (Thermo Scientific). Antibodies used for characterisation of iPS cells: Nanog (Cell Signaling 4903 rabbit monoclonal IgG), Oct4 (Cell Signaling 2840 rabbit monoclonal IgG), Sox2 (Cell Signaling 3579 rabbit monoclonal IgG), SSEA4 (Thermo Scientific MA1-21 mouse monoclonal IGG), Claudin6 (R&D Systems MAB3656 mouse monoclonal IGG). Antibodies used for characterisation of hepatic-like cells Alpha Fetoprotein (Dako A 0008, rabbit polyclonal), HNF4a (Abcam ab92378, rabbit monoclonal), Albumin (R&D Systems mab14-55, mouse monoclonal), Cytokeratin 18 (Abcam ab82254, mouse monoclonal), MRP2. Alexa Flour 488 conjugated antibody goat anti-rabbit and Alexa Fluor 633 conjugated antibody goat anti-mouse (Thermo Scientific) were used as secondary antibodies.

4.3. In vitro spontaneous differentiation

The iPSCs colonies were detached from the plate using Versene (LifeTechnologies) and suspended in Essential 6 medium (LifeTechnologies). The cell aggregates were cultured in suspension on low attachment Petri dishes to generate embryoid bodies. After 7 days,

embryoid bodies were transferred to Geltrex-coated 6-well plates and cultured for another 14 days. Afterwards, cells were stained (as described before) for markers for neurons (Neurofilament heavy Novus Bio NB300-135, rabbit polyclonal) and muscle cells (Alpha-Smooth muscle actin Sigma A5228, mouse monoclonal).

4.4.Karyotype analysis

Chromosomal analysis was performed after GTG-banding by Dr. Heidrun Holland (Team Leader, Authentication, Stability, and Identity of Cells, SIKT and Faculty of Medicine Leipzig University, Philipp- Rosenthal Str. 55, Leipzig, Germany). Seventeen metaphases were counted and three karyograms analysed with no evidence of numerical or structural chromosomal aberrations.

4.5.RNA isolation

The total RNA was isolated from cells at day 24 of hepatic differentiation protocol using RNeasy Mini Kit (Qiagen). Briefly, cells were lysed and homogenised using lysis buffer after washing with PBS. Then ethanol was added according to protocol and sample was loaded onto the RNeasy silica membrane column. Purification of contaminants was performed by washing with provided buffers and spinning the column. Pure, concentrated RNA was eluted by washing with 50 µl of DNase free water. RNA concentration and quality were measured by ND1000 Spectrophotometer (NanoDrop). Isolated RNA was stored at -80°C.

4.6.Quantitative PCR

The gene expression of hepatocyte-specific proteins (Protein phosphatase 1 - PP1, Hepatocyte Nuclear Factor 4 alpha - HNF4a, Albumin - ALB, Alpha-fetoprotein - AFP, Human Serpin peptidase inhibitor - A1AT) were validated using qPCR. Isolated RNA was reverse transcribed using Superscript III Reverse Transcriptase (Thermo Fisher Scientific) according to

manufacturer protocol. The expression of target mRNAs was quantified using Applied Biosystems 7500 Real-Time PCR System with CYBR Green PCR master mix. Each reaction was performed in triplicate in conditions: 95°C 5min followed by 40 cycles of 95°C for 15s denaturation, 60°C 15s annealing and 72°C for 30s extension. Protein phosphatase 1 (PP1) gene was the endogenous control. The Ct value was normalised against endogenous control to obtain Δ Ct. Fold difference was calculated using $2^{-\Delta\Delta}$ Ct method. The following primers were used: Human Hepatocyte Nuclear Factor 4 (HNF4 α) F 5'-ATG GCT CTC CTG AGA GTG GA-3', R 5'-CAG CGC AAG ACC TAA TGA CA - 3', Albumin (Alb) F 5'-GAA ACA TTC ACC TTC CAT GC-3', R 5'-ACA AAA GCT GCG AAA TCA TC-3', Alpha-fetoprotein (AFP) F 5'-CAT ATG TCC CTC CTG CAT TC-3', R 5'-TTA AAC TCC CAA AGC AGC AC-3', Human Serpin peptidase inhibitor (A1AT) F 5'-ATG ATC TGA AGA GCG TCC TG-3', R 5'-AGC TTC AGT CCC TTT CTC GT-3', PP1 F 5'-TTC ATC TGC ACT GCC AAG AC-3', R 5'-TCG AGT TGT CCA CAG TCA GC-3'.

4.7. Periodic acid-schiff (PAS) staining

The cells at day 24 of differentiation were stained using Periodic Acid-Schiff (PAS) staining system (Sigma-Aldrich) according to the manufacturer's instruction. Briefly, cells were first fixed with Formalin-Ethanol Fixative Solution then washed with water. Next cells were incubated 5 min in Periodic Acid Solution followed with distilled water washing. Then cells were immersed in Schiff's Reagent for 15 min. After washing with water, nucleuses were counterstain with hematoxylin and analysed.

4.8. Indocyanine green uptake and release

Indocyanine green (ICG, Cardiogreen, Sigma-Aldrich) was dissolved in DMSO (Sigma-Aldrich) and then added to the medium for 1 h. The final concentration of the resulting ICG solution was 1 mg/ml. After incubation medium was exchanged and images representing ICG uptake was taken with the microscope. After 6h, functional ability of hepatocytes to remove the dye was inspected again with the microscope.

4.9. Plasmid transfection

The plasmid was detailed described in the previous section. The transfection was done using Lipofectamine 3000 (Invitrogen). Before transfection, 1 mg plasmid and 2 mL Lipofectamine 3000 separately was diluted with 50 mL serum-free Opti-MEM I (Invitrogen) and incubated for 5 min. Then, solutions were mixed and incubated additionally for 20 min at room temperature. After incubation mixture was added to the medium and mixed gently. The medium was replaced with a new culture medium after 24h.

4.10. Hepatic differentiation

For the hepatic differentiation, the previously described protocol was used (Yu et al., 2012). Briefly, when cells reach 70% confluency medium was changed for RPMI1640 media containing B27 Supplements Minus Insulin (Invitrogen), 100 ng/mL Activin A (R&D Systems), 20 ng/ml fibroblast growth factor 2 (FGF2) (R&D Systems) and 10 ng/ml bone morphogenetic protein 4 (BMP4) (Peprotech) to induce endoderm. After 8 days of the culture, dishes were moved to hypoxia (4%O₂) in RPMI/B27 Supplements (Invitrogen) medium with 20 ng/mL BMP4 and 10 ng/mL FGF2 for 5 days. Next medium was changed to RPMI/B27 supplemented with 20 ng/mL hepatocyte growth factor (HGF, Peprotech) for additional 5 days in hypoxia. The final stage of differentiation was in HCM™ hepatocyte culture medium (Lonza, but omitting the EGF) supplemented with 20 ng/mL Oncostatin M (R&D Systems) for 5 days in normoxia (21%O₂). The medium was prepared freshly and changed daily.

4.11. Wheat Germ Agglutinin staining

Wheat Germ Agglutinin (WGA), Alexa Fluor® 488 Conjugate can be used to visualise cell membrane in the fluorescent microscope. WGA binds to sialic acid and N-acetylglucosaminyl residues in the cell membrane and in combination with fluorochrome can be easily detected. Staining was performed according to manufacturer protocol, briefly, WGA conjugate stock solution was dissolved in medium to the concentration of 5.0 µg/mL. The cells were

incubated with the mixture for 10 min at 37°C. Then cells were counterstain with DAPI and fixed with 4% paraformaldehyde for 15 min prior to secure the sample during transport to the confocal microscope.

4.12. Validation of hepatic differentiation efficiency

To validate the efficiency, cells were cultured on two wells slides (Thermo Fisher Scientific Inc) and after the hepatic differentiation, stained as described above for HNF4a and ALB. Whole slides were scanned (Bioquant, University Heidelberg), and using image analysis tool ImageJ (Schnider), area of double-positive cells was measured. Scans of four wells were analysed per condition.

4.13. RNA isolation and sequencing

The total RNA, including short RNAs, was purified from frozen hepatocytes (pooled 10 donors HMCS10, GIBCO) and cells at day 20 and 24 of hepatic differentiation using the miRNeasy Micro Kit (Qiagen) and quantified by Nanodrop spectrophotometer. The total RNA was used in the small RNA protocol with the TruSeq™ Small RNA sample prekit v2 (Illumina) according to the instructions of the manufacturer. The barcoded libraries were size restricted between 140 and 165bp, purified and quantified using the Library Quantification Kit - Illumina/Universal (KAPA Biosystems) according to the instructions of the manufacturer. Sequencing was performed with an IlluminaHighScan-SQ sequencer at the sequencing core facility of the IZKF Leipzig (Faculty of Medicine, University Leipzig). Hepatic-like cells were cultured and harvested at two different time points: day 20 of hepatic differentiation (hepatoblast stage of HD) and day 24, the last day of differentiation.

4.14. Bioinformatic Analysis

4.14.1. Sequencing quality and mapping

The raw reads were analysed with fastqc for a quality control of the sequencing. Reads were trimmed from adapters and prepared for mapping to the human genome assembly hg38. Mapping was performed with segemehl (Hoffmann et al., 2009), which allows multiple read mapping. Subsequently, the mapped reads were overlapped with gene annotation GENCODE v24 and RepeatMasker track (retrieved from UCSC) using rna-counter and bedtools (Quinlan, 2014), respectively. Additionally, human snoRNA annotations were taken from literature (Jorjani et al., 2016).

4.14.2. Analysis of differentially expressed ncRNAs

The count data were normalized and differentially expressed miRNAs and snoRNAs genes were identified using EdgeR a Bioconductor software package for every group pairwise comparison (Robinson et al., 2010). The differentially expressed miRNAs and snoRNAs were selected by a false discovery rate (FDR) less than 0.001 and sorted by the adjusted fold change (including only genes with normalised fold change higher than 2).

4.14.3. Target pathways prediction of differentially expressed miRNAs

In order to identify predicted targets of the differentially expressed miRNAs, the DIANA mirPath tool V3.0 was used. This online tool allows detecting KEGG pathways by mapping target genes. For every comparison, up to 50 significant miRNAs were analysed. DIANA-TarBase v7.0 was used to analyse gene interactions. This database contains more than half a million miRNA-gene interactions. The advantage of this database is also that every interaction is experimentally validated, which makes it the most relevant in the field. Fisher's exact test was applied for statistical pathways union meta-analysis.

4.14.4. Identification of novel ncRNAs candidates

The obtained expression signals identified in all samples (HLCs day 20, HLCs day 24 and hepatocytes) were within a certain distance were transformed to loci. Next, loci were labeled by the type of transcript and only not annotated loci remained on the list for future analysis. Loci overlapping with Nuclear insertions of mitochondrial sequences (NuMTs) were removed. The NuMTs track available for the human hg19 assembly at UCSC Table Browser was mapped to hg38 using liftOver and intersected with the loci. Then tRNAScan (Schattner, Brooks, & Lowe, 2005) was applied to recognize and remove loci coding for transfer RNA. To identify novel snoRNA candidates in the remaining loci, snoReport (Hertel, Hofacker, & Stadler, 2008) or RNAz 2.0 (Gruber, Findeiß, Washietl, Hofacker, & Stadler, 2010) was used. For each remaining locus, the conservation was checked by searching for homologous sequences in other deuterostomes species using blast (Altschul, Gish, Miller, Myers, & Lipman, 1990) with settings: E-value: 1e-3, minimal base identity: 50%, minimal score: 60 and minimal length of query: 50%. Found homologous were used as queries in the subsequent blast search in the next species. Repetitive loci (having more than 100 accepted blast hits in a species) were rejected from the further comparative analysis. Alignments containing all found homologous sequences were computed with MUSCLE (Edgar, 2004). Consensus secondary structures were computed using RNAlifold (Bernhart, Hofacker, Will, Gruber, & Stadler, 2008) under emacs RALEE mode (Griffiths-Jones, 2005). To identify snoRNA sequences that have not been recognised by snoReport, first putative box motifs were identified using position weight matrices of the snoRNA boxes C, D, C', D', H, and ACA constructed from all annotated human snoRNAs (Jorjani et al., 2016). If a sequence harbors motifs C and D, or H and HACA in correct order and distance, the sequence was next checked for its ability to fold into the typical snoRNA secondary structure using RNAfold (Bernhart, Hofacker, Will, Gruber, & Stadler, 2008). For sequences identified as putative snoRNAs in this manner, homologs were search using the SnoStrip pepline (Bartschat, Kehr, Tafer, Stadler, & Hertel, 2013).

5. Results

5.1. Generation of iPSCs using episomal vectors

To generate a new iPSCs line, non-viral and non-integrating episomal vectors were used. To make transfection easy and accessible, a lipotransfection agent was applied. This method is commonly practiced worldwide in order to transfect many types of cells. Plasmids oriP/EBNA1 (Epstein–Barr nuclear antigen-1)-based episomal vectors (Yu et al., 2009) were purchased from System Biosciences. The plasmid expression system contains well-known genes for reprogramming: transcription factors – Oct4, Sox2, Klf4, L-myc, Lin28. This, together with a cluster of miRNA – miR302/367, which can reprogram cells alone, and shRNA-p53 for the inhibition of potential reprogramming caused apoptosis. This system is also provided with the reporter gene GFP to allow for the fast and non-invasive verification of transfection efficiency. This system supports reprogramming with 0,1 % efficiency when 30% of cells were positive for GFP.

5.1.1. Cell transfection

Human fibroblasts isolated from a 6-year-old boy were transfected in order to obtain a new iPSCs line (Fig.6). Cells were divided into three groups: transfected 1, 2, or 3 times (every second day). Plasmids for transfection contains a GFP gene that allows tracking the efficiency and plasmid degradation. Therefore, cells after lipotransfection were inspected for fluorescence marker expression. Representative images of the transfected cells are shown from day 7 and 14 of reprogramming (Fig. 7.A and 7.B). The efficiency of transfection was estimated at 30% of initial seeding density. During the process of reprogramming, cells expanded notably. There was no visual evidence for cell cytotoxicity after transfection.

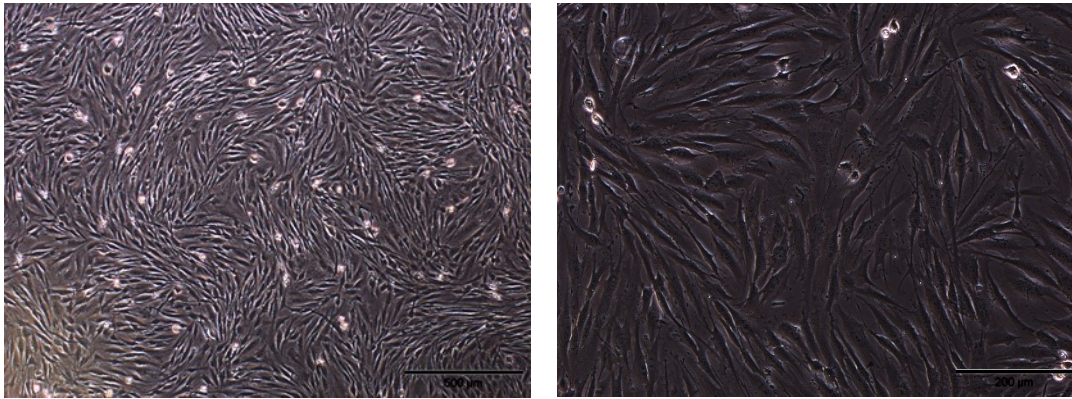


Figure 6 Morphology of fibroblasts on day 0 of reprogramming.

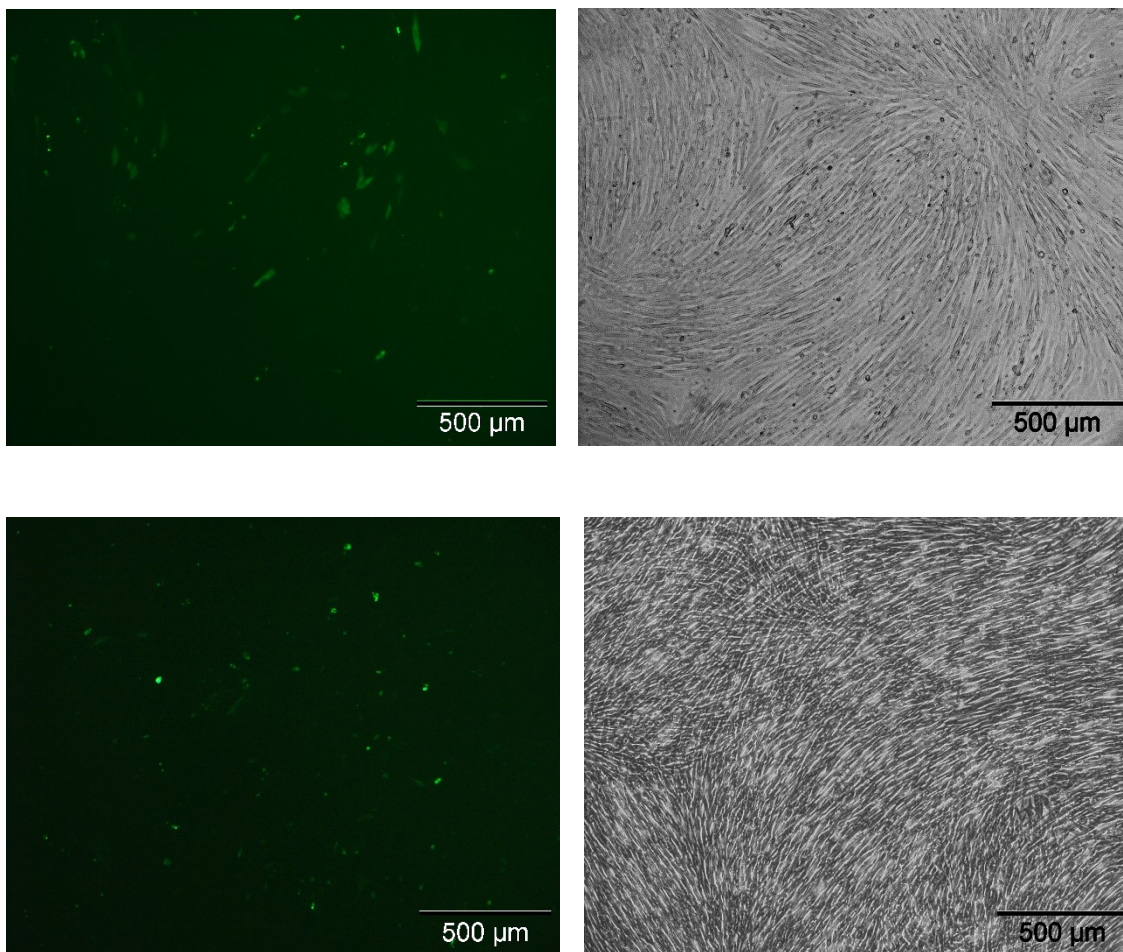


Figure 7 Transfection of fibroblasts with episomal vectors – efficiency on day A) 7 and B) 14.

Left image: GFP positive cells in green; right image: bright field image of the culture in the same spot. Pictures are representative of three experiments.

5.1.2. Establishment of iPSCs line

15 days after the first transfection, the medium was changed to the one suitable for pluripotent stem cells. The first iPSCs colonies appeared on day 21 (Fig. 8). They were easily distinguishable from the surrounding fibroblasts. On day 24, colonies were manually picked up and placed into a Geltrex-coated 96 wells plate, based on their morphology. The high quality iPSCs displayed colonies with defined borders that were densely packed with small round cells containing a large nuclei and tight intercellular contacts. Every colony was transferred into a separate well for clonal expansion. After 5 days in the culture, the best clones were selected and passaged for further expansion (Fig. 9). The clone selected for characterisation was derived from a group of fibroblasts transfected two times. The new iPSCs line resembled the morphology of embryonal stem cells. The GFP expression was constantly inspected in order to track the presence of the vectors. After 30 days from the first transfection, there was no evidence of GFP expression. Cells after passage 4 could be successfully frozen and thawed without morphological changes, which affirm pluripotency of these cells (Fig. 10).

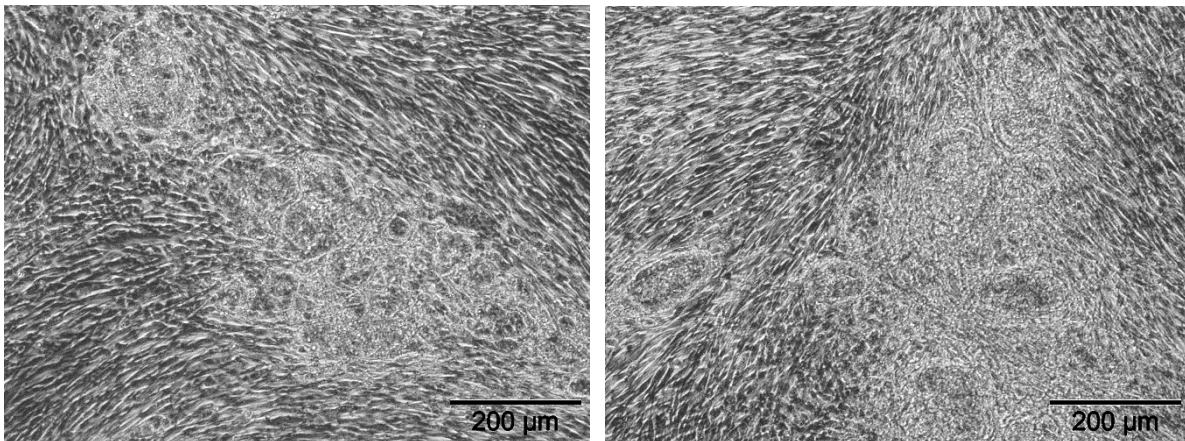


Figure 8 iPSCs appearing colonies on day 21 (left) and 23 (right).

Original magnification x100, representative images of three experiments.

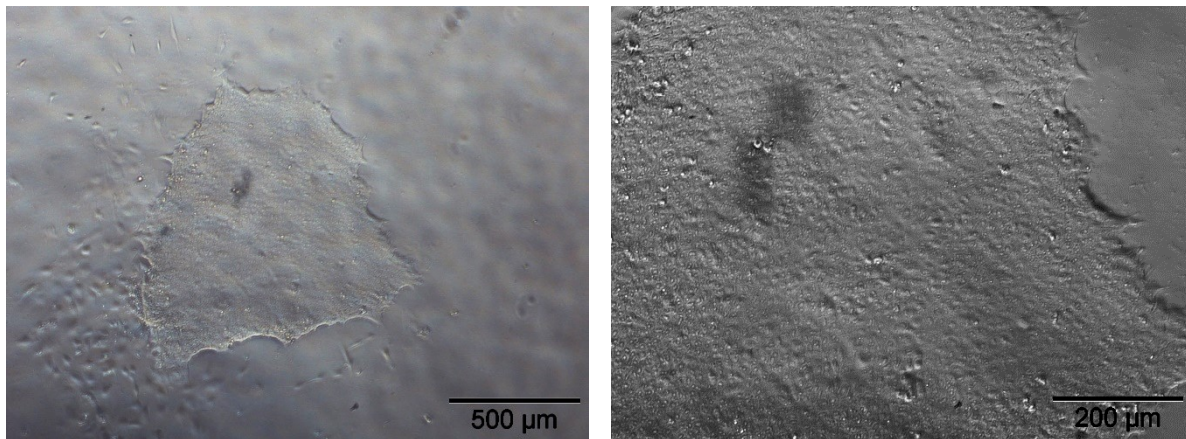


Figure 9 iPSCs colony chosen for future expansion.

Representative images of clone chosen for expansion.

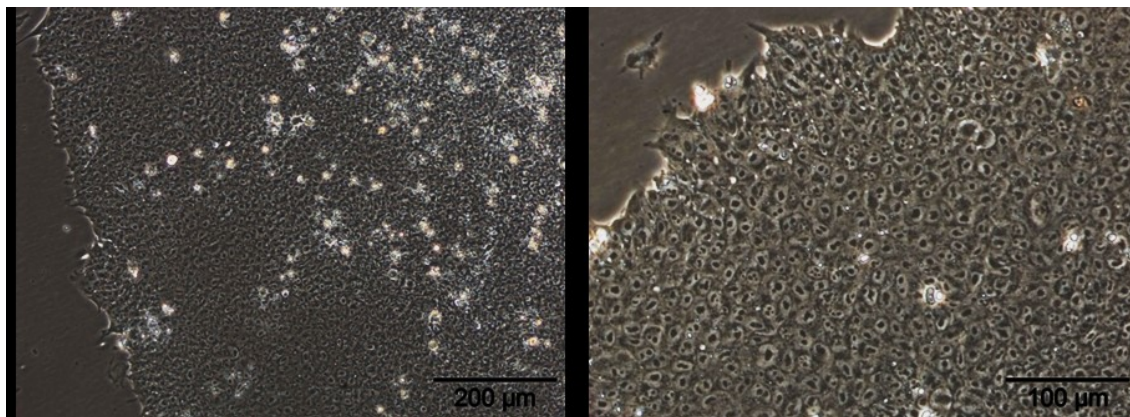


Figure 10 Morphology of iPSCs in the culture after cryopreservation.

Pictures are representative of three independent experiments.

5.2. Pluripotency characterisation of the iPSCs

5.2.1. Pluripotency markers

To confirm the expression of pluripotency markers in newly obtained iPSCs, cells were immunostained with the antibodies against Oct4, Nanog, Sox2, SSEA4 and Claudin6. Cells were separately stained with antibodies or as a double staining of cells at a different passage number. A commercial iPSCs line was used as a positive control. The negative control was

parental fibroblasts. The results of immunostaining showed the expression of pluripotency markers in iPSCs colonies (Fig. 11).

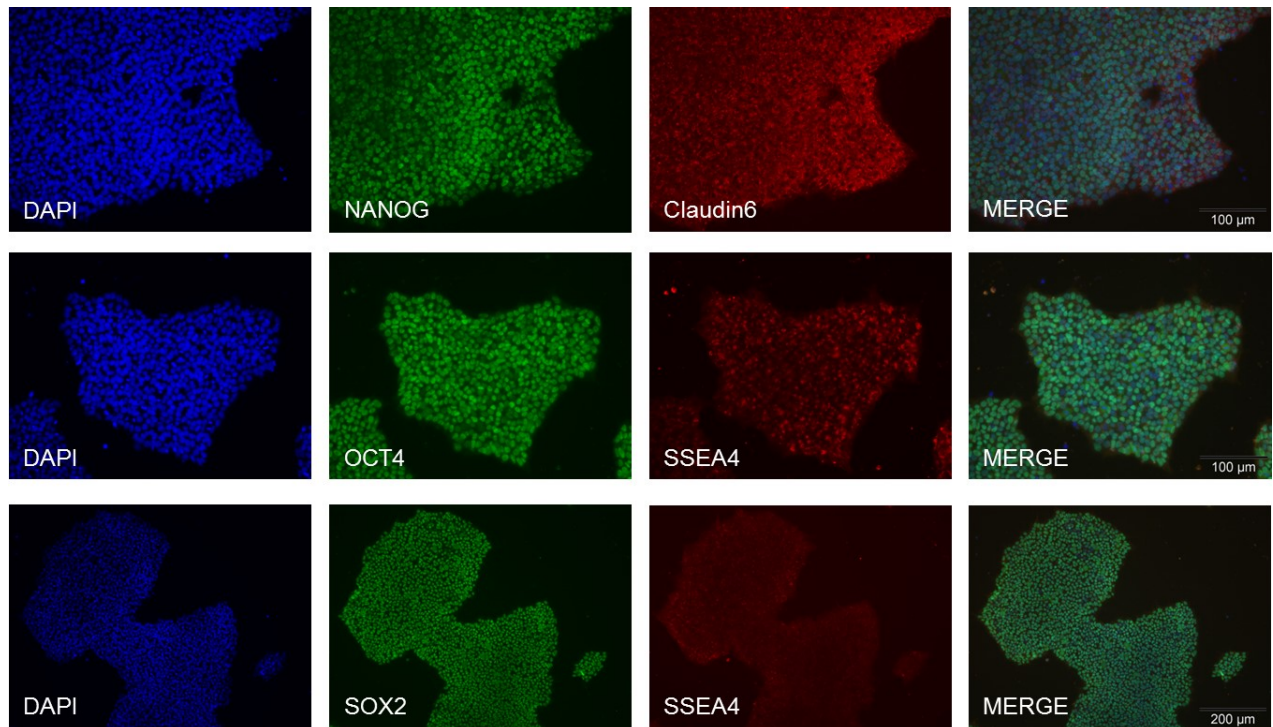


Figure 11 Immunostaining of iPSCs showing expression of pluripotency markers: OCT4, SOX2, NANOG, SSEA4 and Claudin6 (Skrzypczyk et al., 2016).

Pictures are representative of five independent experiments.

5.2.2. Spontaneous differentiation assay

In order to demonstrate the *in vitro* differentiation potential of newly generated iPSCs, spontaneous differentiation assay was performed. First, embryoid bodies were created by culturing cells in suspension without bFGF and TGF β (Fig.12). Next, cells were matured by culturing them on Geltrex-coated plates. Using *in vitro* studies, iPSCs have been shown to differentiate into every germ lineage that includes neurons and muscle cells (Fig.13). This, together with results of directed differentiation into hepatocytes, prove a pluripotent character of newly generated iPSCs.

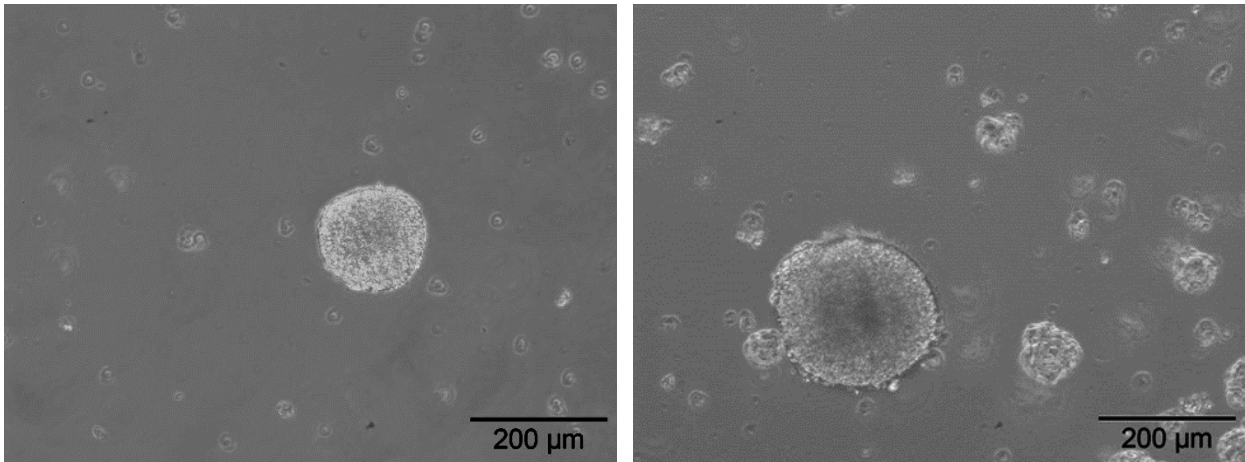


Figure 12 Embryoid bodies; left image 2 days and right image 4 days in suspension culture.

Pictures are representative of three independent experiments.

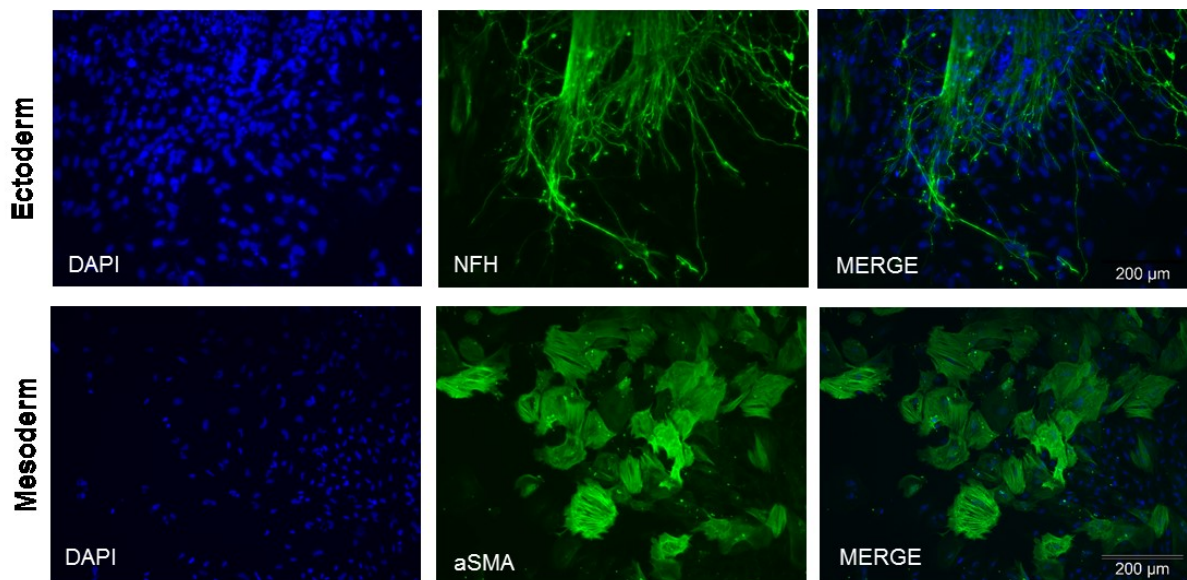


Figure 13 Differentiation potential of iPSCs (Skrzypczyk et al., 2016).

Immunocytochemical staining of in vitro spontaneous differentiation: Neurofilament heavy (NFH), smooth muscle actin (α SMA), DAPI for nucleic acid stain. Original magnification x200. Pictures are representative of three independent experiments.

5.2.3. Karyotype

To determine if chromosomal aberrations occurred during the reprogramming process, GTG-banding analysis was performed. The analysis was done by Dr. Heidrun Holland (Team Leader, Authentication, Stability, and Identity of Cells, SIKT and Faculty of Medicine at Leipzig University, Philipp- Rosenthal Str. 55, Leipzig, Germany). Seventeen metaphases were counted and three karyograms were analysed with no evidence of numerical or structural chromosomal aberrations (Fig. 14).



Figure 14 Karyogram of the iPSCs passage number 20 (Skrzypczyk et al., 2016).

5.3. Hepatic differentiation of iPSCs and HLCs characterisation

5.3.1. iPSCs hepatic differentiation

Controlled generation of hepatocytes *in vitro* is a crucial step in the advancement of iPSCs research from the laboratory to its clinical application. However, the molecular mechanisms that regulate the expression of mature liver genes remain a central challenge. Since the liver is responsible for detoxification, there is a priority to obtain cells that are capable of acquiring those functions.

In order to differentiate iPSCs into HLCs, cells were seeded into Geltrex-coated 6 well plates. The medium with cytokines was changed daily, according to the protocol (Yu et al. 2012). The differentiation of a commercial line and a new cell line proceeded similarly. During differentiation, stem cell morphology gradually changed towards the polygonal shape of hepatocytes. After 22 days of differentiation, it was possible to observe binucleated cells and the accumulation of lipid droplets (Fig. 15). To obtain images of cell shape, 3D confocal microscopy imaging was applied. The cells were stained with WGA AF488-conjugated to visualise the cell membrane (Fig. 16).

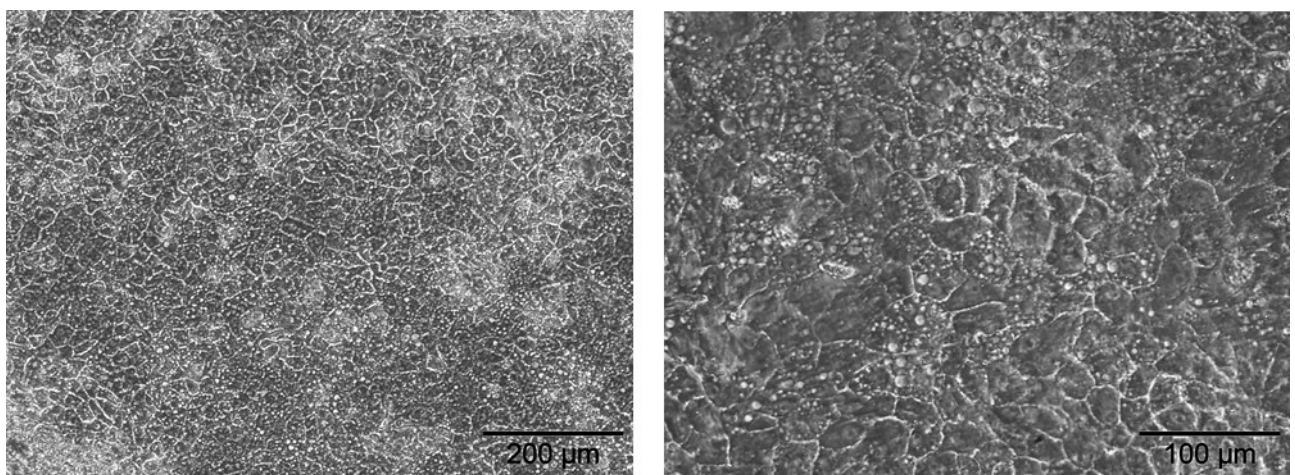


Figure 15 Morphology of HLCs obtained from differentiation of new iPSCs.

Pictures are representative of five independent experiments.

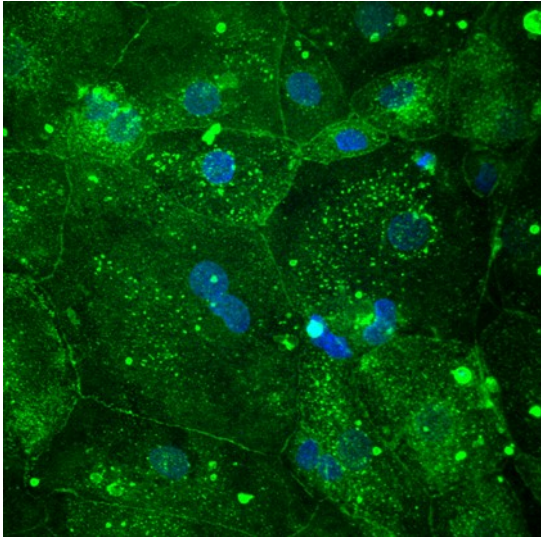


Figure 16 VEGEA confocal staining of HLCs shape.

Hepatic differentiation of commercial iPSCs. Nucleuses stained with DAPI. Magnification 400x. Pictures are representative of three independent experiments.

5.3.2. Expression of hepatic markers

To confirm the expression of hepatic markers in obtained HLCs, cells were immunostained with the antibodies against HNF4a, ALB, CK18, MRP2, and the fetal marker AFP. Hepatic marker MRP2 was detected in cells, but only locally. The HepG2 cell line was used as a positive control and fibroblasts as a negative. Cells were stained separately or with a double staining with specific antibodies. The results of immunostaining showed the expression of mature hepatic markers and the fetal marker AFP (Fig. 17).

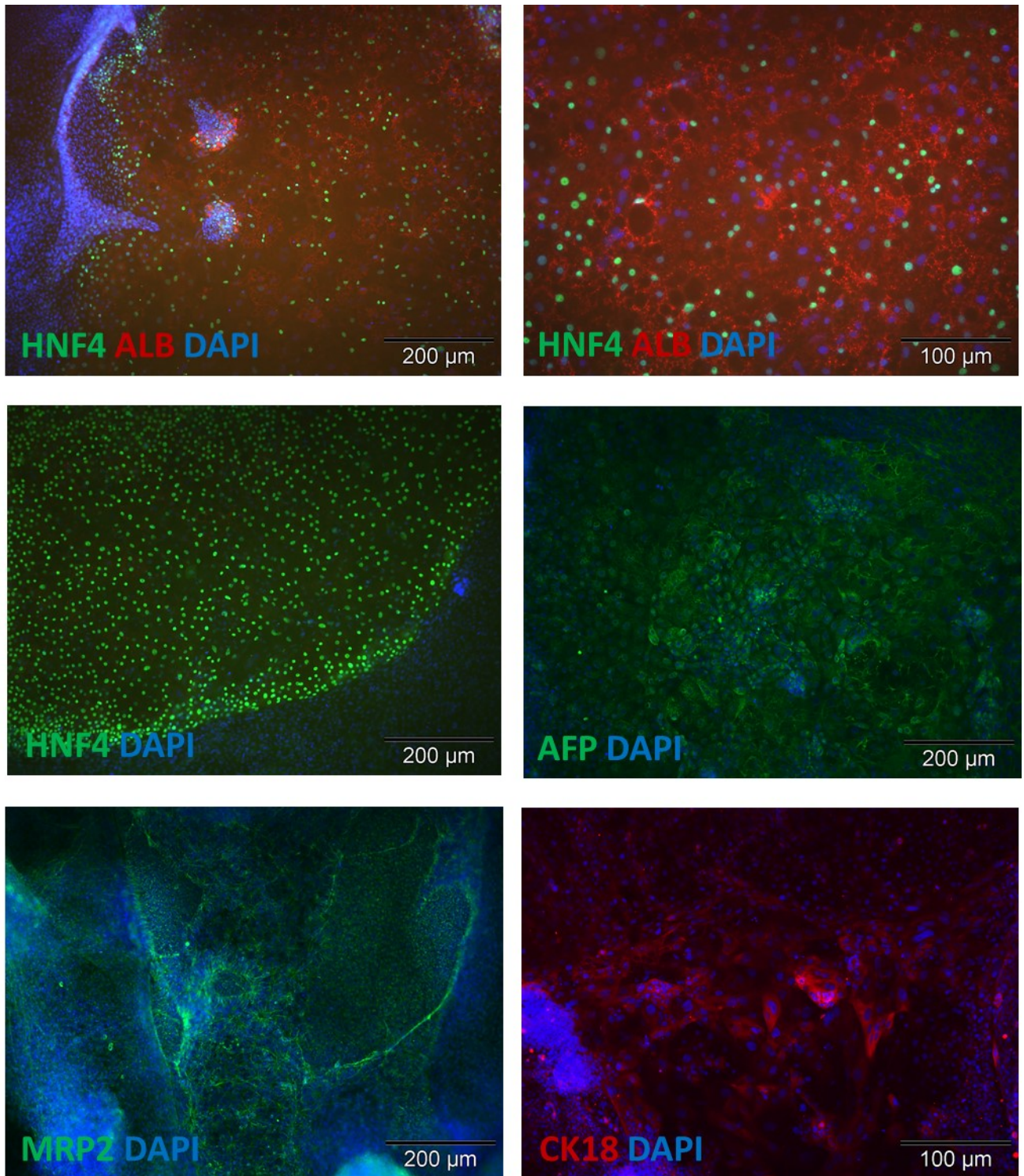


Figure 17 Expression of hepatic markers in new iPSCs-derived HLC: HNF4a, ALB, AFP, MRP2 and CK18.

Pictures are representative of three independent experiments.

5.3.3. Hepatic gene expression in HLCs

In order to confirm successful differentiation, the expression of hepatic genes was quantified using q-PCR. The RNA isolated from HLCs day 24, HepG2 cell line, frozen hepatocytes, and iPSCs were used for q-PCR. The results demonstrated that hepatocytes have the highest expression of mature hepatic genes: A1AT, HNF4a, and Albumin, as suspected (Fig. 18). HepG2 cells expressed mature hepatic genes, but in a lower level than in hepatocytes and they also expressed AFP. Tested HLCs expressed mature hepatic genes, but at a much lower level than hepatocytes. Additionally, HLCs had a high expression of fetal liver marker AFP. In a negative control for hepatic genes – iPSCs there is a lack of expression of those genes, which confirms their pluripotent character.

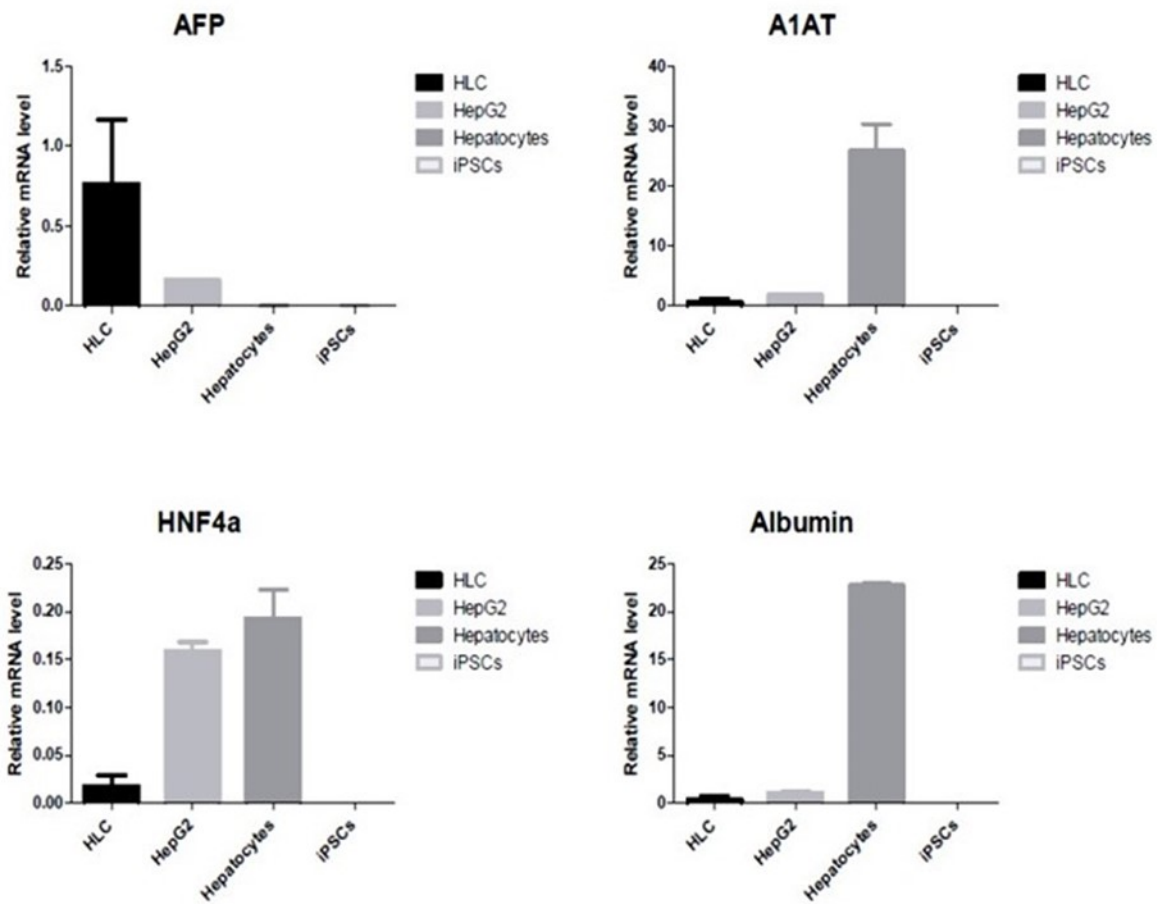


Figure 18 Quantitation of hepatic genes: AFP, A1AT, HNF4a, Albumin mRNA levels by qPCR analysis in HLCs, HepG2, hepatocytes and iPSCs.

Data shown are from three separate experiments and are normalized to PP1 gene expression; without significant changes between HLCs and HepG2 or hepatocytes.

5.3.4. Hepatic functions in HLCs

To show that cells after differentiation have a specific hepatocytes functions, PAS staining and ICG metabolism testing were done. The glycogen serves as a buffer to maintain blood-glucose levels in the body. In a functional liver, the concentration of glycogen is 10% of its weight. The glycogen forms granules in the cytosol of hepatocytes and can be detected by PAS staining (Berg, Tymoczko, & Stryer, 2002). The results of PAS staining in HLCs are shown on Figure 19. The obtained HLCs had a purple-red colour, which indicates glycogen presence in cytosol.

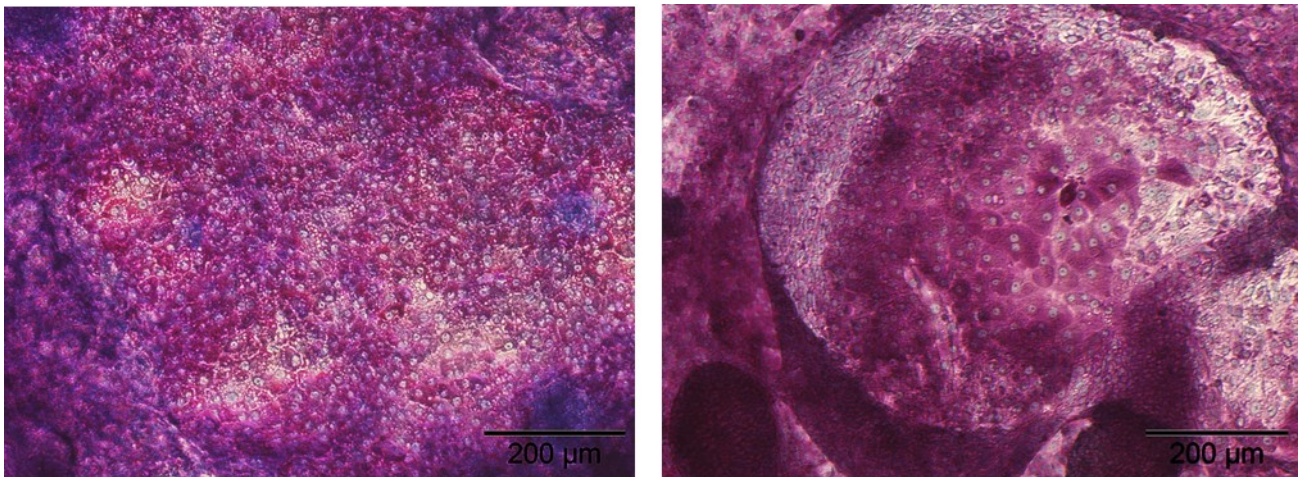


Figure 19 Representative images of PAS staining to detect glycogen storage in HLCs.

Glycogen in purple-red colour, nuclei stained by haematoxylin – dark blue. Pictures are representative of three independent experiments.

An important function of hepatocytes is detoxification. ICG testing is widely used to assess the in vitro function of iPSCs-derived HLCs. ICG is taken up exclusively by hepatocytes via the transporter organic anion transport protein OATP-C, which is also known as SLCO1B1 (Solute carrier organic anion transporter family member 1B1). This transporter is located in the basolateral membrane of hepatocytes. ICG is then actively excreted into the bile canaliculi by MRP2. The results showed that HLCs were turning green after incubation with ICG. After 6 hours, the ICG was released by the cells (Fig. 20). The green colour loss in the cells and the appearance of ICG in the culture medium was detected microscopically (Ho et al., 2012).

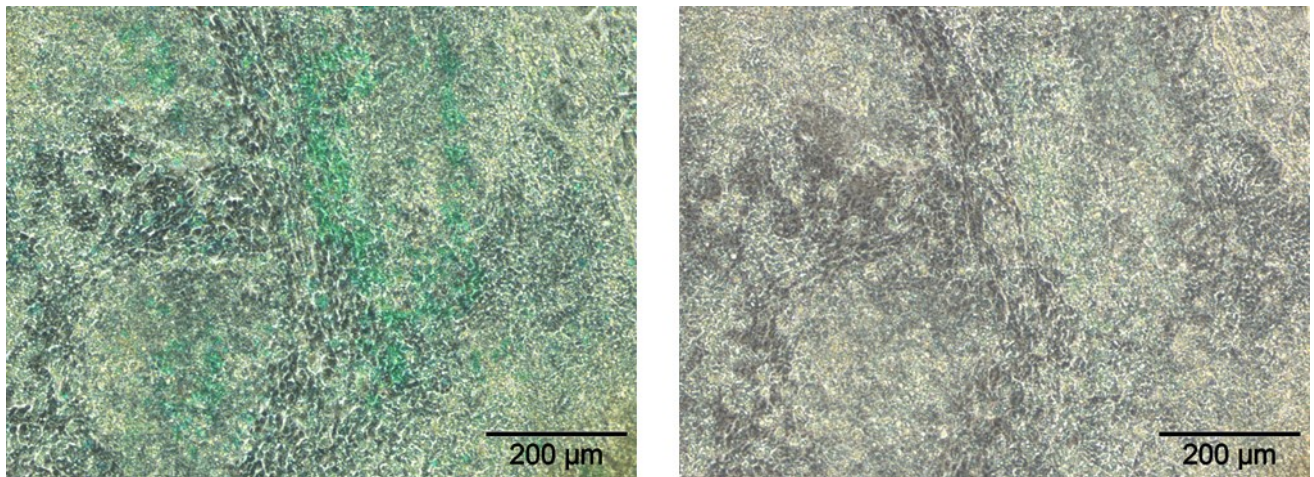


Figure 20 Representative images of ICG assay.

ICG uptake (left) and release in HLCs after 6h (right). Pictures are representative of three independent experiments.

5.4.HNF4a overexpression during differentiation

5.4.1. Cell transfection during differentiation

Commercial iPSCs were differentiated, as previously described, into HLCs. On day 7 of differentiation, using a lipotransfection agent, cells were transfected with a plasmid that contained human HNF4a gene. There was no evidence for cell cytotoxicity after transfection. The cells were immunostained with the antibodies against HNF4a and Albumin (Fig. 21). The results showed that the transfection with plasmid containing an open reading frame for the HNF4a gene, indeed caused overexpression of this transcriptional factor. The overexpression of HNF4a was visible also in the cytosol, represented locally in the cells.

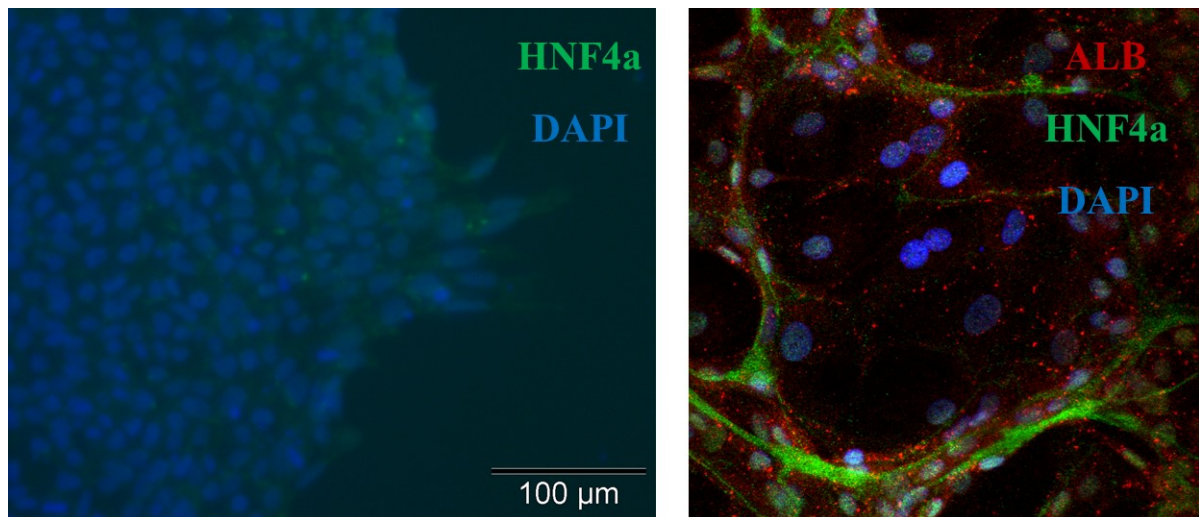


Figure 21 Overexpression of HNF4a after transfection in cells during differentiation.

Non-nuclear localisation spots. Left image - cells 48h after transfection, fluorescent microscope; right image – cells after 24 days of differentiation from confocal microscope, magnification x200. Pictures are representative of three independent experiments.

5.4.2. Comparison of hepatic differentiation efficiency

The cells during differentiation with a modified protocol behaved as previously described. Their morphology was typical for HLCs and there were no visible differences when compared to HLCs obtained with an unmodified protocol. HLCs obtained from a protocol with HNF4a overexpression were immunostained for hepatic markers as before. Results showed an expression of mature hepatic markers (HNF4a, Albumin, CK18), but also the fetal liver marker AFP (Fig. 22). Obtained HLCs were able to store glycogen and metabolise ICG, which indicates that those cells have hepatic functions (Fig. 23). There were no visible differences between standard protocol and with HNF4a overexpression in the hepatic marker expression and functions.

To compare protocols based on hepatic gene expression, q-PCR of RNA isolated from HLCs with overexpression was performed (Fig. 24). The results showed that protocol with plasmid transfection produced HLCs with lower hepatic gene expression, which can indicate that HNF4a overexpression is not sufficient for improving hepatic differentiation of iPSCs.

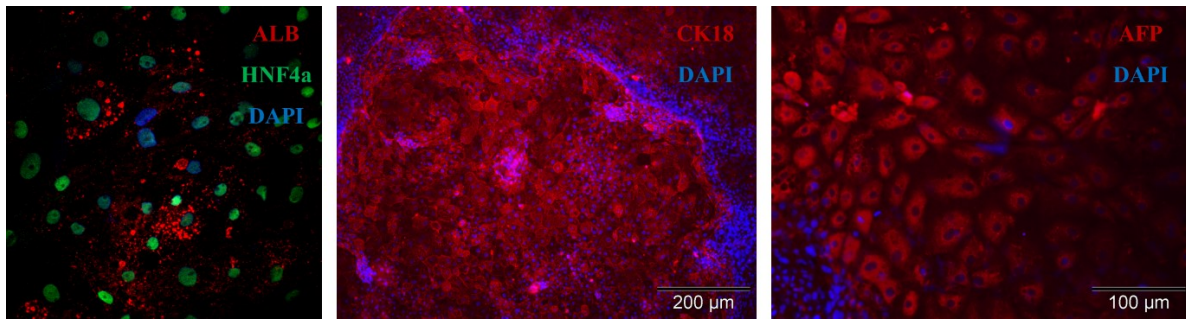


Figure 22 Expression of hepatic markers in HLCs obtained with HNF4a overexpression.

HNF4a and ALB confocal image magnification x200; AFP, CK18 fluorescence microscope images. Nucleuses stained with DAPI. Pictures are representative of three independent experiments.

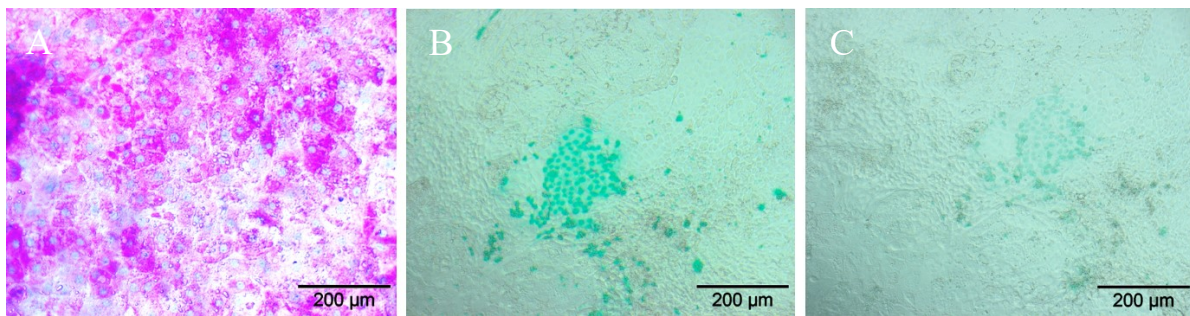


Figure 23 Representative images of hepatic functions in HLCs obtained with overexpression of HNF4a; A) PAS staining, B) ICG uptake; C) ICG release after 6h.

Glycogen in purple-red colour, nucleuses stained by haematoxylin – dark blue. Green colour in cells indicates ICG metabolism. Pictures are representative of three independent experiments.

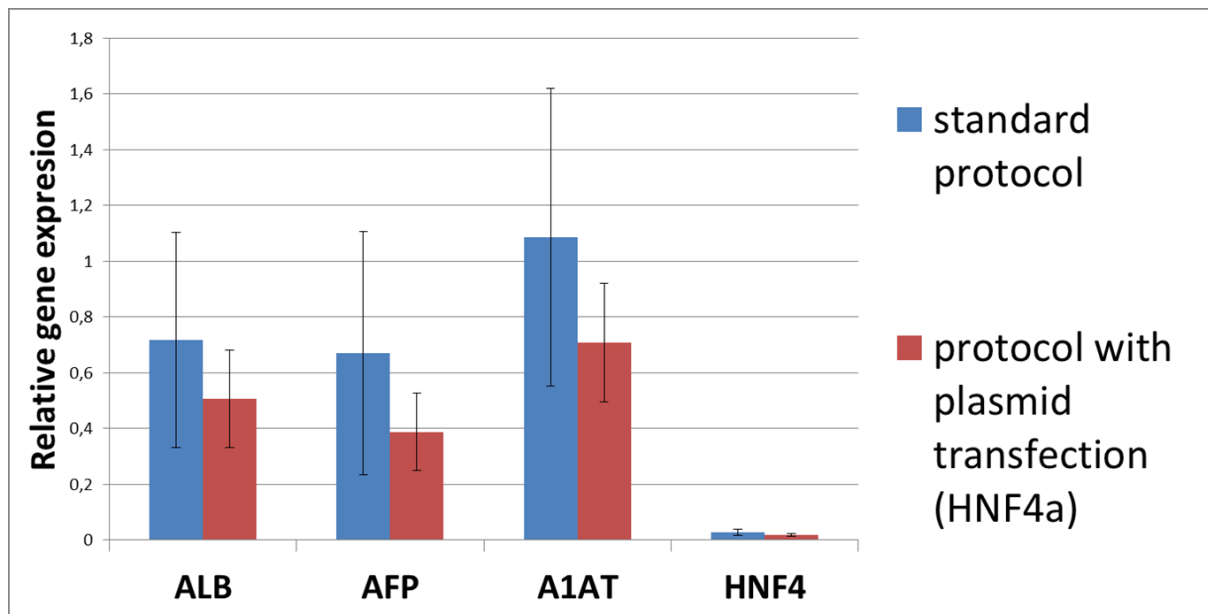


Figure 24 Comparison of the hepatic differentiation protocols by qPCR results.

Hepatic gene expression in HLCs; results from three independent experiments, without significant changes.

5.4.3. Whole slide scanning

To evaluate the efficiency of differentiation by using different protocols, the entire slides with cells were scanned to create virtual slides. To detect truly differentiated HLCs, cells were first differentiated inside slides and then stained for the presence of mature hepatic markers: HNF4a and Albumin. Slides were then scanned to visualise areas of double positive cells for hepatic markers. The virtual slides were created in collaboration with Heidelberg University (Fig. 25). Using an image analysis, the area of double positive HLCs were calculated and compared after two protocols (Fig. 26). The results indicate that the efficiency of hepatic differentiation was 30% of the area of cultivated cells. However, the AFP positive cells cover the slide in almost 90% of the area (visual observations, data not shown). Protocol with HNF4a overexpression produced comparable numbers of HLCs which demonstrates that this approach is not sufficient to improve hepatic differentiation of iPSCs.

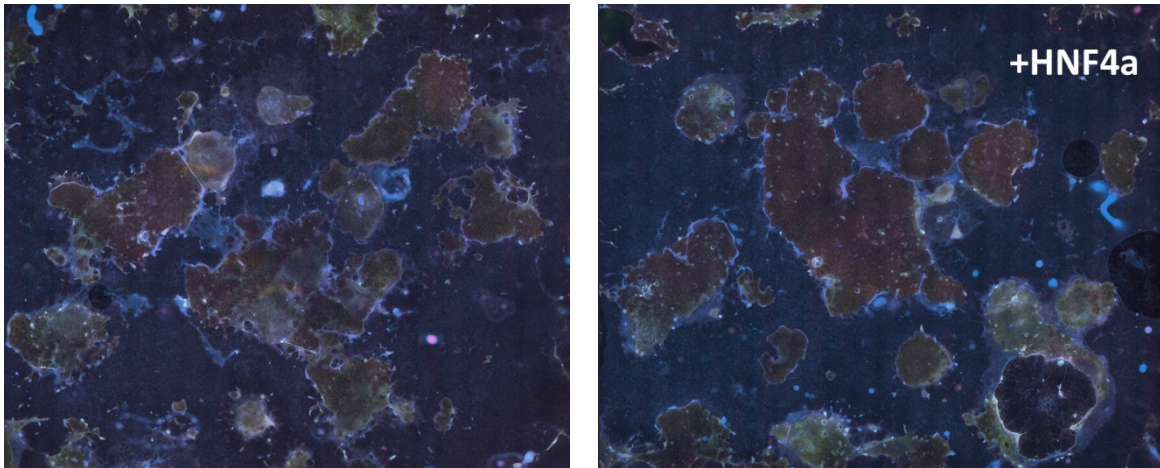


Figure 25 Representative virtual slide.

The whole area of one well from each of slides/protocols as a virtual slide; separate pictures with magnification x400 were combined to create virtual slide in order to calculate efficiency of the whole differentiation area; chromatin DAPI – blue, Albumin – red, HNF4a – green.

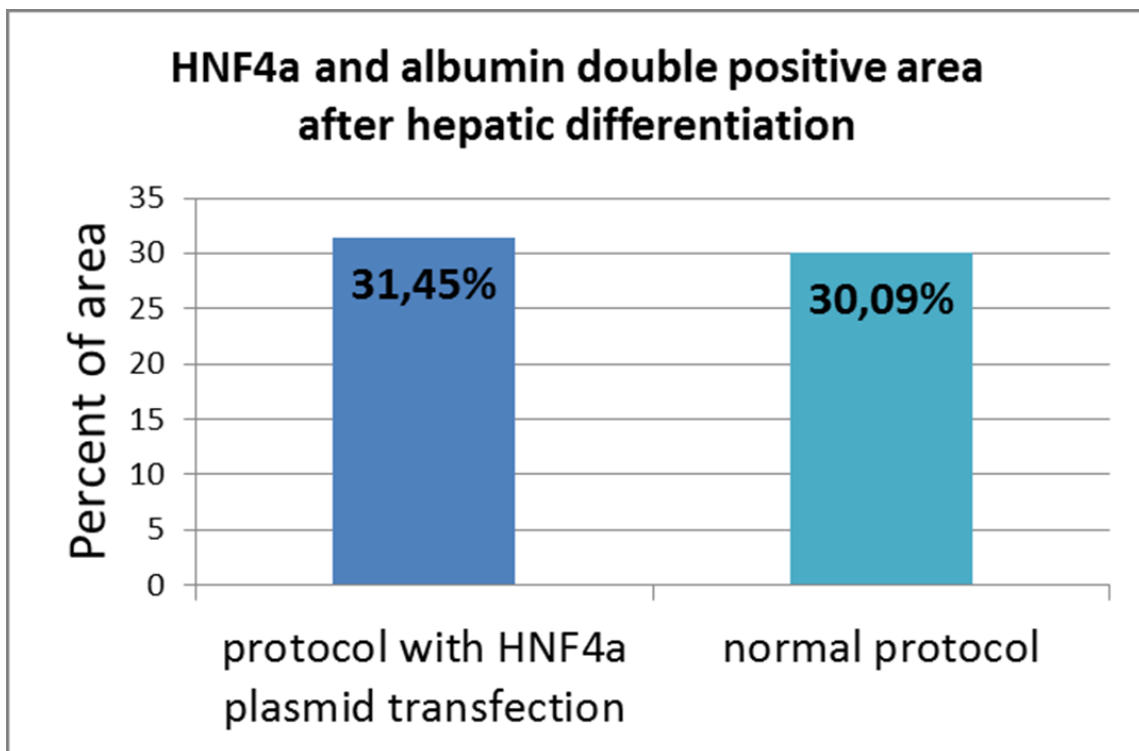


Figure 26 Image analysis of slides after scanning.

Percent of the area with colocalization of HNF4a and Alb expression in HLCs (two wells slide for each protocol); no significant difference.

5.5. Non-coding RNA analysis

5.5.1. Non-coding RNA sequencing quality

The quality of sequencing was analysed by FastQC software (chapter 4.14.1). In brief, there were no deviations from the standard Illumina sequencing. The RNA sequencing resulted in reads between 8.3 M and 25.2 M. 73% to 80% of the reads were longer than 17 nucleotides after adapter clipping. Most of the obtained clipped sequences (92% to 94%) were successfully mapped (Fig. 27). Between 345k and 1.45 M reads were identified as miRNA, while as snoRNA – between 4.14 M and 11.9 M reads (Fig. 28). Around 15% of the reads that were identified as a snoRNA contained adapter sequences. Those reads were up to 20 nt long (referred as short snoRNA reads). Among the sequenced reads, other types of transcripts were identified, including rRNA (between 6.5% and 16.5%), snRNA, long intergenic noncoding RNAs (lincRNA, about 1%) and protein coding (between 0.6% and 7%) (Fig. 29).

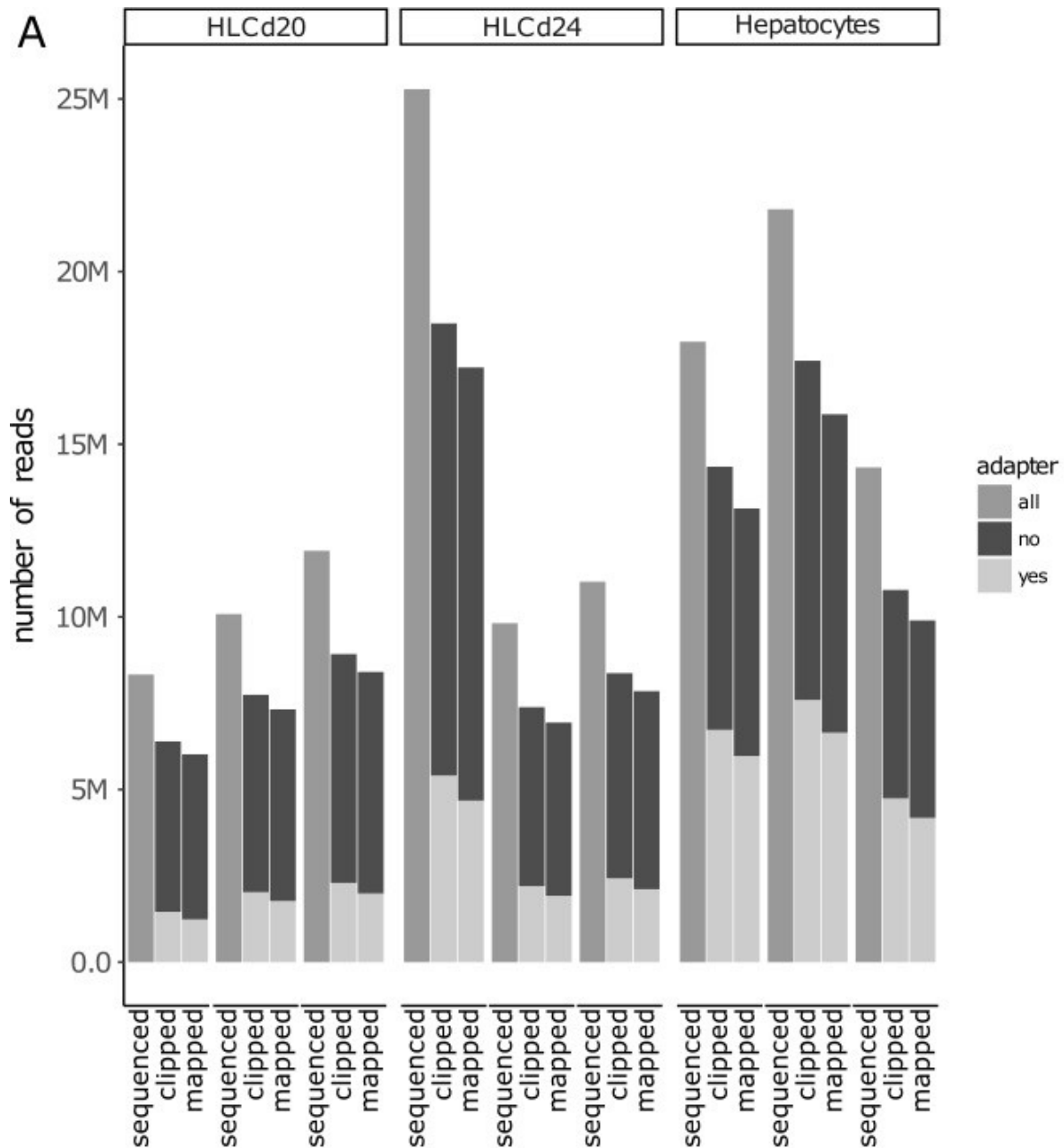


Figure 27 Total number of sequenced reads, reads after clipping and mapped reads.

“All” symbolised all reads obtained after sequencing. The bar showing clipped reads contains reads that could be processed by cutting the helper sequences. Mapped reads bar show reads aligned to a reference genome. Clipped and mapped reads are divided into reads containing an adapter (length below 50 nt) and reads that do not contain an adapter (length ≥ 50 nt).

HLCd20, HLCd24 shows reads from HLCs day 20 and day 24 of differentiation respectively, in comparison to reads from hepatocytes (Skrzypczyk et al., 2017, manuscript in preparation).

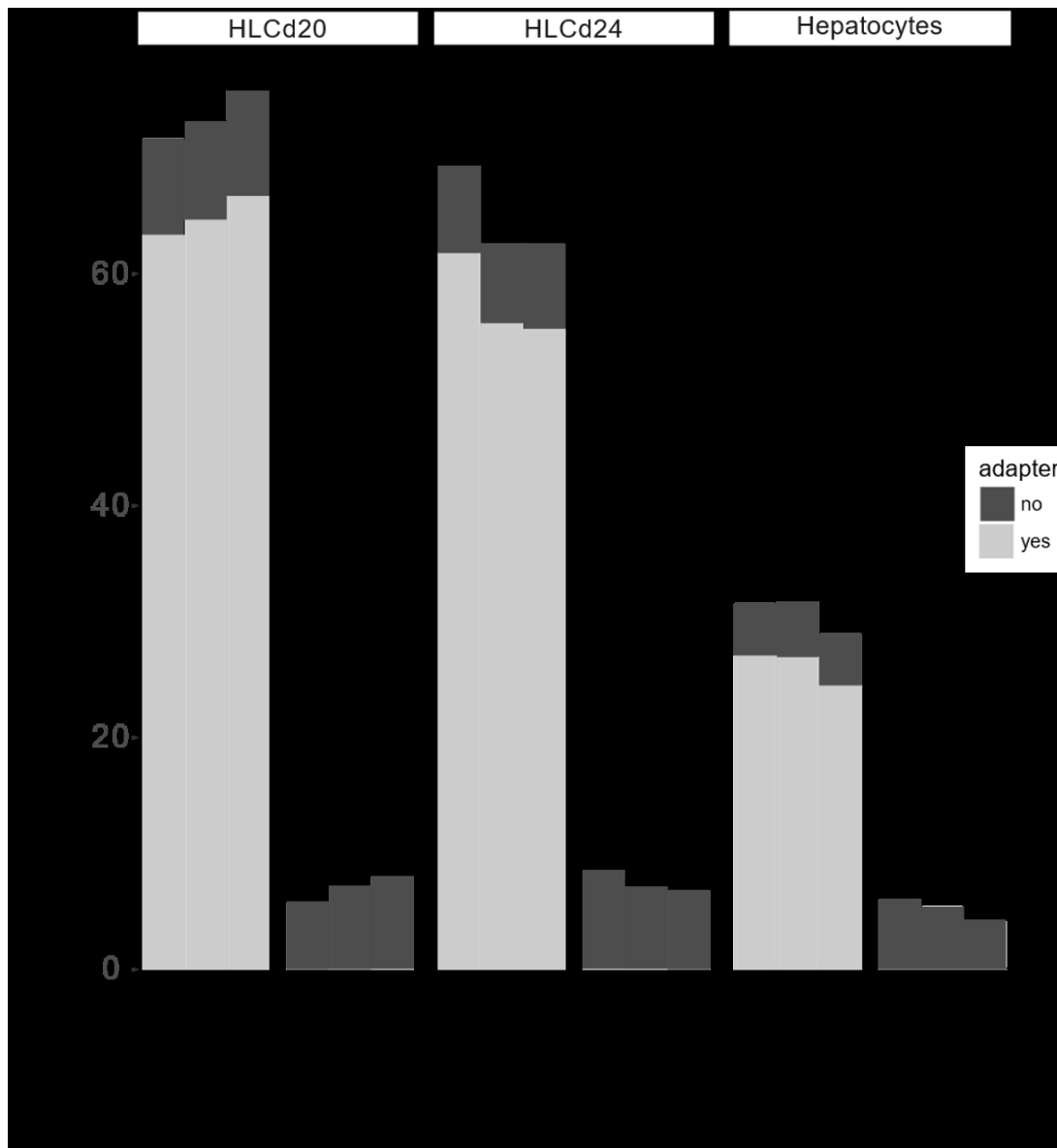


Figure 28 Percentage of mapped reads with an adapter.

Mapped reads of miRNA and snoRNA are divided into reads containing an adapter (length below 50 nt) and reads that do not contain an adapter (length ≥ 50 nt). HLCd20, HLCd24 shows reads from HLCs day 20 and day 24 of differentiation respectively, in comparison to reads from hepatocytes (Skrzypczyk et al., 2017, manuscript in preparation).

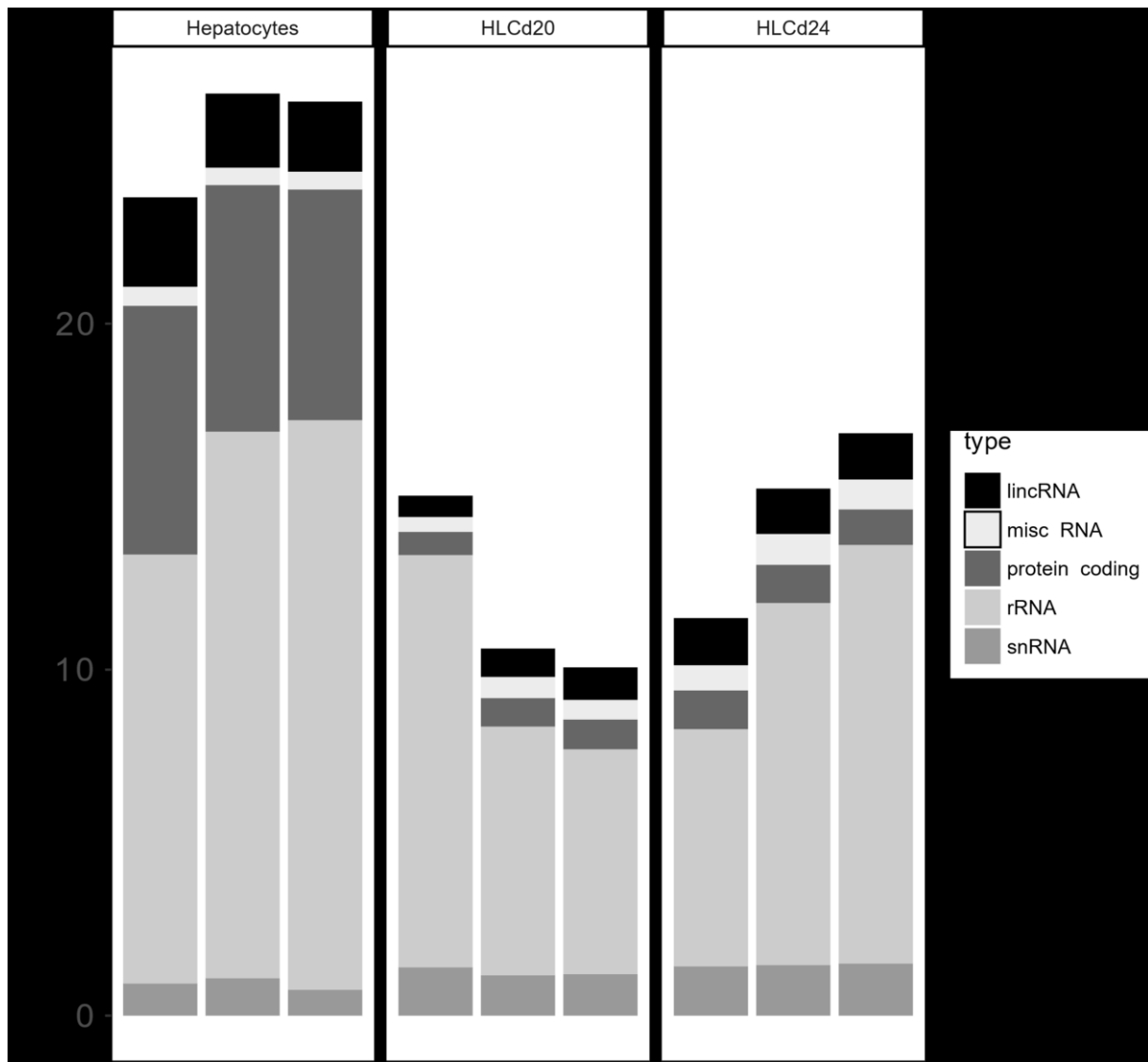


Figure 29 Percentage of different transcript types in the sequencing.

Identified ncRNA without miRNAs and snoRNAs transcripts which were successfully mapped and overlapped genome annotations. HLCd20, HLCd24 shows transcripts from HLCs day 20 and day 24 of differentiation respectively, in comparison to transcripts from hepatocytes (Skrzypczyk et al., 2017, manuscript in preparation).

To visualize the consistency between replicates and global changes between the studied samples, a hierarchical clustering of all detected ncRNA was performed (Fig.30). This revealed a strong separation between the hepatocytes and hepatic-like cells, and good homogeneity within each group.

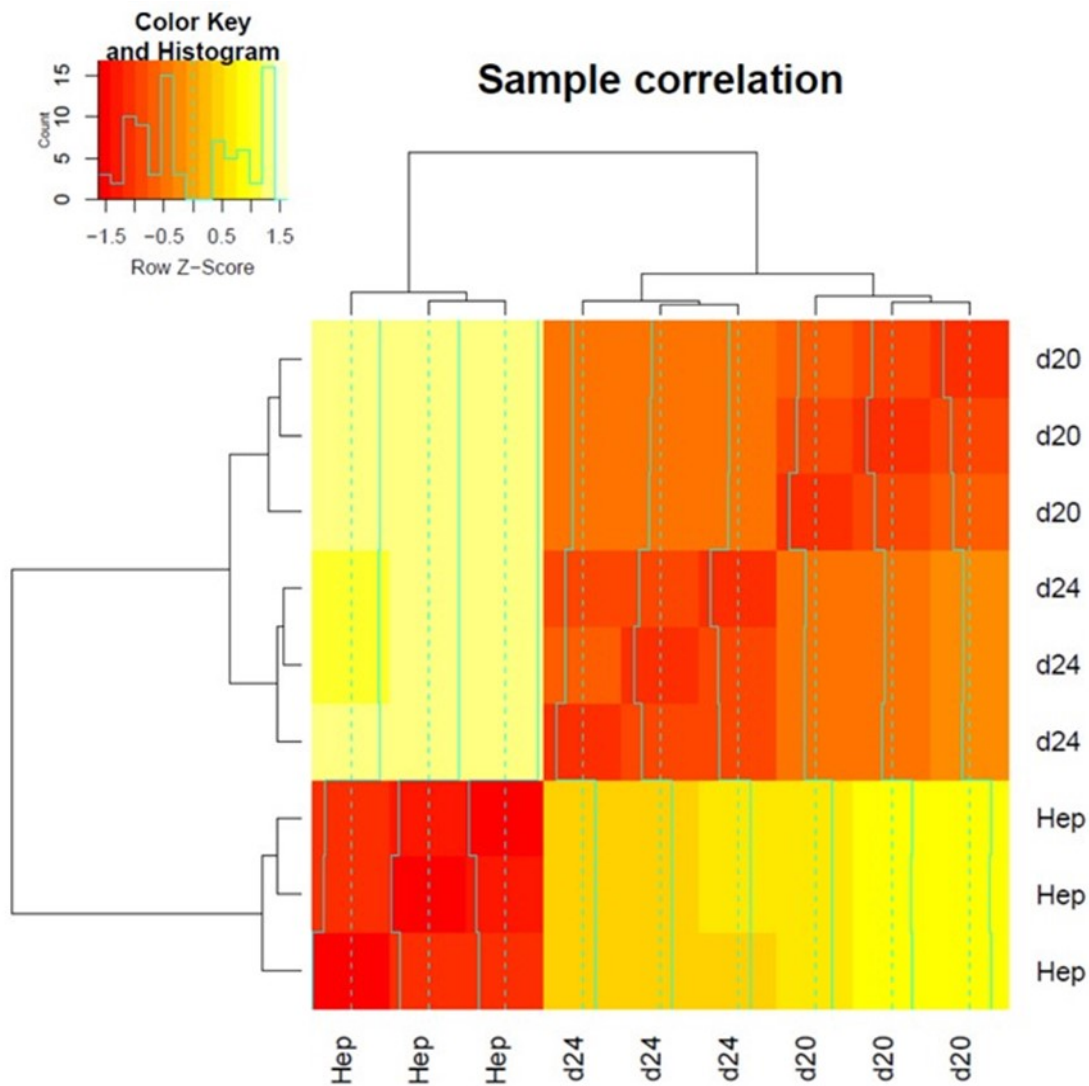


Figure 30 Cluster heat map of gene expression data.

Hierarchical clustering was generated using Euclidean measure to obtain a distance matrix and correlation coefficients of log₂- transformed expression values. The colour scale indicates the degree of correlation (white, low correlation; red, high correlation, see legend).

5.5.2. MicroRNA analysis

First, hepatic specific miRNA genes (from literature) were investigated. MiR-122-5p, miR-27b-3p, miR-23b-3p, miR-148-3p, miR-146b-5p and miR-194-5b were upregulated in hepatocytes, however their expression in the HLCs was decreased (Fig. 31). Nevertheless, upregulation of a mature hepatic miRNAs in HLCs on day 24 shows hepatic lineage

commitment during differentiation. The miRNAs which had elevated expression in the HLCs on day 24 were reported to be specific for fetal hepatocytes: miR-23a-3p, miR-30a-5p, miR483-3p, miR-92b-3p (Fig. 32). Upregulation of the fetal liver miRNAs and lower expression of the mature liver miRNAs in HLCs shows that differentiated cells resemble a fetal characteristic, as previously described. Remarkably, a several upregulated miRNAs at the end of differentiation (day 24) indicate an epithelial phenotype of HLCs. Those miRNAs, previously described as blocking EMT, were plotted separately: EMT related (miR-200c-3p miR-200b-3p, miR-204-5p, miR-199b-3p, miR-199a-3p and miR-429, Fig. 33). The selected miRNAs: miR-21-3p, miR-21-5p, miR-214, miR-216a, were also highlighted (Fig. 34). Expression of those miRNAs has been previously shown to increase during the last stage of hepatic differentiation of embryonic stem cells (ESC). Those miRNAs are connected to PI3K signalling and hepatic differentiation.

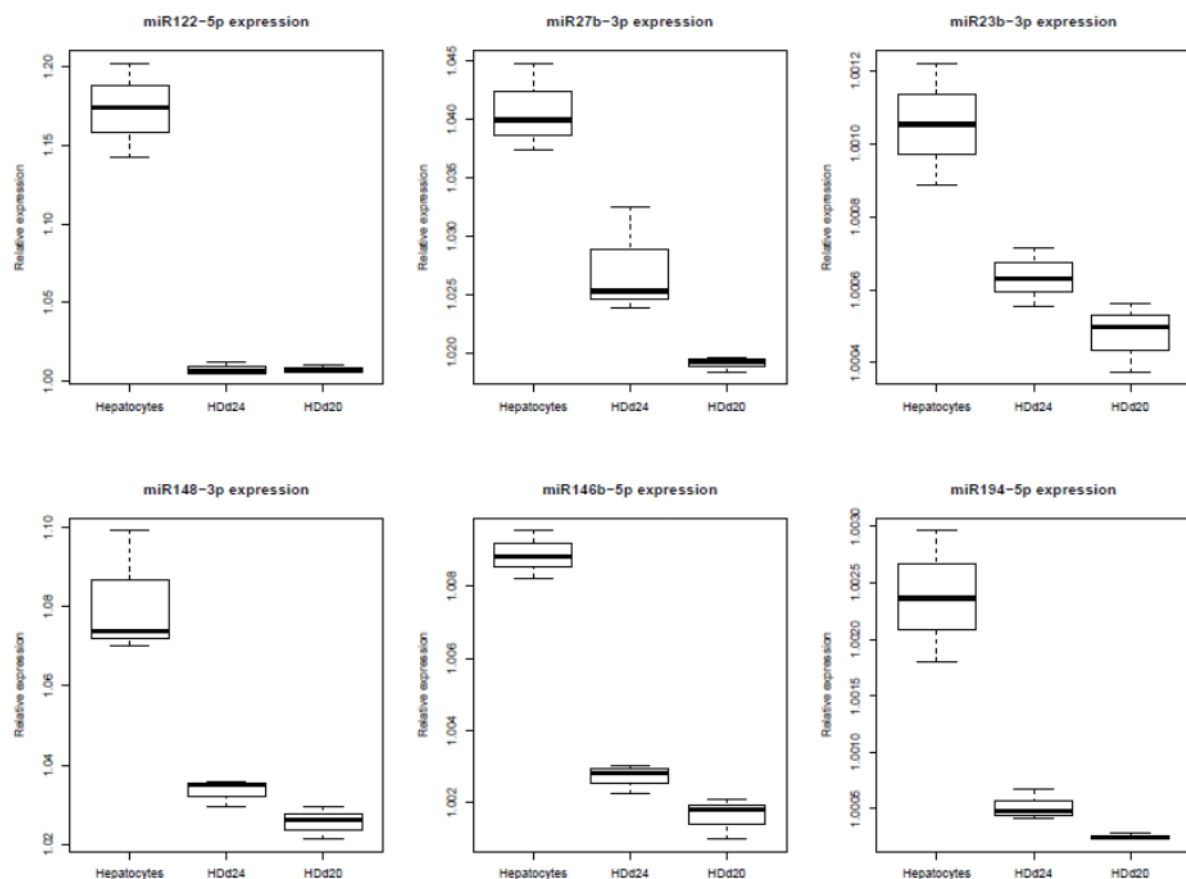


Figure 31 Expression of hepatic specific miRNAs.

MiR-122-5p, miR-27b-3p, miR-23b-3p, miR-148-3p, miR-146b-5p and miR-194-5b were upregulated in hepatocytes in comparison to HLCs at day 20 or 24 of differentiation.

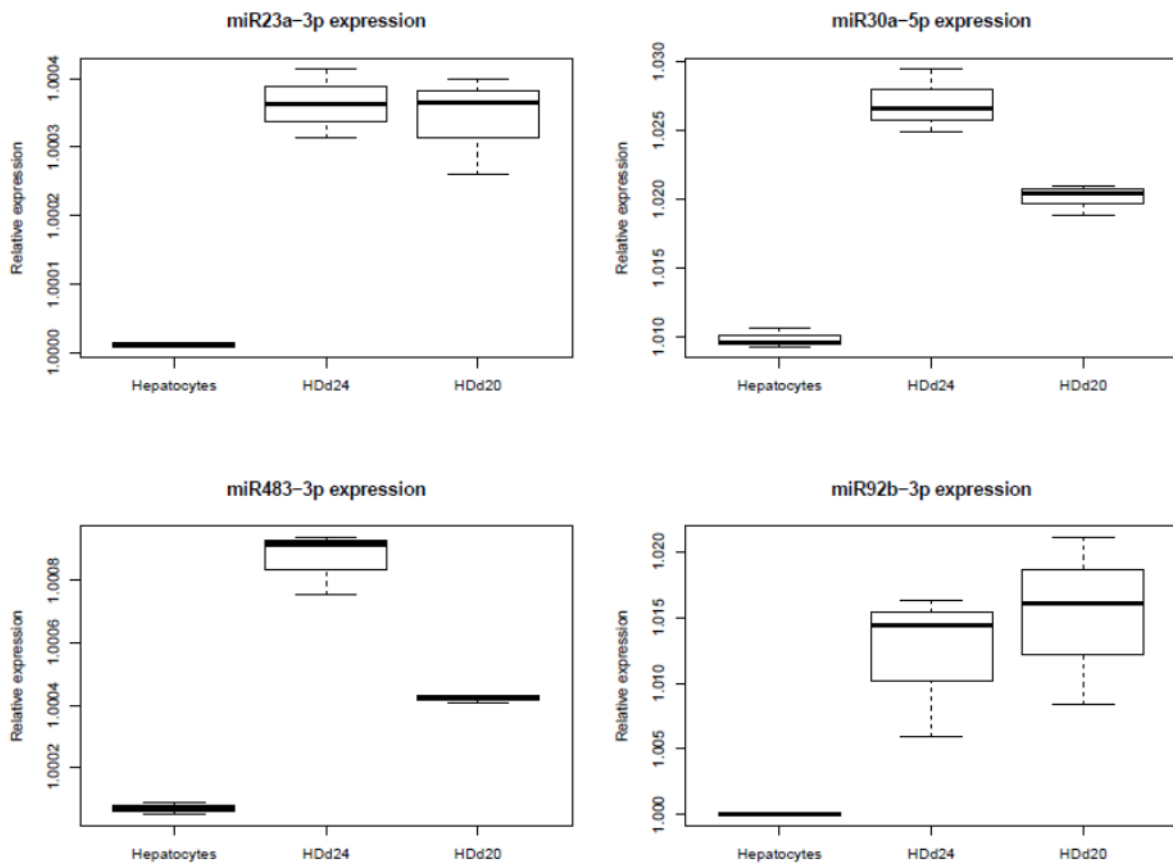


Figure 32 Expression of fetal liver miRNAs.

MiR-23a-3p, miR-30a-5p, miR483-3p, miR-92b-3p were upregulated in HLCs day 24 in comparison to hepatocytes.

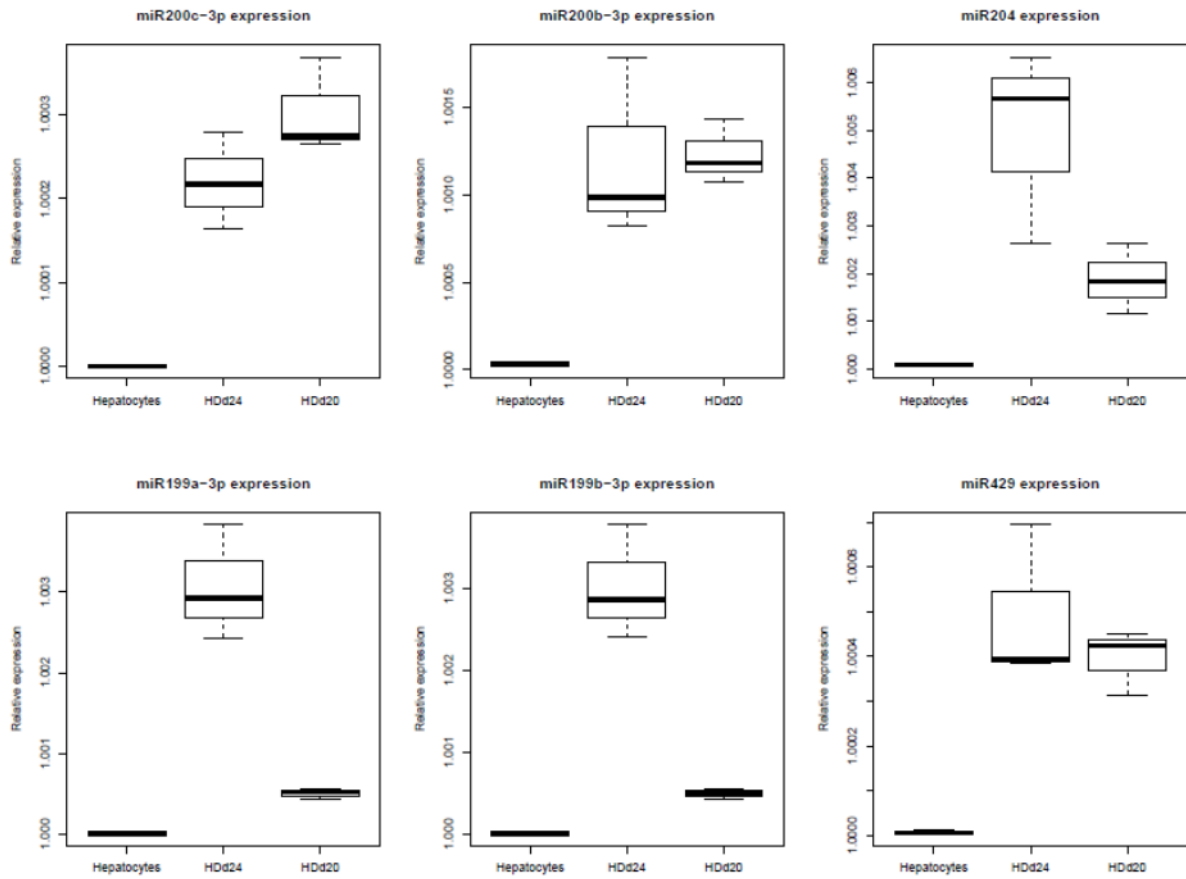


Figure 33 Expression of miRNAs related to MET.

MiR-200c-3p miR-200b-3p, miR-204-5p, miR-199b-3p, miR-199a-3p and miR-429 were upregulated in HLCs day 24 in comparison to hepatocytes.

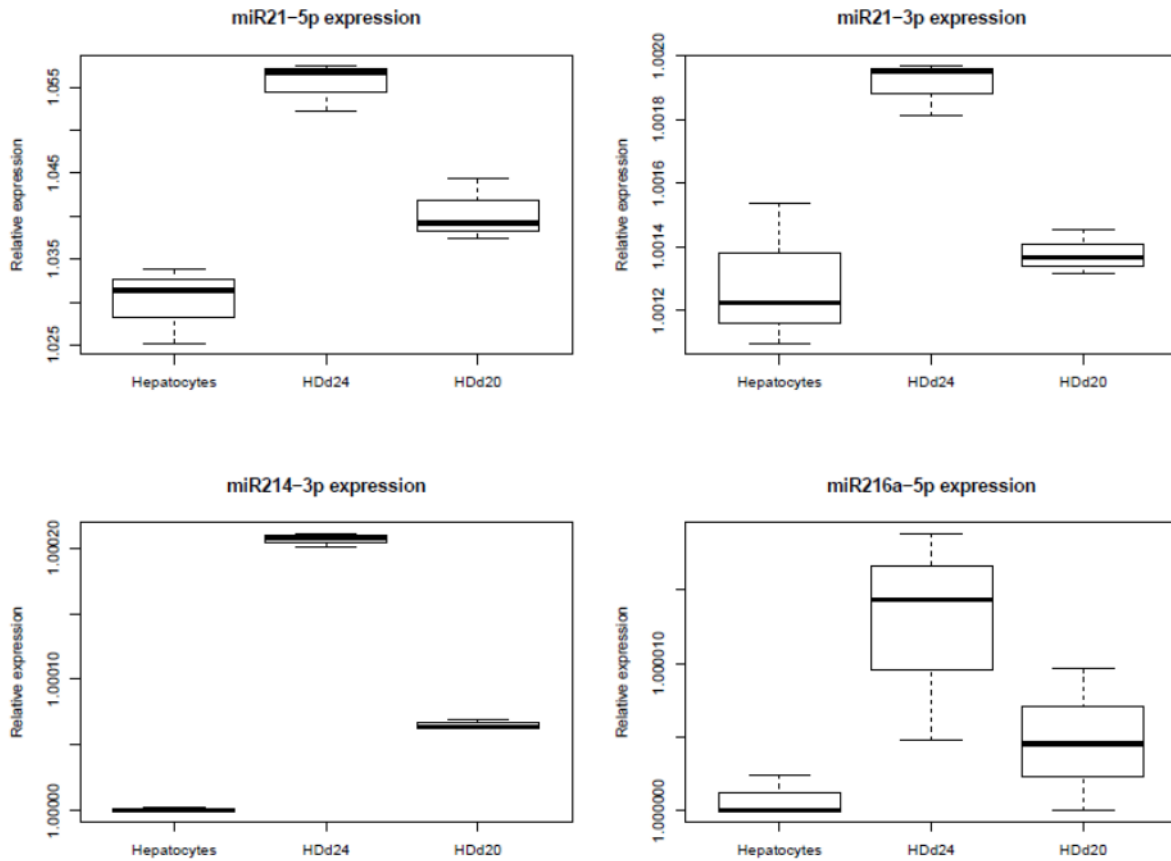


Figure 34 Expression of PI3K related miRNAs shown to be upregulated during hepatic differentiation.

MiR-21-3p, miR-21-5p, miR-214, miR-216a were upregulated in HLCs day 24 in comparison to hepatocytes and HLCs in day 20 of differentiation.

The differentially expressed miRNAs between control hepatocytes and the different stages of differentiation (day 20, day 24) were identified. Those with adjusted low-p values (FDR) and with high fold changes at the same time are marked and visualized in the volcano plots (Fig. 35, 36 and 37). MiRNAs expression changed during hepatic differentiation. Briefly, 14 differentially expressed miRNAs with a threshold of $FDR > 0.05$ were identified. 5 miRNAs were downregulated in HLCs day 24 including miR-367, miR-302, and also miR-516 in comparison to HLCs at day 20. 19 miRNAs were upregulated: miR-199a, miR-199b, miR-211 and miR-214 in HLCs day 24 in comparison to HLCs at day 20. When compared to the hepatocytes, a greater number of miRNAs were differentially expressed. With a threshold of $FDR < 0.001$ in the HLCs day 24, 228 miRNAs were downregulated when compared to the

hepatocytes, including miR-181d, miR-199a, miR-214, miR-200c, and miR-205. 88 miRNAs were upregulated in the hepatocytes including: let-7b-5p, miR-29c, let-7f-5p, let-7g-5p miR-612, and miR-195, among others. 75% of the differentially expressed miRNAs in the hepatocytes compared with the HLCs day 24 were also differentially expressed in the hepatocytes compared with the HLCs day 20. Figure 38 presents a heatmap of the 100 most differentially expressed miRNAs for visualisation. A list of differentially expressed miRNAs is provided in the appendix.

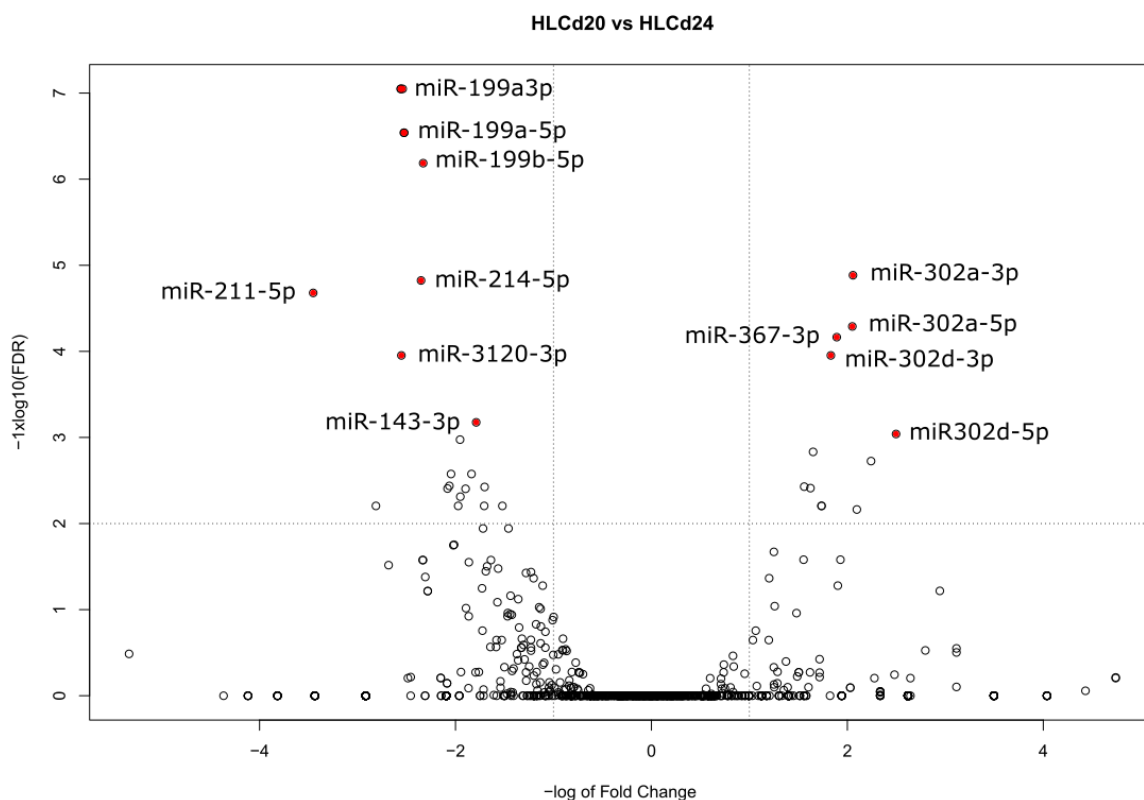


Figure 35 The volcano plot of differentially expressed miRNAs between HLCs day 20 and HLCs day 24.

The x-axis indicates a difference of expression level on a log scale, while the y-axis represents corresponding adjusted P values (FDR) on a negative log scale; statistically significant differences extends vertically. Red points indicate genes with the significance level of $FDR > 0.001$. Labels are given for the most significant differentially expressed miRNAs.

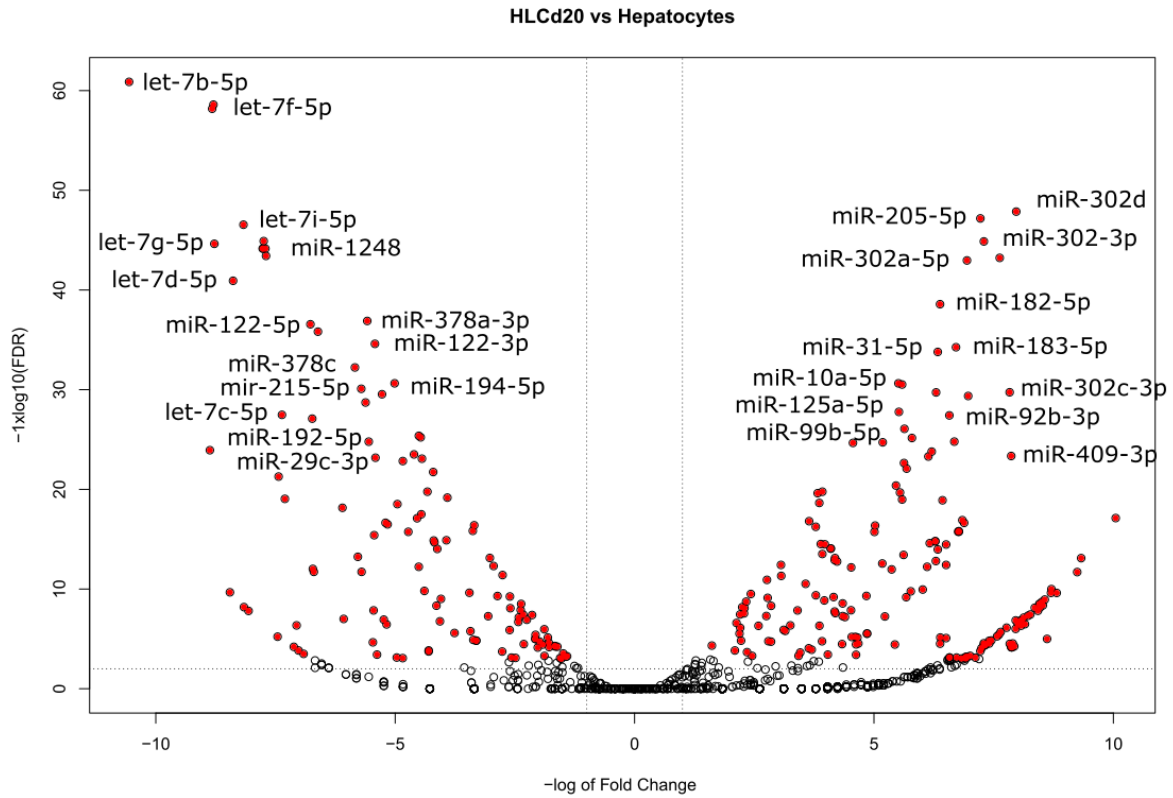


Figure 36 The volcano plot of differentially expressed miRNAs between HLCs day 20 and Hepatocytes.

The x-axis indicates a difference of expression level on a log scale, while the y-axis represents corresponding adjusted P values (FDR) on a negative log scale; statistically significant differences extends vertically. Red points indicate genes with the significance level of $FDR > 0.001$. Labels are given for the most significant differentially expressed miRNAs.

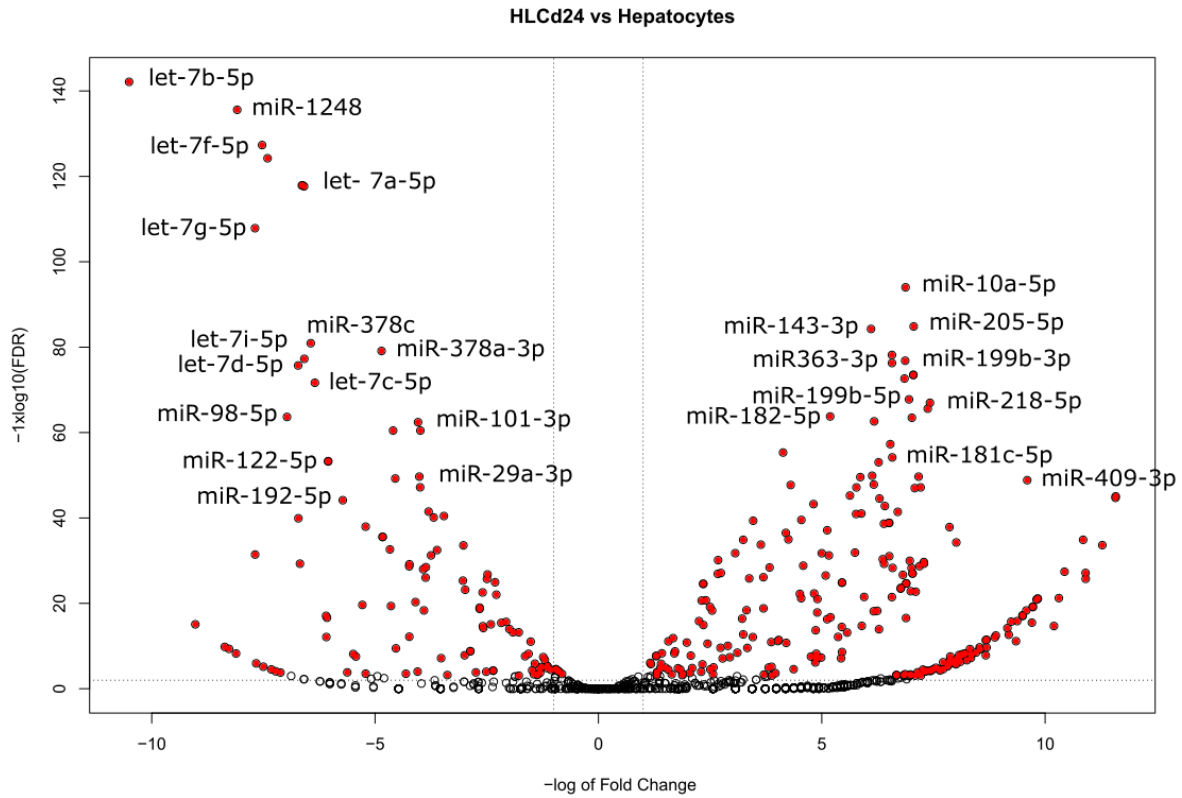


Figure 37 The volcano plot of differentially expressed miRNAs between HLCs day 24 and Hepatocytes.

The x-axis indicates a difference of expression level on a log scale, while the y-axis represents corresponding adjusted P values (FDR) on a negative log scale; statistically significant differences extends vertically. Red points indicate genes with the significance level of $\text{FDR} > 0.001$. Labels are given for the most significant differentially expressed miRNAs.

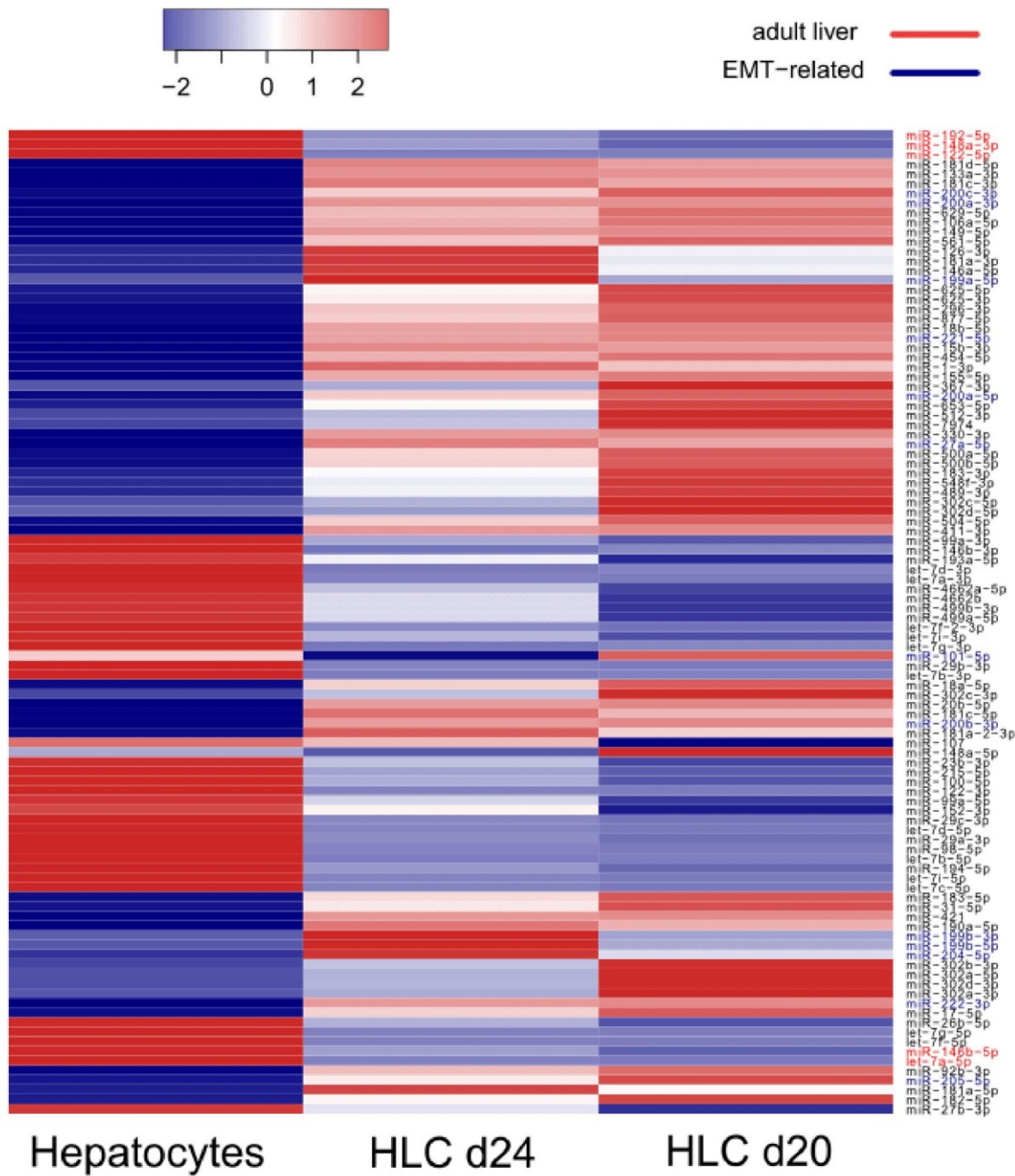


Figure 38 Heatmap showing the differentially expressed miRNAs.

Differentially expressed miRNAs are represented in shades of blue (decreased expression) and red (increased) in HLCs day 20 (HLCd20), day 24 (HLCd24) and hepatocytes.

Additionally, mature liver and EMT related miRNAs are marked in colour.

To identify genes and pathways controlled by differentially expressed miRNAs, the DIANA-miRPath v3.0 online tool was used (Vlachos et al., 2015). A posteriori approach (pathway union) was applied to increase the stringency of the prediction. The enrichment of the KEGG gene ontology terms related to differentially expressed miRNAs target genes is presented in Table 4. The differentially expressed miRNAs at HLCs day 20 in comparison to hepatocytes are related mostly to the signalling pathways regulating the pluripotency of stem cells, since they are miRNAs which induce pluripotency. The upregulated miRNAs in HLCs day 24 are involved in fatty acid biosynthesis, ECM-receptor interaction fatty acid metabolism, proteoglycans in cancer, the Hippo signalling pathway, steroid biosynthesis, and the adherens junction. Interestingly, the steroid biosynthesis pathway is special in this comparison. The differentially expressed enriched miRNAs from HLCs compared to hepatocytes additionally control lysine degradation, prion diseases, viral carcinogenesis, pathways in cancer, and the p53 signaling pathway. The HLCs d20 genes exclusively regulate 2 further pathways: microRNAs in cancer and the cell cycle. The pathway - transcriptional misregulation in cancer is unique for miRNAs from HLC d24 in comparison to hepatocytes. The hepatic upregulated miRNAs regulate pathways typical for those cells, like Hepatitis B, endodermal cell cancers, the PI3K-Akt signaling pathway, focal adhesion, TGF-beta signaling pathway, and also the Thyroid hormone signaling pathway. Intriguingly, the FoxO signaling pathway, protein processing in the endoplasmic reticulum, and endocytosis were restricted for the differentially expressed miRNAs in hepatocytes when compared with HLC d24.

Table 4 Gene ontology categories of differentially expressed miRNAs targets (pathway union).

Comparison	KEGG pathway	p-value	#genes	#miRNAs
Differentially expressed miRNAs in HLC d24 compared to HLC d20	Fatty acid biosynthesis	0	1	2
	ECM-receptor interaction	0	10	4
	Fatty acid metabolism	5.984709e-10	2	2
	Proteoglycans in cancer	2.928118e-09	31	3
	Hippo signaling pathway	0.0001180971	13	3
	Steroid biosynthesis	0.004048092	2	2
	Adherens junction	0.01782237	11	2
	Base excision repair	0.02708153	4	2
Differentially expressed miRNAs in HLC d20 compared to HLC d24	Lysine degradation	1.389225e-08	9	2
	Chronic myeloid leukemia	0.0001602018	13	2
	Proteoglycans in cancer	0.0002270705	12	1
	Wnt signaling pathway	0.0006146658	12	1
	FoxO signaling pathway	0.003220974	18	2
	Cell cycle	0.003295535	9	1

	Pathways in cancer	0.004235095	17	1
	Progesterone-mediated oocyte maturation	0.03364343	8	1
	Oocyte meiosis	0.03398087	5	1
	Signaling pathways regulating pluripotency of stem cells	0.05899564	9	1
Differentially expressed miRNAs in HLC d20 compared to hepatocytes	Fatty acid biosynthesis	0	4	4
	ECM-receptor interaction	0	29	10
	Lysine degradation	0	26	17
	Proteoglycans in cancer	0	115	18
	MicroRNAs in cancer	2.065015e-14	55	3
	Adherens junction	1.92849e-10	56	14
	Fatty acid metabolism	2.435736e-07	12	5
	Hippo signaling pathway	2.854731e-07	76	15
	Prion diseases	3.567319e-07	2	1
	Viral carcinogenesis	4.563306e-07	90	10
	Pathways in cancer	7.078609e-05	155	11
	Cell cycle	0.0002485214	62	9
	p53 signaling pathway	0.02762094	42	10
	Transcriptional misregulation in cancer	0.02815897	70	8
Differentially expressed miRNAs in hepatocytes compared to HLC d20	Fatty acid biosynthesis	0	4	7
	ECM-receptor interaction	0	39	15
	Lysine degradation	0	26	17
	Cell cycle	0	92	17
	Viral carcinogenesis	0	129	19
	Hippo signaling pathway	0	92	23
	Proteoglycans in cancer	0	140	23
	Pathways in cancer	1.110223e-16	235	20
	Adherens junction	8.881784e-16	59	20
	Hepatitis B	3.774758e-15	83	13
	Chronic myeloid leukemia	3.940404e-12	54	18
	Colorectal cancer	3.432521e-11	43	17
	Glioma	9.944934e-11	43	15
	Fatty acid metabolism	1.771966e-06	14	8
	p53 signaling pathway	2.456315e-06	47	16
	Small cell lung cancer	8.452771e-06	57	14
	Oocyte meiosis	1.56543e-05	65	12
	Thyroid hormone signaling pathway	2.996244e-05	64	11
	Steroid biosynthesis	8.629469e-05	7	12
	Prostate cancer	0.0004910115	65	13
	PI3K-Akt signaling pathway	0.001506451	118	10
	Focal adhesion	0.001709285	81	9
	TGF-beta signaling pathway	0.004683835	48	9
Differentially expressed miRNAs in HLC d24 compared to hepatocytes	Prion diseases	0	2	2
	Fatty acid biosynthesis	0	4	6
	Fatty acid metabolism	0	14	9
	Proteoglycans in cancer	0	107	15
	ECM-receptor interaction	0	34	18
	Adherens junction	2.136489e-10	52	16
	Viral carcinogenesis	2.367215e-07	84	11
	Hippo signaling pathway	8.686167e-05	76	14

	Pathways in cancer	0.001098215	135	8
	Lysine degradation	0.001337938	24	10
	Transcriptional misregulation in cancer	0.003591186	53	7
	p53 signaling pathway	0.04591601	39	11
Differentially expressed miRNAs hepatocytes compared to HLC d24	Fatty acid biosynthesis	0	4	7
	Hepatitis B	0	91	15
	ECM-receptor interaction	0	41	16
	Lysine degradation	0	27	18
	Cell cycle	0	93	18
	Viral carcinogenesis	0	132	18
	Pathways in cancer	0	247	21
	Hippo signaling pathway	0	91	22
	Proteoglycans in cancer	0	143	23
	Adherens junction	5.662137e-15	58	19
	Chronic myeloid leukemia	1.465494e-14	58	19
	Glioma	8.104628e-14	46	16
	Colorectal cancer	8.277157e-12	45	18
	p53 signaling pathway	2.698853e-08	47	17
	Oocyte meiosis	1.888721e-07	67	13
	Small cell lung cancer	5.78931e-07	61	15
	Thyroid hormone signaling pathway	1.055741e-05	64	11
	Prion diseases	2.777397e-05	6	2
	Steroid biosynthesis	4.649816e-05	10	11
	TGF-beta signaling pathway	6.111763e-05	52	11
	Prostate cancer	0.0001105553	66	13
	Fatty acid metabolism	0.0001381028	13	7
	PI3K-Akt signaling pathway	0.0001991286	138	11
	FoxO signaling pathway	0.001107838	84	15
	Focal adhesion	0.001779401	90	9
	Bladder cancer	0.002833066	27	12
	Melanoma	0.01182136	41	10
	Protein processing in endoplasmic reticulum	0.01436954	105	12
	Endocytosis	0.01445943	97	12

5.5.3. SnoRNA analysis

In this study, expression of 18 non-canonical SNORD-like, and six candidate snoRNA genes reported in a study of Jorjani et al. was confirmed (Jorjani et al., 2016). Analogous to miRNAs, differentially expressed snoRNAs were identified. The volcano plots represent differentially expressed snoRNAs (Fig. 39, 40 and 41). A total of 77,6% of the differentially expressed snoRNAs in the hepatocytes compared with the HLCs day 20 were also

differentially expressed in the hepatocytes compared with the HLCs day 24. Among 210 common differentially expressed snoRNAs were: SCARNA17, SNORD118, SNORA46, SNORA60 and SNORA81. With selected FDR, only 29 snoRNAs were differentially expressed between HLCs day 20 and day 24, including SNORA38, SNORA101B, SNORA38B. The differentially expressed snoRNAs are visualized in a heatmap (Fig. 42). Of those, 68% were box C/D snoRNAs, which is 44% of all box C/D snoRNAs. A list of all differentially expressed snoRNAs is provided in the appendix.

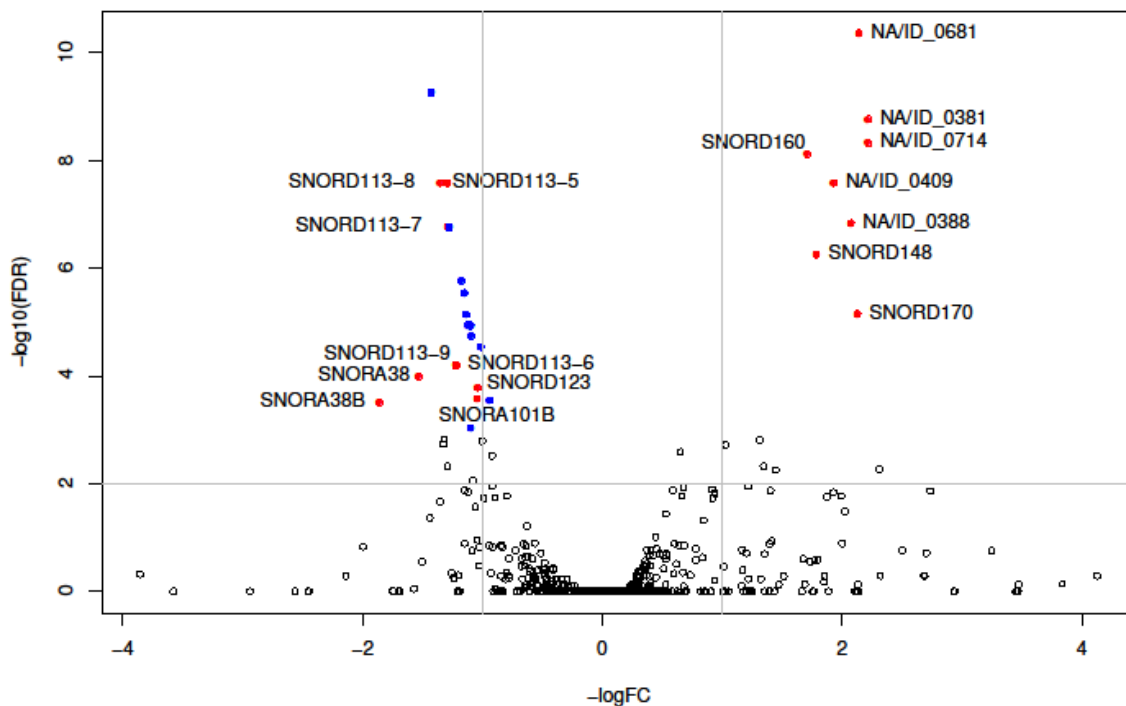


Figure 39 The volcano plot of differentially expressed snoRNAs between HLCs day 20 and HLCs day 24.

The x-axis indicates difference of expression level on a log scale, while the y-axis represents corresponding adjusted P values (FDR) on a negative log scale; statistically significant differences extends vertically. Red points indicate genes with the significance level of $\text{FDR} > 0.001$. Blue points represent SNORD114. Labels are given for the most significant differentially expressed snoRNAs (Skrzypczyk et al., 2017, manuscript in preparation).

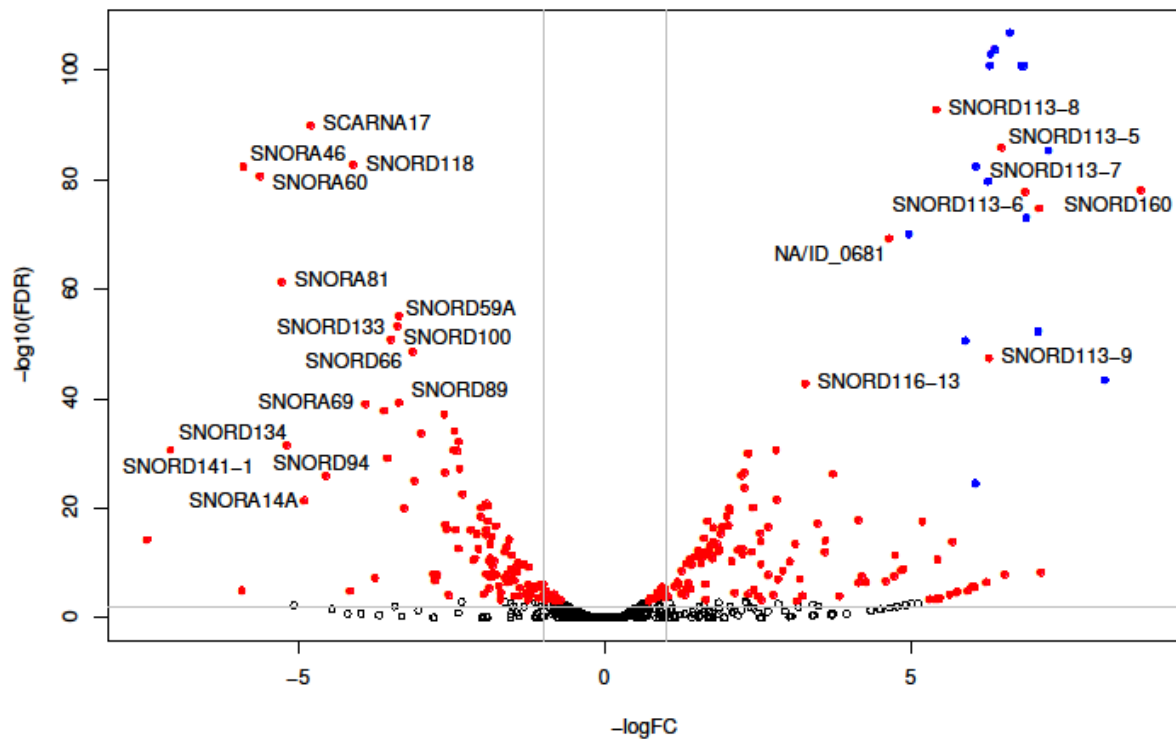


Figure 40 The volcano plot of differentially expressed snoRNAs between HLCs day 20 and Hepatocytes.

The x-axis indicates difference of expression level on a log scale, while the y-axis represents corresponding adjusted P values (FDR) on a negative log scale; statistically significant differences extends vertically. Red points indicate genes with the significance level of $FDR > 0.001$. Blue points represent SNORD114. Labels are given for the most significant differentially expressed snoRNAs (Skrzypczyk et al., 2017, manuscript in preparation).

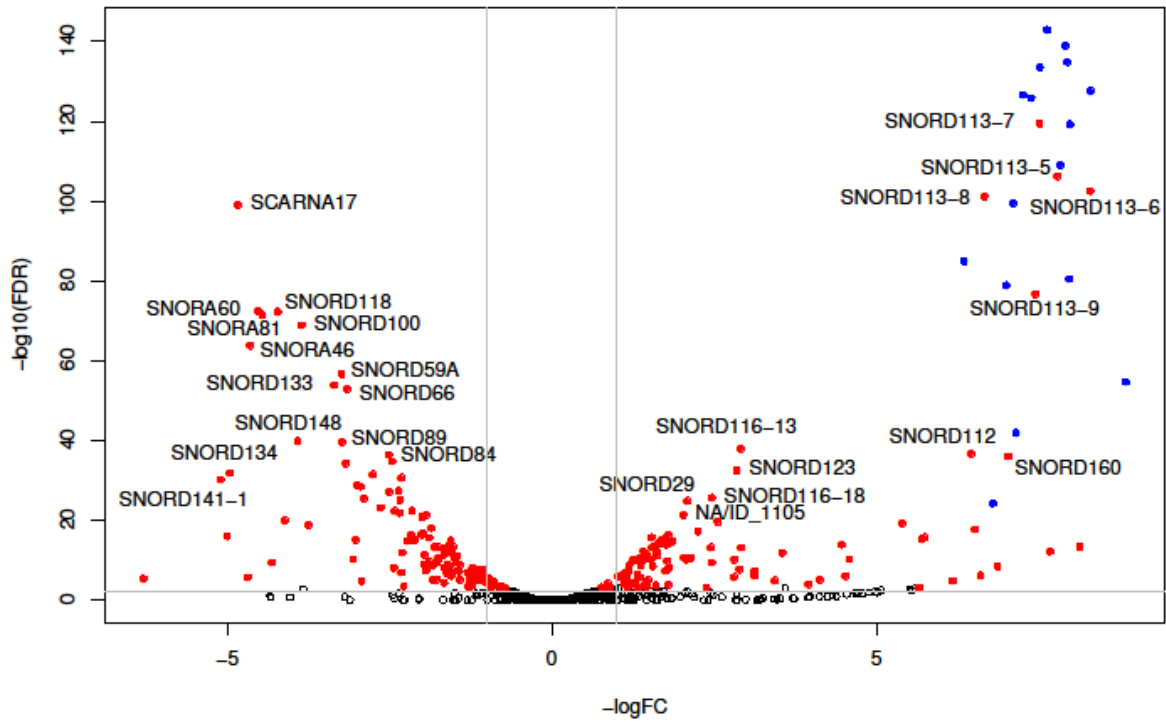


Figure 41 The volcano plot of differentially expressed snoRNAs between HLCs day 24 and Hepatocytes.

The x-axis indicates difference of expression level on a log scale, while the y-axis represents corresponding adjusted P values (FDR) on a negative log scale; statistically significant differences extends vertically. Red points indicate genes with the significance level of $FDR > 0.001$. Blue points represent SNORD114. Labels are given for the most significant differentially expressed snoRNAs (Skrzypczyk et al., 2017, manuscript in preparation).

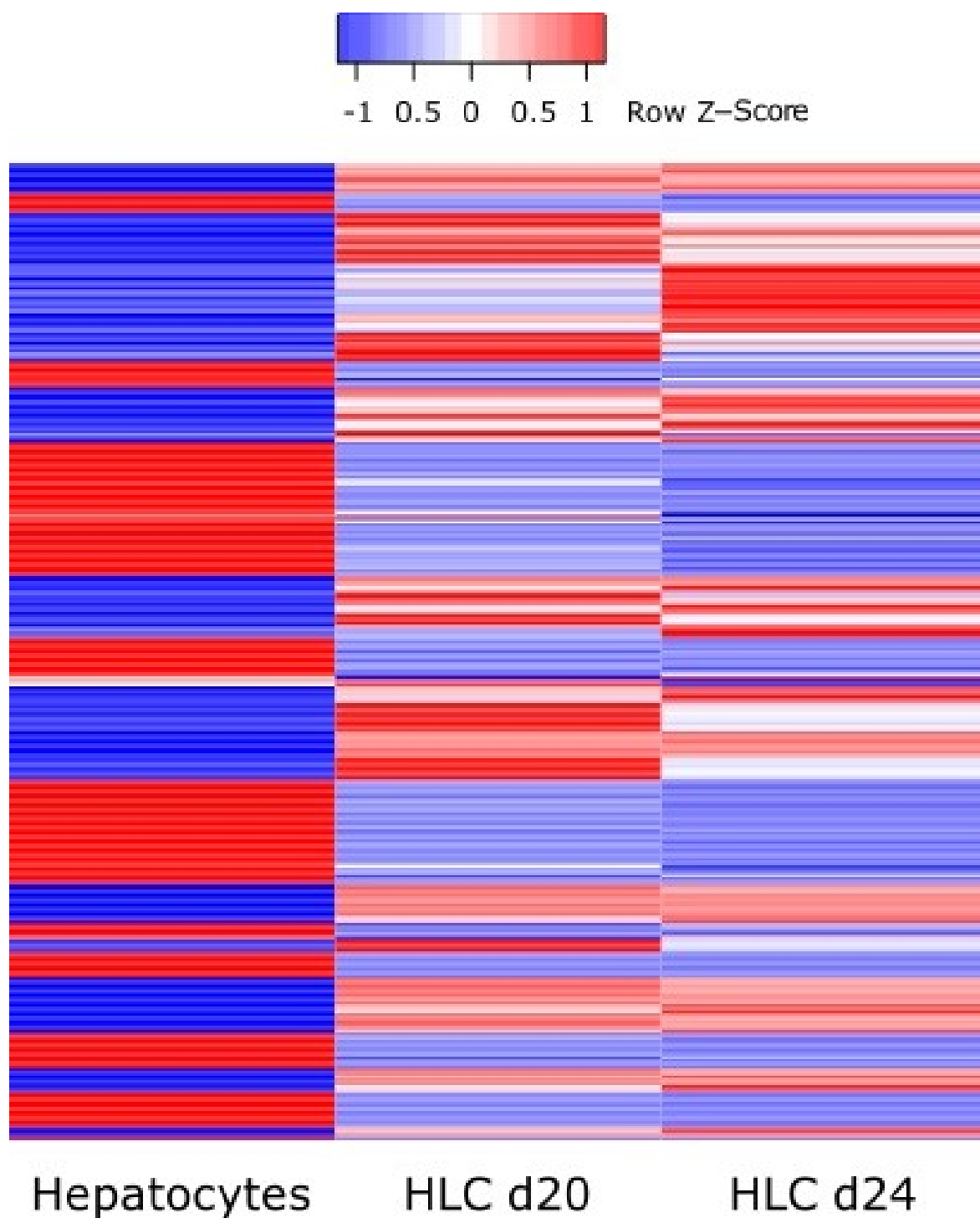


Figure 42 Heatmap showing the differentially expressed snoRNAs.

Differentially expressed snoRNAs are represented in shades of blue (decreased expression) and red (increased) in HLCs day 20 (HLCd20), day 24 (HLCd24) and hepatocytes (Skrzypczyk et al., 2017, manuscript in preparation).

5.5.4. Short reads snoRNA analysis

During standard miRNA sequencing, a fraction of snoRNAs sequenced can be small and limited to short length reads of snoRNAs with adapters as a result of fractioning done before sequencing. The obtained dataset was created from the fraction of longer ncRNA and could be divided into short reads with adapters and full length reads. The short snoRNA reads cover 15% of all mapped snoRNAs. In order to investigate whether the analysis of short (~20nt) reads alone give reasonable results for the snoRNA analysis, differential expression analysis on only the short snoRNA reads was performed and compared with results from all snoRNA reads analysis. An identified differentially expressed snoRNA with an FDR of 0.001 from short reads were in 85% to 90% also differentially expressed in the full data set. Of these, still significantly different reads, only a maximum of 1% showed a different direction in expression change. This result shows that datasets generated for the miRNA analysis can also be used to reliably investigate the snoRNome. To visualise a clear correlation between the analysed short reads and all dataset snoRNAs, a dot plot was prepared (Fig. 43). The figure shows the correlation between all investigated group pairs.

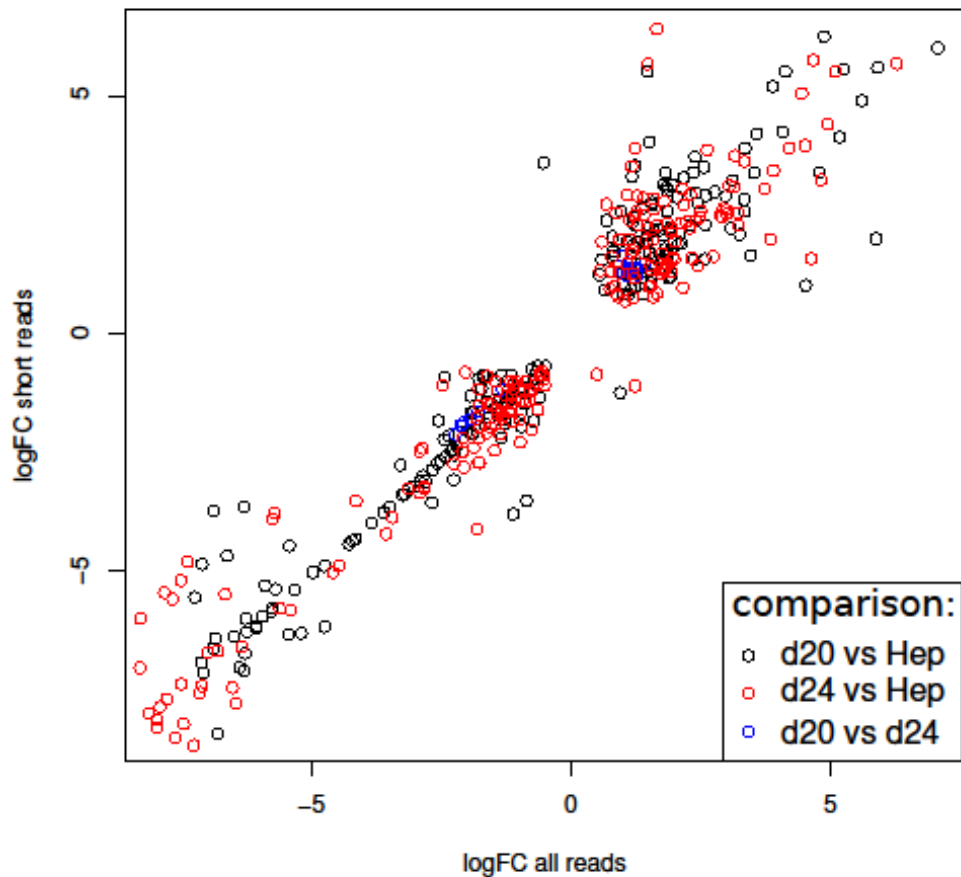


Figure 43 Correlation of fold changes between short reads and all reads mapping snoRNA genes.

Analysis of snoRNA genes with FDR below 0.001; y-axis – logarithmic transformation of fold change of short reads only analysis, x-axis – logarithmic transformation of fold change when considering all reads. Comparison of results from differentially gene expression analysis of HLCd20 and hepatocytes- in black, HLCd24 and hepatocytes – in red and in blue HLCd20 and HLCd24 (Skrzypczyk et al., 2017, manuscript in preparation).

5.5.5. New gene candidates

In the expressed loci that do not overlap gene or repeats annotations, it was possible to identify novel ncRNAs. These include 9 novel box C/D snoRNAs, 10 box H/ACA snoRNAs and 4 detected with structurally conserved regions (detected by RNAz software based on

support vector machines). Most of the new RNA sequences were conserved during evolution (Table 5). One box C/D snoRNA could only be identified in humans and three snoRNA families of each type are identified as primate-specific. Another seven families are also conserved in other eutherian species. A list of all annotated novel genes is provided in Table 6.

Table 5 Conservation of novel RNA candidates

Method	Type	Count	Conservation
snoReport	CD	3	Boreoeutheria
SnoStrip	CD	3	Primates
		1	Human
		1	Homininae
		1	Boreoeutheria
SnoStrip	HACA	2	Theria
		1	Eutheria
		3	Primates
		2	Boreoeutheria
		2	Euarchontoglires
RNAz	-	2	Primates
		1	Eutheria
		1	Boreoeutheria

Table 6 List of novel ncRNAs

Position	Type	Host gene
chr1:113824553-113824673	HACA-snoRNA	PTPN22
chr1:181362152-181362263	HACA-snoRNA	-
chr1:40773163-40773278	HACA-snoRNA	-
chr1:153969534-153969592	CD-snoRNA	CREB3L4
chr3:168093129-168093244	HACA-snoRNA	GOLIM4
chr3:79560919-79561042	HACA-snoRNA	ROBO1
chr5:163294865-163294994	HACA-snoRNA	RP11-541P9.3
chr5:6757562-6757670	HACA-snoRNA	-
chr7:33591095-33591209	HACA-snoRNA	BBS9
chr9:122744852-122744927	CD-snoRNA	-

chr11:71300629-71300727	CD-snoRNA	-
chr11:98956624-98956737	CD-snoRNA	-
chr13:59018873-59018998	HACA-snoRNA	-
chr17:39725613-39725692	CD-snoRNA	ERBB2
chr21:39475295-39475353	CD-snoRNA	SH3BGR
chrY:6441667-6441790	HACA-snoRNA	-
chr5:116653307-116653431	CD-snoRNA	-
chr9:79487404-79487526	CD-snoRNA	-
chr10:30457496-30457617	CD-snoRNA	MAP3K8
chr11:2224892-2225019	RNAz	-
chr16:636684-636856	RNAz	MCRIP2
chr5:97539290-97539410	RNAz	LINC01340
chr8:27942407-27942528	RNAz	SCARNA5

6. Discussion

6.1. Methodical strategy

The iPSCs were discovered 10 years ago, and during this time cell reprogramming techniques changed. Currently, episomal vectors are the most popular tool to obtain a temporary overexpression of reprogramming factors. Traditionally, the electroporation method was performed to deliver those vectors to reprogramming cells. In the current study, episomal vectors were delivered to the reprogrammed cells using Lipofectamine 3000. A combination of repeated lipotransfection and the highly efficient reprogramming factors makes the generation of iPSCs effective and safe. The transfection method used here can be successfully reproduced by other laboratories worldwide, without using expensive machines for electroporation. Additionally, there was no symptom of cytotoxicity during reprogramming which makes this method stable and predictive.

A cell's gene expression changes in time and condition-specific situations. It is an important issue to completely understand the regulatory mechanisms of gene expression during human development. This study can have a potential implication in clinical medicine. During recent years, miRNAs profiles were discovered in many cell types. Several researchers identified that miRNAs are involved in differentiation and cancerogenesis. However, the mechanism of miRNA orchestrating the hepatic differentiation of stem cells is still poorly understood. Therefore, identification of such miRNAs may be used to improve the generation of stem cell-derived hepatocytes for cell replacement therapies. In the current study, a new line of iPSCs was differentiated into hepatocytes and ncRNA profiling was performed. Several methods were developed for miRNAs quantification. NcRNA sequencing using the Illumina platform was the chosen strategy here. This approach is a reliable procedure in order to identify miRNAs that are differentially expressed between the cell types. However, this method cannot predict the functional relevance of the discovered differentially expressed miRNAs. Hence, functional studies and target validation have to be performed in order to assert how miRNA contributes to cell condition. Nevertheless, ncRNA sequencing also allows the detection of novel genes. To filter new ncRNA candidates, the bioinformatic approach was used as the most valid method today.

6.2.Characterisation of generated iPSCs

After the generation of new iPSCs, it was necessary to validate their pluripotent character with the standard pluripotency tests. For this purpose, the colonies were assessed for expression of pluripotency markers, the ability for differentiation into three germ layers, and genetic stability following reprogramming.

The iPSCs showed ESCs-typical morphology, expression of pluripotency markers, and the ability to differentiate into all three germ layers. Karyotyping reveals that these iPSCs have no chromosomal aberrations. The reprogramming process did not cause the incorporation of vector carrying genes. The obtained new cell line had a stable karyotype during the long-term culture. To our knowledge, this is the first report of the generation of iPSCs using oriP/EBNA1 (Epstein–Barr nuclear antigen-1)-based episomal vectors combined with repeated lipotransfection. This method is a combination of many pluripotency inducers and gentle transfection using liposomes. The episomal vectors were delivered twice in order to increase the reprogramming efficiency. This method can be successfully applied in many laboratories without the necessity of using an electroporator. An evaluation of generated cells was done by a comparison with commercial iPSCs (Life Technologies). The newly derived iPSCs were exhibit morphology, proliferation, pluripotency markers, and differentiation potential comparable to the commercial iPSCs line. Comparison with the ESCs would be interesting as well, however, the University of Leipzig has no license for the cultivation of ESCs.

6.3.Hepatic differentiation of iPSCs

6.3.1. Characterisation of HLCs

To determine the hepatic characteristic of the cells after differentiation, hepatic markers and genes were examined, as well as hepatic functions. The obtained HLCs expressed mature hepatic markers: HNF4a, ALB, CK18 and MRP2, but also the fetal marker AFP. A gene expression analysis showed that expression of AFP was the highest in the HLCs when compared to the HepG2. There was no expression of AFP in the hepatocytes, while all mature hepatic genes – A1AT, HNF4a and Albumin were highly expressed. In the HLCs, expression

of HNF4a was lower than HepG2. However, A1AT and Albumin expression were approximately the same as in HepG2. The HLCs could store glycogen as shown by PAS staining and metabolise ICG. These functional tests revealed a hepatic characteristic of obtained cells. On the other hand, expression of the fetal liver marker AFP, indicated inhibition of hepatic maturation. Amount of characterisation tests was reduced due to limited funds. However, these results are consistent with the previous description of HLCs obtained with this differentiation protocol (Baxter et al., 2015; Yu et al., 2012).

6.3.2. Protocol with HNF4a overexpression

Hepatic differentiation protocol of iPSCs was changed by adding HNF4a overexpression as an attempt to improve the process since HNF4a is a master transcriptional factor regulating hepatic differentiation. The results showed that HNF4a overexpression caused local storage of the transcription factor in the cells cytosol, however, it was limited to a few spots in the culture vessels of the cells. The episomal vectors are normally lost during cell division, but during differentiation cells stop their proliferation. The observed overexpression could be a result of vector storage during differentiation. The obtained HLCs expressed hepatic markers: Albumin, HNF4a, CK18, AFP and could store glycogen and metabolise ICG, which shows hepatic cell commitment. Comparison of the hepatic gene expression indicates that HLCs from the modified protocol were expressing: A1AT, HNF4a, Albumin and AFP on the lower level. The evaluation of hepatic differentiation efficiency by image analysis of double positive cells for HNF4a and ALB markers on the slides demonstrates that there is no difference between the two protocols. The area covered by “mature” HLC was around 30 % of the slide. It was shown that hepatic differentiation efficiency varies between protocols and the iPSCs lines used for the study (Kajiwara et al., 2012). Nevertheless, modification of protocol by HNF4a overexpression was not enough to improve hepatic differentiation and maturation.

6.3.3. Differentially expressed miRNA

In this study, the miRNA profiles of iPSCs-derived HLCs were investigated. To detect potential inhibitors of hepatic maturation, obtained miRNAs profiles were compared.

Previously, some attempts to explore miRNA profiles during hepatic differentiation of ESCs were made (Kim et al., 2011; Raut & Khanna, 2016). However, analysis of ncRNA sequencing from iPSCs derived HLCs were not investigated before. The comparison of the miRNA profiles reveals that hepatic specific miRNAs (miR-122-5p, miR-27b-3p, miR-23b-3p, miR-148-3p, miR-146b-5p and miR-194-5b among others) are expressed at the lower level in the HLCs compared to hepatocytes. However, expression of those hepatic specific miRNAs rose during the differentiation process in the HLCs when day 20 and day 24 were compared. Additionally, fetal hepatic miRNAs (miR-23a-3p, miR-30a-5p, miR483-3p, miR-92b-3p among others) are expressed in the HLCs especially on day 24 of differentiation, indicating that HLCs undergo hepatic differentiation into immature hepatocytes. Analysis of differentially expressed miRNAs implicates that upregulated miRNAs in the HLCs when compared to hepatocytes are involved in differentiation, inhibition of proliferation, and maintaining epithelial phenotype. Remarkably, analysis of differentially expressed miRNAs between HLCs day 20 and day 24 shows that in HLCs day 24, miR-199 is strongly upregulated along with miR-214. These miRNAs are regulators of skeleton formation, cardiogenesis, and cancer (Gu & Chan, 2012). An inhibition of miR-199a-5p expression, improved the hanging drop hepatic differentiation of ESC and liver repopulation ability of obtained HLC (Möbus et al., 2015). Authors of this research also identified new targets of miR-199a-5p which directly regulate hepatocyte development. This finding might have implications that improve hepatic maturation in the future. MiR-199a was also identified as being involved in liver fibrosis through deposition of an extracellular matrix and a pro-fibrotic cytokines release, together with the miR-200 family (Murakami et al., 2011; Jiang, Ai, Wan, Zhang, & Wu, 2017). The miR-200 family (miR-200a, miR-200b, miR200c, miR-141, miR-429) is known epithelial marker which was recently linked to the inhibition of EMT by repressing ZEB1, ZEB2 and Snail (Gregory et al., 2008). Expression of those miRNAs is visible in HLCs and could inhibit EMT during maturation. It has been previously reported in the study of MSC-derived HLCs by Raut et al. (human umbilical cord Wharton's jelly-derived MSCs) that EMT related miRNAs had elevated expression in the last days of hepatic differentiation (Raut & Khanna, 2016). During the embryo development, both EMT and Mesenchymal to Epithelial Transition (MET) are essential processes. EMT can be characterised by the repression of the E-cadherin expression, change in morphology and loss of cell adhesion. At the same time, cells increase migration and expression of mesenchymal markers like N-cadherin, Vimentin and Fibronectin (Lamouille, Subramanyam, Blelloch, & Derynck, 2013). During liver development, the EMT event is visible in stroma cells when the

liver supports haematopoiesis (Chagraoui, Lepage-Noll, Anjo, Uzan, & Charbord, 2003; Sicklick et al., 2006; Li, Zheng, Sano, & Taniguchi, 2011). Inhibition of EMT can potentially block hepatic differentiation. However, this hypothesis must be interpreted with caution. During liver development, EMT is a natural process of hepatic differentiation, but it is also involved in cancerogenesis (Yoshida, 2016; Du et al., 2014). There are several possible explanations for this result. For example, low differentiation efficiency leads to a heterogeneous population after differentiation, including other kinds of endodermal cells, as speculated before (Godoy et al., 2015). Nevertheless, evidence of EMT inhibition was previously reported and should be resolved by additional studies. Some attempts have already been made. The SNAI-1 mesenchymal transcription factor (Snail, inducer of EMT) proved to be important for hepatic cell maturation (Goldman, Valdes, Ezhkova, & Gouon-Evans, 2016). E-cadherin (epithelial cadherin) overexpression during hepatic differentiation of mice ESCs influences vascular network structures by accelerating angiogenesis (Hu et al., 2013).

In the present study, elevated expressed miRNAs have been similar to those described during ESCs hepatic differentiation by Kim et al. (Kim et al., 2011). The obtained HLCs had a high expression of miRNAs (miR-21, miR-214, miR-216a) involved in phosphatidylinositol-3-kinases (PI3K) pathway. However, results of this experiment show no evidence of upregulation of those miRNAs in the adult hepatocytes. At the same time, analysis of the differentially expressed miRNAs from hepatocytes by DIANA miRpath shows that they control the PI3K pathway. This indicates that the PI3K signaling pathway might be maintained in the hepatocytes by different miRNAs during differentiation and in the mature state. Another highly upregulated miRNA in HLCs- miR-181, which is also abundant in the fetal liver, was linked to hepatocarcinoma (Ji et al., 2009). In cancer cells, the expression of an epithelial cell adhesion molecule (EpCAM) was related to high level of miR-181. This miRNA, however, targets the epithelial gene caudal type homeobox transcription factor 2 (CDX2), which promotes EMT. It suggests that the expression of miR-181 might be essential for the balance between the epithelial and mesenchymal phenotype in hepatocytes.

A crosslink between miRNA profiles and pathways related to differences in cells is difficult to assess. Many of those miRNAs still do not have validated targets. An analysis of a large number of genes can lead to a statistical bias. Nevertheless, KEGG pathways related to differentially expressed miRNAs were identified by using the DIANA-miRPath v3.0 online tool (Vlachos et al., 2015). The analysis of KEGG pathways related to differentially expressed miRNAs in hepatocytes shows that they control pathways, as mentioned before in regards not

only to PI3K-Akt signaling but also with focal adhesion, TGF-beta signaling pathway and the Thyroid hormone signaling pathway. It was shown that transient hypothyroidism increased expression of miRs-1, 206, 133a and 133b in liver cells (Dong et al., 2010). Interestingly, miR-1-3p and miR-133a are in the group of differentially expressed miRNAs from the HLCs. An appropriate thyroid hormone level is critically important for development and differentiation. It is also well known that the liver regulates the hormone level by secreting carrier proteins (Malik & Hodgson, 2002). The potential influence of the thyroid hormone on hepatic differentiation should be resolved in future research. The differentially expressed and enriched miRNAs from the HLCs compared to the hepatocytes, control the following: fatty acid biosynthesis and metabolism, ECM-receptor interaction, proteoglycans in cancer, the Hippo signalling pathway, the adherens junction, lysine degradation, prion diseases, viral carcinogenesis, pathways in cancer, the p53 signaling pathway, and the cell cycle. Fatty acid biosynthesis and metabolism is a typical liver function, which can be accelerated by insulin added to the medium. The hippo signaling pathway is a central mechanism that regulates organ size by control of cell proliferation and apoptosis (Pan, 2010). The HLCs miRNAs control those pathways as a result of the differentiation process. Furthermore, HLCs have fetal character and tissue remodelling processes take place. Pathways listed here could be involved in any differentiation process, however this result shows again that the obtained HLCs are immature and undergo many metabolic changes. Some differentially expressed miRNAs in HLCs are involved in cancer. Additional research must be done to clarify miRNAs interplay between genes and chemical molecules used in differentiation. The hepatic differentiation process is still limited; however, the ncRNA expression profiles obtained in this study will be helpful in understanding the mechanism of differentiation and thus indicate the way of future research.

6.3.4. Differentially expressed snoRNA

Strong evidence of differentially expressed snoRNAs was found in the dataset. Most of those snoRNAs belong to the box C/D class. There is evidence that small fragments derived from the box C/D snoRNAs accumulate in cells having conserved patterns. This sdRNA have been shown to influence splicing or translation (Scott et al., 2012; Falaleeva & Stamm, 2013b). Additionally, it has been shown that patients with metastatic prostate cancer have a higher expression of SNORD78 and its derived small fragments (Martens-Uzunova et al., 2015).

This demonstrates that the differentially expressed snoRNAs can be useful diagnostic biomarkers for many conditions. In this study, differences in expression of many snoRNAs that potentially can be differentiation markers were reported, nevertheless, future investigation is needed. Many of the differentially expressed snoRNAs belong to an imprinted locus (24 copies of SNORD115, 7 copies of SNORD113, 18 copies of SNORD114 and 20 copies of SNORD116). Previously, hepatic snoRNAs from imprinted regions were compared with 10 other human tissues by Castle et al. (Castle et al., 2010). Expression of imprinted snoRNA genes was low in the liver. However, in this study, copies of SNORD113, SNORD114 and SNORD116 were downregulated in the liver compared to HLCs, while all copies of SNORD115 were upregulated. This is in line with later reported analysis of the Prader-Willi Syndrome locus by Galiveti et al., where SNORD115 had higher expression than SNORD116 in the liver (Galiveti, Raabe, Konthur, & Rozhdestvensky, 2014). What is interesting in other endodermal tissues (small intestine, colon, spleen, lungs and trachea) is that expression of SNORD115 is lower and SNORD116 higher. Moreover, it was shown that SNORD115 can regulate SNORD116 expression and activity (Falaleeva, Surface, Shen, La Grange, & Stamm, 2015). Intriguing correlation between our data and previous research can be noticed. These findings, while preliminary, suggest that there are metabolic changes in mature hepatocytes, which can potentially lead to a characteristic snoRNA expression pattern. Another aspect of a differential snoRNA expression is that it can lead to specialised ribosomes in the hepatocytes. The liver is an essential organ that has multiple functions. Highly active metabolic ribosomes of hepatocytes might require special rRNA modifications. A recent investigation of sequencing data generated across the circadian cycle in the mouse liver indicates cyclical variations of snoRNAs (Aitken & Semple, 2017). Furthermore, those variations were independent of the host gene expression and identified SNORD115 as a cyclical snoRNA.

Additionally, shown here analysis of short snoRNA reads (with adapters) and a comparison to the whole snoRNAsome is a very useful methodological result. Results show that the presence of snoRNAs during standard miRNA sequencing can be analysed with approximately 85% accuracy. Differential expression of snoRNAs can be detected and quantified reliably from standard short ncRNA sequencing data and does not require sequencing of RNAs in size range geared towards detecting snoRNAs.

6.4. Novel snoRNA genes

From obtained sequencing data, 19 candidate snoRNA genes and four unclassified ncRNAs were identified. Conservation analysis shows that most novel genes are evolutionarily young, suggesting that the repertoire of small structured RNAs is subject to rapid expansions. Potentially these newly identified snoRNAs are exclusively expressed in endodermal lineage and therefore have not been detected before. The novel snoRNAs require further investigation for their functions in hepatocytes. Recent research on snoRNAs revealed that functions of snoRNAs go beyond guidance of chemical modification of ribosomal and snRNAs. Therefore, those novel genes need further investigation.

7. Summary

Zusammenfassung der Arbeit

Dissertation zur Erlangung des akademischen Grades

DOCTOR RERUM NATURALIUM (Dr. rer. nat.)

an der Medizinischen Fakultät der Universität Leipzig

Titel: Non-coding RNA analysis of iPSCs-derived hepatocyte-like cells

eingereicht von Skrzypczyk Aniela

geboren am 02. Oktober 1988 in Siemianowice Slaskie (Polen)

angefertigt an / in: Universität Leipzig, Biotechnologisch-Biomedizinisches Zentrum,
Zelltechniken und Angewandte Stammzellbiologie

betreut von: Univ.-Prof. Dr. med. Augustinus Bader und Prof. Peter F. Stadler

November 2017

The liver is a crucial human organ with a complex architecture. Although the liver has great regeneration potential, deadly liver diseases are associated with irreversible hepatocytes damage. Currently, a liver transplant is the only treatment for liver failure. A shortage of donors forced extensive research for alternative treatments. The most promising hepatocyte source could be obtained from the differentiation of induced pluripotent stem cells (iPSCs). This technology can give us great amounts of pluripotent cells, without ethical restrictions, which could be available in a variety of haplotypes to minimize the possibility of rejection. There are many reprogramming protocols available. However, there is still no standardised method to obtain clinical grade iPSCs. From those stem cells, it is possible to obtain hepatic-

like cells (HLCs) by direct differentiation in vitro. HLCs express multiple hepatocyte-specific features, but their names signal that they still show fetal liver identity. A variety of hepatic differentiation protocols were described, although the process of hepatic differentiation must be improved in order to be translated into the clinic. Along with genes, microRNA (miRNA) is the well-known controller of cell fate. MiRNA is a type of non-coding RNA (ncRNA) which can influence gene transcription by inhibiting gene expression. In contrast to genes, many of the miRNAs can affect up to thousands of genes simultaneously. Another group of ncRNA, which is a subject of potential differences are small nucleolar RNA (snoRNA). SnoRNA are involved in RNA chemical modifications by acting as a guide, mostly for ribosomal RNA (rRNA), but some of them have additional functions.

In this study, a new iPSCs line was generated from skin fibroblasts using lipotransfection of episomal vectors. This method is free from exogene integration and shows low cytotoxicity. A pluripotency of generated cells was confirmed by morphological assessment, immunocytochemical staining, and spontaneous differentiation assay. To be sure that the chromosomes of the cells were not changed, karyotype analysis was performed. Next, HLCs were derived from those iPSCs using a four-stage hepatic differentiation protocol. The obtained HLCs were then characterised using a hepatic gene expression analysis, among others. Cells after differentiation express mature and fetal hepatic markers, which is consistent with previous results. The attempt to improve differentiation using transient overexpression of master hepatic transcription factor – HNF4 α , was not sufficient, as shown by gene expression analysis and whole slide scanning.

Previous studies failed to point out the genetic inhibitors of hepatic maturation and non-coding RNA (ncRNA) profiles of iPSCs – derived HLCs were not investigated. In this study, the sequencing of ncRNA was performed in order to compare the expression profiles of HLCs on two stages of differentiation (Day 20 and 24) with mature hepatocytes. The obtained results indicate that HLCs express miRNA, which control hepatic differentiation and maintain their fetal liver character. In comparison to mature hepatocytes, differentially expressed miRNAs in HLCs control the pathways of fatty acid metabolism and synthesis, proteoglycan in cancer, the Hippo signaling pathway, ECM-receptor interaction and adherens junction. Some of those highly expressed miRNAs can potentially block maturation by inhibiting epithelial-mesenchymal transition (EMT) which has a huge impact during hepatic differentiation. However, this should be resolved in future research. In this work, differentially expressed snoRNA were also identified. A total of 68% of differentially

expressed snoRNAs was box C/D class. This is interesting because this snoRNA class was previously indicated as capable to be processed by a miRNA processing pathway. Many of the differentially expressed snoRNAs belong to the imprinted loci, in which a different expression in a human was analysed before. In obtained dataset, copies of SNORD115 were upregulated in a liver, but not in HLCs, which is consistent with an earlier comparison of a liver and other endoderm organs. Additionally, an analysis of obtained sequencing data allowed for a discovery of 19 novel snoRNA genes.

In summary, this work shows a new approach to the reprogramming of a fibroblast and investigates the involvement of miRNAs and snoRNAs in the dynamics of hepatic differentiation. Novel snoRNA genes were annotated which enriches the pool of known snoRNA. A dataset generated here could also be the foundation for a hepatic-specialised ribosomes theory. This study has shed a light on the molecular and regulatory mechanisms that underlie the complex process of liver differentiation. The results obtained here will hopefully be found useful in overcoming existing problems with the medical use of iPSCs-derived hepatocytes.

8. References

- Abbas, Q., Raza, S. M., Biyabani, A. A., & Jaffar, M. A. (2016). A Review of Computational Methods for Finding Non-Coding RNA Genes. *Genes*, 7(12), 113.
- Adam, R., McMaster, P., O'Grady, J. G., Castaing, D., Klempnauer, J. L., Jamieson, N., . . . Pollard, S. (2003). Evolution of liver transplantation in Europe: report of the European Liver Transplant Registry. *Liver Transplantation*, 9(12), 1231–1243.
- Adewumi, O., Aflatoonian, B., Ahrlund-Richter, L., Amit, M., Andrews, P. W., Beighton, G., . . . Bevan, S. (2007). Characterization of human embryonic stem cell lines by the International Stem Cell Initiative. *Nature biotechnology*, 25(7), 803–816.
- Aitken, S., & Semple, C. A. (2017). The circadian dynamics of small nucleolar RNA in the mouse liver. *Journal of the Royal Society, Interface*, 14(130). <https://doi.org/10.1098/rsif.2017.0034>
- Altschul, S. F., Gish, W., Miller, W., Myers, E. W., & Lipman, D. J. (1990). Basic local alignment search tool. *Journal of molecular biology*, 215(3), 403–410.
- Anokye-Danso, F., Trivedi, C. M., Juhr, D., Gupta, M., Cui, Z., Tian, Y., . . . Epstein, J. A. (2011). Highly efficient miRNA-mediated reprogramming of mouse and human somatic cells to pluripotency. *Cell Stem Cell*, 8(4), 376–388.
- Avior, Y., Sagi, I., & Benvenisty, N. (2016). Pluripotent stem cells in disease modelling and drug discovery. *Nat Rev Mol Cell Biol*, 17(3), 170–182.
- Baghbaderani, B. A., Tian, X., Neo, B. H., Burkall, A., Dimezzo, T., Sierra, G., . . . Fellner, T. (2015). cGMP-manufactured human induced pluripotent stem cells are available for pre-clinical and clinical applications. *Stem cell reports*, 5(4), 647–659.
- Bartschat, S., Kehr, S., Tafer, H., Stadler, P. F., & Hertel, J. (2013). snoStrip: a snoRNA annotation pipeline. *Bioinformatics*, 30(1), 115–116.
- Baptista, P. M., Siddiqui, M. M., Lozier, G., Rodriguez, S. R., Atala, A., & Soker, S. (2011). The use of whole organ decellularization for the generation of a vascularized liver organoid. *Hepatology (Baltimore, Md.)*, 53(2), 604–617. <https://doi.org/10.1002/hep.24067>

- Baxter, M., Withey, S., Harrison, S., Segeritz, C.-P., Zhang, F., Atkinson-Dell, R., . . . Jenkins, R. (2015). Phenotypic and functional analyses show stem cell-derived hepatocyte-like cells better mimic fetal rather than adult hepatocytes. *Journal of hepatology*, 62(3), 581–589.
- Bazeley, P. S., Shepelev, V., Talebizadeh, Z., Butler, M. G., Fedorova, L., Filatov, V., & Fedorov, A. (2008). snoTARGET shows that human orphan snoRNA targets locate close to alternative splice junctions. *Gene*, 408(1), 172–179.
- Berg, J. M., Tymoczko, J. L., & Stryer, L. (2002). *Glycogen Metabolism*: W H Freeman.
- Bernhart, S. H., Hofacker, I. L., Will, S., Gruber, A. R., & Stadler, P. F. (2008). RNAalifold: improved consensus structure prediction for RNA alignments. *BMC bioinformatics*, 9, 474. <https://doi.org/10.1186/1471-2105-9-474>
- Bieth, E., Eddiry, S., Gaston, V., Lorenzini, F., Buffet, A., Auriol, F. C., . . . Arveiler, B. (2015). Highly restricted deletion of the SNORD116 region is implicated in Prader–Willi Syndrome. *European Journal of Human Genetics*, 23(2), 252–255.
- Brameier, M., Herwig, A., Reinhardt, R., Walter, L., & Gruber, J. (2011). Human box C/D snoRNAs with miRNA like functions: expanding the range of regulatory RNAs. *Nucleic acids research*, 39(2), 675–686.
- Burkhardt, M. F., Martinez, F. J., Wright, S., Ramos, C., Volfson, D., Mason, M., . . . Shoukat-Mumtaz, U. (2013). A cellular model for sporadic ALS using patient-derived induced pluripotent stem cells. *Molecular and Cellular Neuroscience*, 56, 355–364.
- Burroughs, A. M., Ando, Y., Hoon, M. L. de, Tomaru, Y., Suzuki, H., Hayashizaki, Y., & Daub, C. O. (2011). Deep-sequencing of human Argonaute-associated small RNAs provides insight into miRNA sorting and reveals Argonaute association with RNA fragments of diverse origin. *RNA biology*, 8(1), 158–177.
- Cai, Y., Yu, X., Hu, S., & Yu, J. (2009). A brief review on the mechanisms of miRNA regulation. *Genomics, proteomics & bioinformatics*, 7(4), 147–154.
- Cameron, K., Tan, R., Schmidt-Heck, W., Campos, G., Lyall, M. J., Wang, Y., . . . Kimber, S. J. (2015). Recombinant laminins drive the differentiation and self-organization of hESC-derived hepatocytes. *Stem cell reports*, 5(6), 1250–1262.

Campbell, K. H. S., McWhir, J., Ritchie, W. A., & Wilmut, I. (1996). Sheep cloned by nuclear transfer from a cultured cell line. *Nature*, 380(6569), 64.

Caralt, M., Velasco, E., Lanas, A., & Baptista, P. M. (2014a). Liver bioengineering: from the stage of liver decellularized matrix to the multiple cellular actors and bioreactor special effects. *Organogenesis*, 10(2), 250–259. <https://doi.org/10.4161/org.29892>

Caralt, M., Velasco, E., Lanas, A., & Baptista, P. M. (2014b). Liver bioengineering: from the stage of liver decellularized matrix to the multiple cellular actors and bioreactor special effects. *Organogenesis*, 10(2), 250–259. <https://doi.org/10.4161/org.29892>

Castle, J. C., Armour, C. D., Löwer, M., Haynor, D., Biery, M., Bouzek, H., . . . Rohl, C. A. (2010). Digital genome-wide ncRNA expression, including SnoRNAs, across 11 human tissues using polyA-neutral amplification. *PloS one*, 5(7), e11779.

Cayo, M. A., Mallanna, S. K., Di Furio, F., Jing, R., Tolliver, L. B., Bures, M., . . . Duncan, S. A. A Drug Screen using Human iPSC-Derived Hepatocyte-like Cells Reveals Cardiac Glycosides as a Potential Treatment for Hypercholesterolemia. *Cell Stem Cell*, 20(4), 478-489.e5. <https://doi.org/10.1016/j.stem.2017.01.011>

Chagraoui, J., Lepage-Noll, A., Anjo, A., Uzan, G., & Charbord, P. (2003). Fetal liver stroma consists of cells in epithelial-to-mesenchymal transition. *Blood*, 101(8), 2973–2982. <https://doi.org/10.1182/blood-2002-05-1341>

Chapman, A. R., & Scala, C. C. (2012). Evaluating the first-in-human clinical trial of a human embryonic stem cell-based therapy. *Kennedy Institute of Ethics Journal*, 22(3), 243–261.

Chen, Y., & Verfaillie, C. M. (2014). MicroRNAs: the fine modulators of liver development and function. *Liver International*, 34(7), 976–990.

Cirillo, L. A., Lin, F. R., Cuesta, I., Friedman, D., Jarnik, M., & Zaret, K. S. (2002). Opening of compacted chromatin by early developmental transcription factors HNF3 (FoxA) and GATA-4. *Molecular Cell*, 9(2), 279–289.

Cohen, J. C., Horton, J. D., & Hobbs, H. H. (2011). Human fatty liver disease: old questions and new insights. *science*, 332(6037), 1519–1523.

Costa, R. H., Kalinichenko, V. V., Holterman, A. L., & Wang, X. (2003). Transcription factors in liver development, differentiation, and regeneration. *Hepatology*, 38(6), 1331–1347.

- Coulouarn, C., Factor, V. M., Andersen, J. B., Durkin, M. E., & Thorgeirsson, S. S. (2009). Loss of miR-122 expression in liver cancer correlates with suppression of the hepatic phenotype and gain of metastatic properties. *Oncogene*, 28(40), 3526–3536.
- Cui, L., Shi, Y., Zhou, X., Wang, X., Wang, J., Lan, Y., . . . Han, Y. (2013). A set of microRNAs mediate direct conversion of human umbilical cord lining-derived mesenchymal stem cells into hepatocytes. *Cell death & disease*, 4, e918. <https://doi.org/10.1038/cddis.2013.429>
- Cullen, B. R. (2004). Transcription and Processing of Human microRNA Precursors. *Molecular Cell*, 16(6), 861–865. <https://doi.org/10.1016/j.molcel.2004.12.002>
- Czysz, K., Minger, S., & Thomas, N. (2015). DMSO efficiently down regulates pluripotency genes in human embryonic stem cells during definitive endoderm derivation and increases the proficiency of hepatic differentiation. *PloS one*, 10(2), e0117689.
- Deng, X., Qiu, R., Wu, Y., Li, Z., Xie, P., Zhang, J., . . . Maharjan, A. (2014). Overexpression of miR-122 promotes the hepatic differentiation and maturation of mouse ESCs through a miR-122/FoxA1/HNF4a-positive feedback loop. *Liver International*, 34(2), 281–295.
- Deutsch, G., Jung, J., Zheng, M., Lóra, J., & Zaret, K. S. (2001). A bipotential precursor population for pancreas and liver within the embryonic endoderm. *Development*, 128(6), 871–881.
- Dhawan, A., Puppi, J., Hughes, R. D., & Mitry, R. R. (2010). Human hepatocyte transplantation: current experience and future challenges. *Nature Reviews Gastroenterology and Hepatology*, 7(5), 288–298.
- Dianat, N., Dubois-Pot-Schneider, H., Steichen, C., Desterke, C., Leclerc, P., Raveux, A., . . . Dubart-Kupperschmitt, A. (2014). Generation of functional cholangiocyte-like cells from human pluripotent stem cells and HepaRG cells. *Hepatology (Baltimore, Md.)*, 60(2), 700–714. <https://doi.org/10.1002/hep.27165>
- Dixon, L. J., Barnes, M., Tang, H., Pritchard, M. T., & Nagy, L. E. (2013). Kupffer cells in the liver. *Comprehensive Physiology*.

- Doddapaneni, R., Chawla, Y. K., Das, A., Kalra, J. K., Ghosh, S., & Chakraborti, A. (2013). Overexpression of microRNA-122 enhances in vitro hepatic differentiation of fetal liver-derived stem/progenitor cells. *Journal of cellular biochemistry*, 114(7), 1575–1583.
- Dong, H., Paquette, M., Williams, A., Zoeller, R. T., Wade, M., & Yauk, C. (2010). Thyroid hormone may regulate mRNA abundance in liver by acting on microRNAs. *PloS one*, 5(8), e12136. <https://doi.org/10.1371/journal.pone.0012136>
- Du, R., Wu, S., Lv, X., Fang, H., Wu, S., & Kang, J. (2014). Overexpression of brachyury contributes to tumor metastasis by inducing epithelial-mesenchymal transition in hepatocellular carcinoma. *Journal of Experimental & Clinical Cancer Research*, 33(1), 105.
- Duncan, S. A. (2003). Mechanisms controlling early development of the liver. *Mechanisms of development*, 120(1), 19–33.
- Dupuis-Sandoval, F., Poirier, M., & Scott, M. S. (2015). The emerging landscape of small nucleolar RNAs in cell biology. *Wiley Interdisciplinary Reviews: RNA*, 6(4), 381–397.
- Edgar, R. C. (2004). MUSCLE: multiple sequence alignment with high accuracy and high throughput. *Nucleic acids research*, 32(5), 1792–1797.
- Ender, C., Krek, A., Friedländer, M. R., Beitzinger, M., Weinmann, L., Chen, W., . . . Meister, G. (2008). A human snoRNA with microRNA-like functions. *Molecular Cell*, 32(4), 519–528.
- Evans, M. J., & Kaufman, M. H. (1981). Establishment in culture of pluripotential cells from mouse embryos. *Nature*, 292(5819), 154–156.
- Falaleeva, M., & Stamm, S. (2013a). Processing of snoRNAs as a new source of regulatory non-coding RNAs. *Bioessays*, 35(1), 46–54.
- Falaleeva, M., & Stamm, S. (2013b). Processing of snoRNAs as a new source of regulatory non-coding RNAs: snoRNA fragments form a new class of functional RNAs. *BioEssays : news and reviews in molecular, cellular and developmental biology*, 35(1), 46–54. <https://doi.org/10.1002/bies.201200117>
- Falaleeva, M., Surface, J., Shen, M., La Grange, P. de, & Stamm, S. (2015). SNORD116 and SNORD115 change expression of multiple genes and modify each other's activity. *Gene*, 572(2), 266–273. <https://doi.org/10.1016/j.gene.2015.07.023>

- Fässler, R., & Meyer, M. (1995). Consequences of lack of beta 1 integrin gene expression in mice. *Genes & development*, 9(15), 1896–1908.
- Fields, M., Cai, H., Gong, J., & Del Priore, L. (2016). Potential of Induced Pluripotent Stem Cells (iPSCs) for Treating Age-Related Macular Degeneration (AMD). *Cells*, 5(4), 44.
- Flasza, M., Shering, A. F., Smith, K., Andrews, P. W., Talley, P., & Johnson, P. A. (2003). Reprogramming in inter-species embryonal carcinoma–somatic cell hybrids induces expression of pluripotency and differentiation markers. *Cloning & Stem Cells*, 5(4), 339–354.
- Freyer, N., Knospel, F., Strahl, N., Amini, L., Schrade, P., Bachmann, S., . . . Zeilinger, K. (2016). Hepatic Differentiation of Human Induced Pluripotent Stem Cells in a Perfused Three-Dimensional Multicompartment Bioreactor. *BioResearch open access*, 5(1), 235–248. <https://doi.org/10.1089/biores.2016.0027>
- Fu, H., Tie, Y., Xu, C., Zhang, Z., Zhu, J., Shi, Y., . . . Zheng, X. (2005). Identification of human fetal liver miRNAs by a novel method. *FEBS letters*, 579(17), 3849–3854.
- Gailhouste, L., Gomez-Santos, L., Hagiwara, K., Hatada, I., Kitagawa, N., Kawaharada, K., . . . Shibata, T. (2013). miR-148a plays a pivotal role in the liver by promoting the hepatospecific phenotype and suppressing the invasiveness of transformed cells. *Hepatology*, 58(3), 1153–1165.
- Galiveti, C. R., Raabe, C. A., Konthur, Z., & Rozhdestvensky, T. S. (2014). Differential regulation of non-protein coding RNAs from Prader-Willi Syndrome locus. *Scientific Reports*, 4, 6445.
- Gebhardt, R. (1992). Metabolic zonation of the liver: regulation and implications for liver function. *Pharmacology & therapeutics*, 53(3), 275–354.
- Girard, M., Jacquemin, E., Munnich, A., Lyonnet, S., & Henrion-Caude, A. (2008). miR-122, a paradigm for the role of microRNAs in the liver. *Journal of hepatology*, 48(4), 648–656. <https://doi.org/10.1016/j.jhep.2008.01.019>
- Gissen, P., & Arias, I. M. (2015). Structural and functional hepatocyte polarity and liver disease. *Journal of hepatology*, 63(4), 1023–1037.

- Godoy, P., Schmidt-Heck, W., Natarajan, K., Lucendo-Villarin, B., Szkolnicka, D., Asplund, A., . . . Campos, G. (2015). Gene networks and transcription factor motifs defining the differentiation of stem cells into hepatocyte-like cells. *Journal of hepatology*, 63(4), 934–942.
- Goldman, O., Valdes, V. J., Ezhkova, E., & Gouon-Evans, V. (2016). The mesenchymal transcription factor SNAI-1 instructs human liver specification. *Stem cell research*, 17(1), 62–68.
- Gordillo, M., Evans, T., & Gouon-Evans, V. (2015). Orchestrating liver development. *Development*, 142(12), 2094–2108.
- Gregory, P. A., Bert, A. G., Paterson, E. L., Barry, S. C., Tsykin, A., Farshid, G., . . . Goodall, G. J. (2008). The miR-200 family and miR-205 regulate epithelial to mesenchymal transition by targeting ZEB1 and SIP1. *Nat Cell Biol*, 10(5), 593–601. <https://doi.org/10.1038/ncb1722>
- Griffiths-Jones, S. (2005). RALEE—RNA ALignment editor in Emacs. *Bioinformatics*, 21(2), 257–259.
- Gruber, A. R., Findeiß, S., Washietl, S., Hofacker, I. L., & Stadler, P. F. (2010). RNAz 2.0: improved noncoding RNA detection. In *Biocomputing 2010* (pp. 69-79).
- Gu, S., & Chan, W.-Y. (2012). Flexible and Versatile as a Chameleon—Sophisticated Functions of microRNA-199a. *International Journal of Molecular Sciences*, 13(7), 8449–8466. <https://doi.org/10.3390/ijms13078449>
- Hamazaki, T., Iiboshi, Y., Oka, M., Papst, P. J., Meacham, A. M., Zon, L. I., & Terada, N. (2001). Hepatic maturation in differentiating embryonic stem cells in vitro. *FEBS letters*, 497(1), 15–19.
- Han, S., Bourdon, A., Hamou, W., Dziedzic, N., Goldman, O., & Gouon-Evans, V. (2012). Generation of functional hepatic cells from pluripotent stem cells. *Journal of stem cell research & therapy*. (8), 1.
- Hautekeete, M. L., & Geerts, A. (1997). The hepatic stellate (Ito) cell: its role in human liver disease. *Virchows Archiv : an international journal of pathology*, 430(3), 195–207.
- Hay, D. C., Fletcher, J., Payne, C., Terrace, J. D., Gallagher, R. C. J., Snoeys, J., . . . Hannoun, Z. (2008). Highly efficient differentiation of hESCs to functional hepatic endoderm requires

ActivinA and Wnt3a signaling. *Proceedings of the National Academy of Sciences*, 105(34), 12301–12306.

Hebert, M. D. (2013). Signals controlling Cajal body assembly and function. *The international journal of biochemistry & cell biology*, 45(7), 1314–1317.

Hertel, J., Hofacker, I. L., & Stadler, P. F. (2008). SnoReport: computational identification of snoRNAs with unknown targets. *Bioinformatics*, 24(2), 158–164.

Ho, C.-M., Dhawan, A., Hughes, R. D., Lehec, S. C., Puppi, J., Philippeos, C., . . . Mitry, R. R. (2012). Use of indocyanine green for functional assessment of human hepatocytes for transplantation. *Asian Journal of Surgery*, 35(1), 9–15. <https://doi.org/10.1016/j.asjsur.2012.04.017>

Ho, L., Lange, G., Zhao, W., Wang, J., Rooney, R., Patel, D. H., . . . Shaughnessy, M. C. (2014). Select small nucleolar RNAs in blood components as novel biomarkers for improved identification of comorbid traumatic brain injury and post-traumatic stress disorder in veterans of the conflicts in Afghanistan and Iraq. *American journal of neurodegenerative disease*, 3(3), 170.

Hoffmann, S., Otto, C., Kurtz, S., Sharma, C. M., Khaitovich, P., Vogel, J., . . . Hackermüller, J. (2009). Fast mapping of short sequences with mismatches, insertions and deletions using index structures. *PLoS Comput Biol*, 5(9), e1000502.

Hu, A., Shang, C., Li, Q., Sun, N., Wu, L., Ma, Y., . . . He, X. (2013). Epithelial-mesenchymal transition delayed by E-cad to promote tissue formation in hepatic differentiation of mouse embryonic stem cells in vitro. *Stem cells and development*, 23(8), 877–887.

Hu, J., Xu, Y., Hao, J., Wang, S., Li, C., & Meng, S. (2012). MiR-122 in hepatic function and liver diseases. *Protein & cell*, 3(5), 364–371.

Huangfu, D., Osafune, K., Maehr, R., Guo, W., Eijkelenboom, A., Chen, S., . . . Melton, D. A. (2008). Induction of pluripotent stem cells from primary human fibroblasts with only Oct4 and Sox2. *Nature biotechnology*, 26(11), 1269–1275.

Im Sauer, Kardassis, D., Zeillinger, K., Pascher, A., Gruenwald, A., Pless, G., . . . Frank, J. (2003). Clinical extracorporeal hybrid liver support—phase I study with primary porcine liver cells. *Xenotransplantation*, 10(5), 460–469.

- Inui, M., Martello, G., & Piccolo, S. (2010). MicroRNA control of signal transduction. *Nature Reviews Molecular Cell Biology*, 11(4), 252–263.
- Isakov, O., Ronen, R., Kovarsky, J., Gabay, A., Gan, I., Modai, S., & Shomron, N. (2012). Novel insight into the non-coding repertoire through deep sequencing analysis. *Nucleic acids research*, 40(11), e86-e86.
- Ji, J., Yamashita, T., Budhu, A., Forgues, M., Jia, H., Li, C., . . . Ye, Q. (2009). Identification of microRNA-181 by genome-wide screening as a critical player in EpCAM-positive hepatic cancer stem cells. *Hepatology*, 50(2), 472–480.
- Jiang, X.-P., Ai, W.-B., Wan, L.-Y., Zhang, Y.-Q., & Wu, J.-F. (2017). The roles of microRNA families in hepatic fibrosis. *Cell & Bioscience*, 7, 34. <https://doi.org/10.1186/s13578-017-0161-7>
- Jones, E. A., Tosh, D., Wilson, D. I., Lindsay, S., & Forrester, L. M. (2002). Hepatic differentiation of murine embryonic stem cells. *Experimental cell research*, 272(1), 15–22.
- Jorjani, H., Kehr, S., Jedlinski, D. J., Gumienny, R., Hertel, J., Stadler, P. F., . . . Gruber, A. R. (2016). An updated human snoRNAome. *Nucleic acids research*, gkw386.
- Jungermann, K., & Kietzmann, T. (2000). Oxygen: modulator of metabolic zonation and disease of the liver. *Hepatology*, 31(2), 255–260.
- Kajiwara, M., Aoi, T., Okita, K., Takahashi, R., Inoue, H., Takayama, N., . . . Uemoto, S. (2012). Donor-dependent variations in hepatic differentiation from human-induced pluripotent stem cells. *Proceedings of the National Academy of Sciences*, 109(31), 12538–12543.
- Kamiya, A., Kinoshita, T., Ito, Y., Matsui, T., Morikawa, Y., Senba, E., . . . Kishimoto, T. (1999). Fetal liver development requires a paracrine action of oncostatin M through the gp130 signal transducer. *The EMBO journal*, 18(8), 2127–2136.
- Kang, L., Wang, J., Zhang, Y., Kou, Z., & Gao, S. (2009). iPS cells can support full-term development of tetraploid blastocyst-complemented embryos. *Cell Stem Cell*, 5(2), 135–138.
- Khella, H. W. Z., Bakhet, M., Allo, G., Jewett, M. A. S., Girgis, A. H., Latif, A., . . . Yousef, G. M. (2013). miR-192, miR-194 and miR-215: a convergent microRNA network suppressing tumor progression in renal cell carcinoma. *Carcinogenesis*, 34(10), 2231–2239.

- Kim, N., Kim, H., Jung, I., Kim, Y., Kim, D., & Han, Y. (2011). Expression profiles of miRNAs in human embryonic stem cells during hepatocyte differentiation. *Hepatology Research*, 41(2), 170–183.
- Kinoshita, T., & Miyajima, A. (2002). Cytokine regulation of liver development. *Biochimica et Biophysica Acta (BBA)-Molecular Cell Research*, 1592(3), 303–312.
- Kishore, S., Khanna, A., Zhang, Z., Hui, J., Balwierz, P. J., Stefan, M., . . . Stamm, S. (2010). The snoRNA MBII-52 (SNORD 115) is processed into smaller RNAs and regulates alternative splicing. *Human Molecular Genetics*, 19(7), 1153–1164.
- Kiss, T. (2002). Small nucleolar RNAs: an abundant group of noncoding RNAs with diverse cellular functions. *Cell*, 109(2), 145–148.
- Kmiec, Z. (2001). Cooperation of liver cells in health and disease. *Advances in anatomy, embryology, and cell biology*, 161, III-XIII, 1-151.
- Knop, E., Bader, A., Böker, K., Pichlmayr, R., & Sewing, K. (1995). Ultrastructural and functional differentiation of hepatocytes under long-term culture conditions. *The Anatomical Record*, 242(3), 337–349.
- Krützfeldt, J., Rösch, N., Hausser, J., Manoharan, M., Zavolan, M., & Stoffel, M. (2012). MicroRNA-194 is a target of transcription factor 1 (Tcf1, HNF1 α) in adult liver and controls expression of frizzled-6. *Hepatology*, 55(1), 98–107.
- Kumar, A., & Riely, C. A. (1995). Inherited liver diseases in adults. *Western Journal of Medicine*, 163(4), 382.
- Laker, M. F. (1990). Liver function tests. *BMJ: British Medical Journal*, 301(6746), 250.
- Lamouille, S., Subramanyam, D., Blelloch, R., & Derynck, R. (2013). Regulation of epithelial–mesenchymal and mesenchymal–epithelial transitions by microRNAs. *Cell regulation*, 25(2), 200–207. <https://doi.org/10.1016/j.ceb.2013.01.008>
- Lanford, R. E., Hildebrandt-Eriksen, E. S., Petri, A., Persson, R., Lindow, M., Munk, M. E., . . . Ørum, H. (2010). Therapeutic silencing of microRNA-122 in primates with chronic hepatitis C virus infection. *science*, 327(5962), 198–201.

- Laudadio, I., Manfroid, I., Achouri, Y., Schmidt, D., Wilson, M. D., Cordi, S., . . . Schuit, F. (2012). A feedback loop between the liver-enriched transcription factor network and miR-122 controls hepatocyte differentiation. *Gastroenterology*, 142(1), 119–129.
- Laustriat, D., Gide, J., & Peschanski, M. (2010). Human pluripotent stem cells in drug discovery and predictive toxicology. *Biochemical Society Transactions*, 38(4), 1051–1057. <https://doi.org/10.1042/BST0381051>
- Lewis, A. P., & Jopling, C. L. (2010). Regulation and biological function of the liver-specific miR-122. *Biochemical Society Transactions*, 38(6), 1553–1557. <https://doi.org/10.1042/BST0381553>
- Li, B., Zheng, Y.-W., Sano, Y., & Taniguchi, H. (2011). Evidence for mesenchymal–epithelial transition associated with mouse hepatic stem cell differentiation. *PloS one*, 6(2), e17092.
- Li, F., Ma, N., Zhao, R., Wu, G., Zhang, Y., Qiao, Y., . . . Luo, S. (2014). Overexpression of miR-483-5p/3p cooperate to inhibit mouse liver fibrosis by suppressing the TGF-beta stimulated HSCs in transgenic mice. *Journal of cellular and molecular medicine*, 18(6), 966–974. <https://doi.org/10.1111/jcmm.12293>
- Liu, D., Fan, J., Zeng, W., Zhou, Y., Ingvarsson, S., & Chen, H. (2010). Quantitative analysis of miRNA expression in several developmental stages of human livers. *Hepatology Research*, 40(8), 813–822.
- Ma, N., Li, F., Li, D., Hui, Y., Wang, X., Qiao, Y., . . . Gao, X. (2012). Igf2-derived intronic miR-483 promotes mouse hepatocellular carcinoma cell proliferation. *Molecular and cellular biochemistry*, 361(1-2), 337–343. <https://doi.org/10.1007/s11010-011-1121-x>
- Malarkey, D. E., Johnson, K., Ryan, L., Boorman, G., & Maronpot, R. R. (2005). New insights into functional aspects of liver morphology. *Toxicologic pathology*, 33(1), 27–34.
- Malik, R., & Hodgson, H. (2002). The relationship between the thyroid gland and the liver. *QJM: An International Journal of Medicine*, 95(9), 559–569.
- Martens-Uzunova, E. S., Hoogstrate, Y., Kalsbeek, A., Pigmans, B., Vredenburg-van den Berg, M., Dits, N., . . . Jenster, G. (2015). C/D-box snoRNA-derived RNA production is

associated with malignant transformation and metastatic progression in prostate cancer. *Oncotarget*, 6(19), 17430–17444. <https://doi.org/10.18632/oncotarget.4172>

Martin, G. R. (1981). Isolation of a pluripotent cell line from early mouse embryos cultured in medium conditioned by teratocarcinoma stem cells. *Proceedings of the National Academy of Sciences*, 78(12), 7634–7638.

Mathapati, S., Siller, R., Impellizzeri, A. A. R., Lycke, M., Vegheim, K., Almaas, R., & Sullivan, G. J. (2016). Small-Molecule-Directed Hepatocyte-Like Cell Differentiation of Human Pluripotent Stem Cells. *Current protocols in stem cell biology*, 38, 1G.6.1-1G.6.18. <https://doi.org/10.1002/cpsc.13>

Matsumoto, K., Yoshitomi, H., Rossant, J., & Zaret, K. S. (2001). Liver organogenesis promoted by endothelial cells prior to vascular function. *science*, 294(5542), 559–563.

Menasché, P., Vanneaux, V., Hagege, A., Bel, A., Cholley, B., Cacciapuoti, I., . . . Tosca, L. (2015). Human embryonic stem cell-derived cardiac progenitors for severe heart failure treatment: first clinical case report. *European heart journal*, 36(30), 2011–2017.

Meng, Z., Fu, X., Chen, X., Zeng, S., Tian, Y., Jove, R., . . . Huang, W. (2010). miR-194 is a marker of hepatic epithelial cells and suppresses metastasis of liver cancer cells in mice. *Hepatology*, 52(6), 2148–2157.

Miller, R. A., & Ruddle, F. H. (1976). Pluripotent teratocarcinoma-thymus somatic cell hybrids. *Cell*, 9(1), 45–55.

Miyoshi, N., Ishii, H., Nagano, H., Haraguchi, N., Dewi, D. L., Kano, Y., . . . Tanaka, F. (2011). Reprogramming of mouse and human cells to pluripotency using mature microRNAs. *Cell Stem Cell*, 8(6), 633–638.

Möbus, S., Yang, D., Yuan, Q., Lüdtke, T. H.-W., Balakrishnan, A., Sgodda, M., . . . Vogel, A. (2015). MicroRNA-199a-5p inhibition enhances the liver repopulation ability of human embryonic stem cell-derived hepatic cells. *Journal of hepatology*, 62(1), 101–110.

Morrison, E. D., & Kowdley, K. V. (2000). Genetic liver disease in adults. Early recognition of the three most common causes. *Postgraduate medicine*, 107(2), 147-52, 155, 158-9. <https://doi.org/10.3810/pgm.2000.02.872>

- Müller, F.-J., Schuldt, B. M., Williams, R., Mason, D., Altun, G., Papapetrou, E. P., . . . Schmidt, N. O. (2011). A bioinformatic assay for pluripotency in human cells. *Nature methods*, 8(4), 315–317.
- Murakami, Y., Toyoda, H., Tanaka, M., Kuroda, M., Harada, Y., Matsuda, F., . . . Shimotohno, K. (2011). The progression of liver fibrosis is related with overexpression of the miR-199 and 200 families. *PloS one*, 6(1), e16081. <https://doi.org/10.1371/journal.pone.0016081>
- Müsch, A. (2014). The unique polarity phenotype of hepatocytes. *Experimental cell research*, 328(2), 276–283.
- Oh, S.-I., Lee, C. K., Cho, K. J., Lee, K.-O., Cho, S.-G., & Hong, S. (2012). Technological Progress in Generation of Induced Pluripotent Stem Cells for Clinical Applications. *The Scientific World Journal*, 2012. <https://doi.org/10.1100/2012/417809>
- Okita, K., Hong, H., Takahashi, K., & Yamanaka, S. (2010). Generation of mouse-induced pluripotent stem cells with plasmid vectors. *Nature protocols*, 5(3), 418–428.
- Pal, R., Mamidi, M. K., Das, A. K., & Bhonde, R. (2012). Diverse effects of dimethyl sulfoxide (DMSO) on the differentiation potential of human embryonic stem cells. *Archives of toxicology*, 86(4), 651–661.
- Pan, D. (2010). The Hippo Signaling Pathway in Development and Cancer. *Developmental Cell*, 19(4), 491–505. <https://doi.org/10.1016/j.devcel.2010.09.011>
- Parviz, F., Matullo, C., Garrison, W. D., Savatski, L., Adamson, J. W., Ning, G., . . . Duncan, S. A. (2003). Hepatocyte nuclear factor 4 α controls the development of a hepatic epithelium and liver morphogenesis. *Nature genetics*, 34(3), 292–296.
- Polejaeva, I. A., Chen, S.-H., Vaught, T. D., Page, R. L., Mullins, J., Ball, S., . . . Ayares, D. L. (2000). Cloned pigs produced by nuclear transfer from adult somatic cells. *Nature*, 407(6800), 86–90.
- Qian, N.-S., Liu, W.-H., Lv, W.-P., Xiang, X., Su, M., Raut, V., . . . Dong, J.-H. (2013). Upregulated microRNA-92b regulates the differentiation and proliferation of EpCAM-positive fetal liver cells by targeting C/EBP β s. *PloS one*, 8(8), e68004. <https://doi.org/10.1371/journal.pone.0068004>

- Quinlan, A. R. (2014). BEDTools: the Swiss-army tool for genome feature analysis. *Current protocols in bioinformatics*, 11.12. 1-11.12. 34.
- Rais, Y., Zviran, A., Geula, S., Gafni, O., Chomsky, E., Viukov, S., . . . Hanna, J. H. (2013). Deterministic direct reprogramming of somatic cells to pluripotency. *Nature*, 502(7469), 65–70.
- Rambhatla, L., Chiu, C.-P., Kundu, P., Peng, Y., & Carpenter, M. K. (2003). Generation of hepatocyte-like cells from human embryonic stem cells. *Cell transplantation*, 12(1), 1–11.
- Raut, A., & Khanna, A. (2016). High-throughput sequencing to identify microRNA signatures during hepatic differentiation of human umbilical cord Wharton's jelly-derived mesenchymal stem cells. *Hepatology Research*.
- Reichow, S. L., Hamma, T., Ferré-D'Amaré, A. R., & Varani, G. (2007). The structure and function of small nucleolar ribonucleoproteins. *Nucleic acids research*, 35(5), 1452–1464.
- Ren, Y., Jiang, H., Hu, Z., Fan, K., Wang, J., Janoschka, S., . . . Feng, J. (2015). Parkin Mutations Reduce the Complexity of Neuronal Processes in iPSC-Derived Human Neurons. *Stem cells*, 33(1), 68–78.
- Rogler, C. E., LeVoci, L., Ader, T., Massimi, A., Tchaikovskaya, T., Norel, R., & Rogler, L. E. (2009). MicroRNA-23b cluster microRNAs regulate transforming growth factor-beta/bone morphogenetic protein signaling and liver stem cell differentiation by targeting Smads. *Hepatology*, 50(2), 575–584.
- Rossi, J. M., Dunn, N. R., Hogan, B. L. M., & Zaret, K. S. (2001). Distinct mesodermal signals, including BMPs from the septum transversum mesenchyme, are required in combination for hepatogenesis from the endoderm. *Genes & development*, 15(15), 1998–2009.
- Runte, M., Hüttenhofer, A., Groß, S., Kiefmann, M., Horsthemke, B., & Buiting, K. (2001). The IC-SNURF–SNRPN transcript serves as a host for multiple small nucleolar RNA species and as an antisense RNA for UBE3A. *Human Molecular Genetics*, 10(23), 2687–2700.
- Saxena, R., Theise, N. D., & Crawford, J. M. (1999). Microanatomy of the human liver—exploring the hidden interfaces. *Hepatology*, 30(6), 1339–1346.

- Schattner, P., Brooks, A. N., & Lowe, T. M. (2005). The tRNAscan-SE, snoscan and snoGPS web servers for the detection of tRNAs and snoRNAs. *Nucleic acids research*, 33(suppl 2), W686-W689.
- Schmidt, C., Bladt, F., Goedecke, S., & Brinkmann, V. (1995). Scatter factor/hepatocyte growth factor is essential for liver development. *Nature*, 373(6516), 699.
- Schulz, T. C. (2015). Concise review: manufacturing of pancreatic endoderm cells for clinical trials in type 1 diabetes. *Stem cells translational medicine*, 4(8), 927–931.
- Schuppan, D., & Afdhal, N. H. (2008). Liver cirrhosis. *The Lancet*, 371(9615), 838–851.
- Schwartz, R. E., Fleming, H. E., Khetani, SR, & Bhatia, S. N. (2014). Pluripotent stem cell-derived hepatocyte-like cells. *Biotechnology advances*, 32(2), 504–513.
- Schwartz, R. E., Trehan, K., Andrus, L., Sheahan, T. P., Ploss, A., Duncan, S. A., . . . Bhatia, S. N. (2012). Modeling hepatitis C virus infection using human induced pluripotent stem cells. *Proceedings of the National Academy of Sciences*, 109(7), 2544–2548. <https://doi.org/10.1073/pnas.1121400109>
- Schwartz, S. D., Regillo, C. D., Lam, B. L., Elliott, D., Rosenfeld, P. J., Gregori, N. Z., . . . Spirn, M. (2015). Human embryonic stem cell-derived retinal pigment epithelium in patients with age-related macular degeneration and Stargardt's macular dystrophy: follow-up of two open-label phase 1/2 studies. *The Lancet*, 385(9967), 509–516.
- Scott, M. S., Ono, M., Yamada, K., Endo, A., Barton, G. J., & Lamond, A. I. (2012). Human box C/D snoRNA processing conservation across multiple cell types. *Nucleic acids research*, 40(8), 3676–3688. <https://doi.org/10.1093/nar/gkr1233>
- Sekine, S., Ogawa, R., Mcmanus, M. T., Kanai, Y., & Hebrok, M. (2009). Dicer is required for proper liver zonation. *The Journal of pathology*, 219(3), 365–372.
- Shinozawa, T., Yoshikawa, H. Y., & Takebe, T. (2016). Reverse engineering liver buds through self-driven condensation and organization towards medical application. *Developmental biology*, 420(2), 221–229. <https://doi.org/10.1016/j.ydbio.2016.06.036>
- Sicklick, J. K., Choi, S. S., Bustamante, M., McCall, S. J., Pérez, E. H., Huang, J., . . . Diehl, A. M. (2006). Evidence for epithelial-mesenchymal transitions in adult liver cells. *American Journal of Physiology-Gastrointestinal and Liver Physiology*, 291(4), G575-G583.

Siller, R., Greenhough, S., Naumovska, E., & Sullivan, G. J. (2015). Small-molecule-driven hepatocyte differentiation of human pluripotent stem cells. *Stem cell reports*, 4(5), 939–952.

Si-Tayeb, K., Duclos-Vallée, J.-C., & Petit, M.-A. (2012). Hepatocyte-like cells differentiated from human induced pluripotent stem cells (iHLCs) are permissive to hepatitis C virus (HCV) infection: HCV study gets personal. *Journal of hepatology*, 57(3), 689–691.

Sivertsson, L., Synnergren, J., Jensen, J., Björquist, P., & Ingelman-Sundberg, M. (2012). Hepatic differentiation and maturation of human embryonic stem cells cultured in a perfused three-dimensional bioreactor. *Stem cells and development*, 22(4), 581–594.

Skrzypczyk, A., Giri, S., & Bader, A. (2016). Generation of induced pluripotent stem cell line from foreskin fibroblasts. *Stem cell research*, 17(3), 572–575. <https://doi.org/10.1016/j.scr.2016.09.014>

Skrzypczyk, A., Kehr, S., Bernhart, S. H., Krystel, I., Giri, S., Bader, A., & Stadler, P. F. (2017). Non-coding RNA transcripts during differentiation of human induced pluripotent stem cells into hepatocytes. Unpublished manuscript.

Sommer, C. A., Stadtfeld, M., Murphy, G. J., Hochedlinger, K., Kotton, D. N., & Mostoslavsky, G. (2009). Induced pluripotent stem cell generation using a single lentiviral stem cell cassette. *Stem cells*, 27(3), 543–549.

Song, Z., Cai, J., Liu, Y., Zhao, D., Yong, J., Duo, S., . . . Deng, H. (2009). Efficient generation of hepatocyte-like cells from human induced pluripotent stem cells. *Cell Res*, 19(11), 1233–1242.

Stadtfeld, M., Maherali, N., Breault, D. T., & Hochedlinger, K. (2008). Defining molecular cornerstones during fibroblast to iPS cell reprogramming in mouse. *Cell Stem Cell*, 2(3), 230–240.

Stadtfeld, M., Nagaya, M., Utikal, J., Weir, G., & Hochedlinger, K. (2008). Induced pluripotent stem cells generated without viral integration. *science*, 322(5903), 945–949.

Su, J., Liao, J., Gao, L., Shen, J., Guarnera, M. A., Zhan, M., . . . Jiang, F. (2016). Analysis of small nucleolar RNAs in sputum for lung cancer diagnosis. *Oncotarget*, 7(5), 5131.

- Tachibana, M., Amato, P., Sparman, M., Gutierrez, N. M., Tippner-Hedges, R., Ma, H., . . . Sritanandomchai, H. (2013). Human embryonic stem cells derived by somatic cell nuclear transfer. *Cell*, 153(6), 1228–1238.
- Takahashi, K., Tanabe, K., Ohnuki, M., Narita, M., Ichisaka, T., Tomoda, K., & Yamanaka, S. (2007). Induction of Pluripotent Stem Cells from Adult Human Fibroblasts by Defined Factors. *Cell*, 131(5), 861–872. <https://doi.org/10.1016/j.cell.2007.11.019>
- Takahashi, K., & Yamanaka, S. (2006). Induction of pluripotent stem cells from mouse embryonic and adult fibroblast cultures by defined factors. *Cell*, 126(4), 663–676.
- Takayama, K., Kawabata, K., Nagamoto, Y., Kishimoto, K., Tashiro, K., Sakurai, F., . . . Furue, M. K. (2013). 3D spheroid culture of hESC/hiPSC-derived hepatocyte-like cells for drug toxicity testing. *Biomaterials*, 34(7), 1781–1789.
- Takebe, T., Koike, N., Sekine, K., Fujiwara, R., Amiya, T., Zheng, Y.-W., & Taniguchi, H. (2014). Engineering of human hepatic tissue with functional vascular networks. *Organogenesis*, 10(2), 260–267. <https://doi.org/10.4161/org.27590>
- Takebe, T., Zhang, R.-R., Koike, H., Kimura, M., Yoshizawa, E., Enomura, M., . . . Taniguchi, H. (2014). Generation of a vascularized and functional human liver from an iPSC-derived organ bud transplant. *Nature protocols*, 9(2), 396–409. <https://doi.org/10.1038/nprot.2014.020>
- Tam, P. P. L., & Rossant, J. (2003). Mouse embryonic chimeras: tools for studying mammalian development. *Development*, 130(25), 6155–6163.
- Tang, Y., Liu, D., Zhang, L., Ingvarsson, S., & Chen, H. (2011). Quantitative analysis of miRNA expression in seven human foetal and adult organs. *PloS one*, 6(12), e28730.
- Taub, R. (2004). Liver regeneration: from myth to mechanism. *Nature Reviews Molecular Cell Biology*, 5(10), 836–847.
- Taylor, C. J., Peacock, S., Chaudhry, A. N., Bradley, J. A., & Bolton, E. M. (2012). Generating an iPSC Bank for HLA-Matched Tissue Transplantation Based on Known Donor and Recipient HLA Types. *Cell Stem Cell*, 11(2), 147–152. <https://doi.org/10.1016/j.stem.2012.07.014>

- Thomson, J. A., Itskovitz-Eldor, J., Shapiro, S. S., Waknitz, M. A., Swiergiel, J. J., Marshall, V. S., & Jones, J. M. (1998). Embryonic stem cell lines derived from human blastocysts. *science*, 282(5391), 1145–1147.
- Trounson, A., & DeWitt, N. D. (2016). Pluripotent stem cells progressing to the clinic. *Nature Reviews Molecular Cell Biology*, 17(3), 194–200. <https://doi.org/10.1038/nrm.2016.10>
- Vlachos, I. S., Zagkanas, K., Paraskevopoulou, M. D., Georgakilas, G., Karagkouni, D., Vergoulis, T., . . . Hatzigeorgiou, A. G. (2015). DIANA-miRPath v3. 0: deciphering microRNA function with experimental support. *Nucleic acids research*, 43(W1), W460–W466.
- Warren, L., Manos, P. D., Ahfeldt, T., Loh, Y.-H., Li, H., Lau, F., . . . Meissner, A. (2010). Highly efficient reprogramming to pluripotency and directed differentiation of human cells with synthetic modified mRNA. *Cell Stem Cell*, 7(5), 618–630.
- Wen, J., & Friedman, J. R. (2012). miR-122 regulates hepatic lipid metabolism and tumor suppression. *The Journal of clinical investigation*, 122(8), 2773–2776.
- Winter, J., Jung, S., Keller, S., Gregory, R. I., & Diederichs, S. (2009). Many roads to maturity: microRNA biogenesis pathways and their regulation. *Nat Cell Biol*, 11(3), 228–234. <https://doi.org/10.1038/ncb0309-228>
- Xu, J., Zhu, X., Wu, L., Yang, R., Yang, Z., Wang, Q., & Wu, F. (2012). MicroRNA-122 suppresses cell proliferation and induces cell apoptosis in hepatocellular carcinoma by directly targeting Wnt/ β -catenin pathway. *Liver International*, 32(5), 752–760.
- Yakubov, E., Rechavi, G., Rozenblatt, S., & Givol, D. (2010). Reprogramming of human fibroblasts to pluripotent stem cells using mRNA of four transcription factors. *Biochemical and biophysical research communications*, 394(1), 189–193.
- Yamanaka, S. (2007). Strategies and new developments in the generation of patient-specific pluripotent stem cells. *Cell Stem Cell*, 1(1), 39–49.
- Yoshida, G. J. (2016). Emerging role of epithelial-mesenchymal transition in hepatic cancer. *Journal of Experimental & Clinical Cancer Research*, 35(1), 141.
- Young, J. E., Boulanger-Weill, J., Williams, D. A., Woodruff, G., Buen, F., Revilla, A. C., . . . Edland, S. D. (2015). Elucidating molecular phenotypes caused by the SORL1 Alzheimer's

disease genetic risk factor using human induced pluripotent stem cells. *Cell Stem Cell*, 16(4), 373–385.

Yu, J., Vodyanik, M. A., Smuga-Otto, K., Antosiewicz-Bourget, J., Frane, J. L., Tian, S., . . . Stewart, R. (2007). Induced pluripotent stem cell lines derived from human somatic cells. *science*, 318(5858), 1917–1920.

Yu, Y., Liu, H., Ikeda, Y., Amiot, B. P., Rinaldo, P., Duncan, S. A., & Nyberg, S. L. (2012). Hepatocyte-like cells differentiated from human induced pluripotent stem cells: relevance to cellular therapies. *Stem cell research*, 9(3), 196–207.

Yusa, K., Rad, R., Takeda, J., & Bradley, A. (2009). Generation of transgene-free induced pluripotent mouse stem cells by the piggyBac transposon. *Nature methods*, 6(5), 363–369.

Zaret, K. S. (2002). Regulatory phases of early liver development: paradigms of organogenesis. *Nature Reviews Genetics*, 3(7), 499–512.

Zhao, R., & Duncan, S. A. (2005). Embryonic development of the liver. *Hepatology*, 41(5), 956–967.

Zhou, H., Wu, S., Joo, J. Y., Zhu, S., Han, D. W., Lin, T., . . . Zhu, Y. (2009). Generation of induced pluripotent stem cells using recombinant proteins. *Cell Stem Cell*, 4(5), 381.

Zimmermann, A., Preynat-Seauve, O., Tiercy, J.-M., Krause, K.-H., & Villard, J. (2012). Haplotype-based banking of human pluripotent stem cells for transplantation: potential and limitations. *Stem cells and development*, 21(13), 2364–2373.

9. Appendix

Table 7 List of differentially expressed miRNA

Differentially expressed miRNAs (top 100): marked in bold are characteristic for one type of comparison, in colour miRNAs specific for: mature liver , fetal liver , EMT inhibition , Pi3K signalling					
HLCs day 24 vs. Hepatocytes					
let-7b-5p	miR-301b-3p	miR-660-5p	miR-424-5p	let-7f-2-3p	miR-382-3p
miR-1248	miR-183-5p	miR-486-3p	miR-18b-5p	miR-125a-3p	miR-582-5p
let-7f-5p	miR-194-5p	miR-486-5p	miR-598-3p	miR-299-3p	miR-188-5p
let-7a-5p	miR-92b-3p	miR-532-5p	let-7a-3p	miR-369-5p	miR-380-3p
let-7g-5p	miR-141-3p	miR-22-3p	miR-449b-5p	miR-4662a-5p	miR-885-3p
miR-10a-5p	miR-373-3p	miR-708-3p	miR-221-5p	miR-4662b	miR-200a-5p
miR-205-5p	miR-146b-5p	miR-501-3p	miR-10b-5p	miR-539-3p	miR-92a-1-5p
miR-143-3p	miR-885-5p	miR-204-5p	miR-126-3p	miR-96-5p	miR-501-5p
miR-378c	miR-190a-5p	miR-3609	miR-135b-5p	miR-652-3p	miR-187-3p
miR-378a-3p	miR-181b-5p	miR-454-3p	miR-181a-2-3p	miR-450a-5p	miR-15b-3p
miR-125a-5p	miR-9-5p	miR-431-5p	miR-873-5p	miR-6515-3p	miR-656-3p
let-7i-5p	miR-195-5p	miR-23b-3p	miR-10a-3p	miR-615-3p	miR-543
miR-99b-5p	miR-449a	miR-99a-5p	miR-107	miR-378b	miR-1305
miR-363-3p	miR-372-3p	miR-26b-5p	miR-369-3p	miR-9-3p	miR-219a-2-3p
let-7d-5p	miR-421	miR-371b-3p	miR-3607-5p	miR-934	miR-18a-3p
miR-199b-3p	miR-3591-5p	miR-371a-5p	miR-29c-5p	miR-654-5p	miR-5589-5p
miR-199a-3p	miR-122-3p	miR-181a-5p	miR-193a-5p	miR-670-3p	miR-129-5p
let-7c-5p	miR-126-5p	miR-3120-5p	miR-1247-5p	miR-136-5p	miR-411-3p
miR-199b-5p	miR-181d-5p	miR-214-3p	miR-542-3p	miR-3653-5p	miR-499b-3p
miR-218-5p	miR-196b-5p	miR-3653-3p	miR-758-3p	miR-582-3p	miR-499a-5p
miR-301a-3p	miR-335-3p	miR-200c-3p	miR-125b-2-3p	miR-1251-5p	miR-376a-3p
miR-98-5p	miR-432-5p	miR-134-5p	miR-493-3p	miR-195-3p	miR-208b-3p
miR-127-3p	miR-148a-3p	miR-152-3p	miR-3607-3p	miR-330-3p	miR-377-5p
miR-182-5p	miR-33b-5p	miR-675-5p	miR-1270	miR-93-3p	miR-433-3p
miR-101-3p	miR-100-5p	miR-675-3p	miR-323a-3p	miR-24-2-5p	miR-485-5p
miR-29c-3p	miR-136-3p	miR-27b-3p	miR-296-5p	miR-487a-3p	miR-5589-3p
miR-302d-3p	miR-130a-3p	miR-493-5p	miR-767-5p	miR-127-5p	miR-5588-5p
miR-222-3p	miR-181a-3p	miR-155-5p	miR-200a-3p	miR-367-3p	miR-101-5p
miR-31-5p	let-7b-3p	miR-487b-3p	miR-141-5p	miR-618	miR-342-5p
miR-122-5p	miR-215-5p	miR-429	miR-454-5p	miR-196a-5p	miR-504-5p
miR-3591-3p	miR-106a-5p	miR-214-5p	miR-193b-5p	miR-1180-3p	miR-548ah-5p
miR-181c-5p	miR-561-5p	miR-3120-3p	miR-370-3p	miR-34b-5p	miR-378f
miR-302a-5p	miR-181c-3p	miR-330-5p	miR-378d	miR-412-5p	miR-612
miR-29a-3p	miR-221-3p	miR-424-3p	miR-146a-5p	miR-653-5p	miR-532-3p
miR-411-5p	miR-449c-5p	miR-769-5p	miR-218-1-3p	miR-1185-1-3p	miR-326
miR-20b-5p	miR-133a-3p	miR-17-5p	miR-135a-5p	miR-371a-3p	miR-98-3p
miR-194-3p	miR-4510	miR-192-3p	miR-625-3p	miR-371b-5p	let-7g-3p
miR-409-3p	miR-99b-3p	let-7d-3p	miR-625-5p	miR-135b-3p	miR-138-5p
miR-34c-5p	miR-29b-3p	miR-378a-5p	miR-376c-3p	miR-323b-3p	miR-27a-5p
miR-500a-3p	miR-149-5p	miR-145-5p	miR-184	miR-584-5p	miR-935
miR-192-5p	miR-887-3p	miR-106b-5p	miR-877-5p	miR-585-3p	miR-4326
miR-381-3p	miR-99a-3p	miR-490-3p	miR-629-5p	miR-500a-5p	let-7i-3p
miR-302b-3p	miR-18a-5p	miR-125b-5p	miR-1247-3p	miR-145-3p	miR-489-3p
miR-654-3p	miR-302c-3p	miR-200b-3p	miR-4751	miR-219b-5p	miR-124-3p

miR-302a-3p miR-199a-5p miR-410-3p miR-6723-5p	miR-708-5p miR-146b-3p miR-450b-5p miR-889-3p	miR-23a-3p miR-497-5p miR-1-3p miR-335-5p	miR-873-3p miR-431-3p miR-502-3p miR-296-3p	miR-1197 miR-4686 miR-500b-5p	miR-495-3p miR-379-5p miR-377-3p
HLCs day 20 vs. Hepatocytes					
let-7b-5p let-7f-5p miR-302d-3p miR-205-5p miR-98-5p let-7i-5p miR-302a-3p let-7g-5p let-7a-5p miR-1248 miR-302a-5p miR-302b-3p let-7d-5p miR-182-5p miR-378a-3p miR-122-5p miR-378c miR-194-5p miR-31-5p miR-183-5p miR-122-3p miR-10a-5p miR-141-3p miR-215-5p miR-302c-3p miR-363-3p miR-192-5p miR-92b-3p miR-194-3p miR-125a-5p let-7c-5p miR-373-3p miR-6723-5p miR-99b-5p miR-101-3p miR-372-3p miR-371a-5p miR-29c-3p miR-127-3p miR-301a-3p miR-885-5p miR-218-5p miR-146b-5p	miR-409-3p miR-99a-3p miR-152-3p miR-29a-3p miR-20b-5p miR-34c-5p miR-125b-2-3p let-7b-3p miR-181c-5p miR-143-3p miR-99a-5p miR-411-5p miR-222-3p miR-148a-3p miR-4510 miR-381-3p miR-561-5p miR-500a-3p miR-100-5p miR-3591-5p miR-146b-3p miR-181d-5p miR-3609 miR-200c-3p miR-190a-5p miR-29b-3p miR-486-5p miR-27b-3p miR-106a-5p miR-421 miR-23b-3p miR-133a-3p miR-33b-5p miR-654-3p miR-192-3p miR-193a-5p miR-125b-5p miR-9-5p miR-18a-5p miR-301b-3p miR-367-3p miR-199a-3p miR-199b-3p	miR-195-5p miR-708-5p miR-181c-3p let-7d-3p miR-26b-5p miR-149-5p miR-141-5p miR-410-3p miR-155-5p miR-199b-5p miR-135b-5p miR-335-3p miR-196b-5p miR-22-3p miR-708-3p miR-378a-5p miR-501-3p let-7a-3p miR-99b-3p miR-29c-5p miR-432-5p miR-107 miR-200b-3p miR-429 miR-450b-5p miR-18b-5p miR-4662b miR-887-3p miR-378d miR-497-5p miR-96-5p miR-371a-3p miR-181b-5p miR-136-3p miR-221-5p miR-3653-3p miR-193b-3p miR-330-5p miR-424-5p miR-126-5p miR-4662a-5p miR-1270	miR-675-5p miR-17-5p miR-454-5p miR-625-5p miR-30e-3p miR-199a-5p miR-1-3p miR-193b-5p miR-454-3p miR-4751 miR-758-3p miR-889-3p miR-532-5p let-7e-5p miR-148a-5p miR-10b-5p let-7f-2-3p miR-181a-3p miR-877-5p miR-598-3p miR-660-5p miR-221-3p miR-431-5p miR-24-3p miR-21-3p miR-187-3p miR-23a-3p miR-625-3p miR-6087 miR-134-5p miR-296-5p miR-455-3p miR-424-3p miR-6515-3p miR-378b miR-653-5p miR-188-5p miR-135b-3p miR-618 miR-3607-5p miR-769-5p miR-10a-3p miR-873-5p	miR-195-3p miR-3591-3p miR-296-3p miR-487b-3p miR-493-5p miR-200a-3p miR-145-5p miR-106b-5p miR-873-3p miR-675-3p miR-3607-3p miR-18a-3p miR-3653-5p miR-500a-5p miR-1295b-5p miR-204-5p miR-512-3p miR-934 miR-574-3p miR-500b-5p miR-4686 miR-767-5p miR-542-3p miR-371b-3p miR-214-3p miR-486-3p miR-371b-5p miR-365a-3p miR-365b-3p miR-1295a miR-125a-3p miR-499a-5p miR-499b-3p miR-629-5p miR-218-1-3p miR-93-3p miR-370-3p miR-92a-1-5p miR-885-3p miR-490-3p miR-449c-5p miR-135a-5p miR-302c-5p	miR-330-3p miR-22-5p miR-489-3p miR-323a-3p miR-449a miR-302d-5p miR-1305 miR-670-3p miR-219b-5p miR-5589-5p miR-9-3p miR-185-5p miR-369-3p miR-200a-5p miR-493-3p let-7i-3p miR-5589-3p miR-502-3p miR-34b-5p miR-5588-5p miR-3613-5p miR-1247-3p miR-7974 miR-612 miR-24-2-5p miR-378f miR-219a-2-3p miR-548f-3p miR-501-5p miR-652-3p miR-183-3p miR-129-5p miR-450a-5p miR-98-3p miR-411-3p miR-3074-5p miR-1251-5p miR-431-3p miR-548ah-5p miR-376c-3p let-7g-3p miR-203b-3p miR-504-5p
HLCs day 24 vs. day 20					
miR-199b-3p miR-199a-3p	miR-199b-5p miR-367-3p	miR-199a-5p miR-211-5p	miR-214-5p miR-302a-3p	miR-302d-5p	miR-3120-3p

Table 8 List of differentially expressed snoRNA

HLCs day 20 vs. Hepatocytes and HLCs day 24 vs. Hepatocytes					
snoID 0310	SCARNA28	SNORA86	SNORD115-18	SNORD125	SNORD49B
snoID 0319	SCARNA4	SNORA96(revised)	SNORD115-19	SNORD126	SNORD4A
snoID 0324	SCARNA5	SNORD10	SNORD115-2	SNORD127	SNORD4B
snoID 0350	SCARNA6	SNORD100	SNORD115-20	SNORD12B	SNORD5
snoID 0369	SCARNA7	SNORD102	SNORD115-21	SNORD12C	SNORD50B
snoID 0370	SCARNA9	SNORD103A	SNORD115-24	SNORD13	SNORD51
snoID 0372	SCARNA9L	SNORD103B	SNORD115-25	SNORD133	SNORD52
snoID 0375	SNORA11	SNORD104	SNORD115-26	SNORD134	SNORD53
snoID 0378	SNORA11D	SNORD105	SNORD115-32	SNORD136	SNORD53B
snoID 0381	SNORA11E	SNORD107	SNORD115-33	SNORD138	SNORD54
snoID 0388	SNORA11G	SNORD109A	SNORD115-39	SNORD141-1	SNORD58A
snoID 0400	SNORA12	SNORD109B	SNORD115-4	SNORD141-2	SNORD58C
snoID 0435	SNORA14A	SNORD111B	SNORD115-42	SNORD143	SNORD59A
snoID 0662	SNORA20	SNORD112	SNORD115-5	SNORD145	SNORD59B
snoID 0668	SNORA24	SNORD113-3	SNORD115-6	SNORD146	SNORD60
snoID 0681	SNORA24B	SNORD113-4	SNORD115-7	SNORD148	SNORD61
snoID 0684	SNORA25	SNORD113-5	SNORD115-8	SNORD14A	SNORD63
snoID 0688	SNORA26	SNORD113-6	SNORD115-9	SNORD14D	SNORD66
snoID 0720	SNORA28	SNORD113-7	SNORD116-1	SNORD150	SNORD68
snoID 0723	SNORA31	SNORD113-8	SNORD116-11	SNORD16	SNORD7
snoID 0730	SNORA35B	SNORD113-9	SNORD116-12	SNORD160	SNORD70
snoID 0731	SNORA36B	SNORD114-1	SNORD116-13	SNORD173	SNORD70B
snoID 0749	SNORA37	SNORD114-10	SNORD116-14	SNORD175	SNORD71
snoID 0757	SNORA4	SNORD114-11	SNORD116-15	SNORD18A	SNORD73A
snoID 0760	SNORA42	SNORD114-12	SNORD116-16	SNORD1A	SNORD74
snoID 0766	SNORA46	SNORD114-13	SNORD116-17	SNORD1B	SNORD75
snoID 0792	SNORA47	SNORD114-14	SNORD116-18	SNORD20	SNORD77
snoID 0796	SNORA53	SNORD114-15	SNORD116-19	SNORD21	SNORD78
snoID 0826	SNORA54	SNORD114-17	SNORD116-2	SNORD23	SNORD79
snoID 1103	SNORA57	SNORD114-20	SNORD116-20	SNORD24	SNORD8
snoID 1104	SNORA58	SNORD114-21	SNORD116-21	SNORD25	SNORD82
snoID 1105	SNORA5A	SNORD114-22	SNORD116-22	SNORD27	SNORD84
snoID 1106	SNORA5C	SNORD114-23	SNORD116-23	SNORD28	SNORD85
snoID 1108	SNORA60	SNORD114-24	SNORD116-24	SNORD29	SNORD86
snoID 1113	SNORA62	SNORD114-25	SNORD116-25	SNORD34	SNORD89
RNU3P3	SNORA64	SNORD114-26	SNORD116-26	SNORD35B	SNORD90
SCARNA10	SNORA65	SNORD114-28	SNORD116-29	SNORD36A	SNORD91A
SCARNA12	SNORA67	SNORD114-3	SNORD116-3	SNORD36C	SNORD91B
SCARNA14	SNORA69	SNORD114-9	SNORD116-5	SNORD38A	SNORD92
SCARNA15	SNORA71B	SNORD115-1	SNORD116-7	SNORD3C	SNORD93
SCARNA17	SNORA73A	SNORD115-10	SNORD116-8	SNORD41	SNORD94
SCARNA18	SNORA74A	SNORD115-12	SNORD116-9	SNORD43	SNORD96A
SCARNA2	SNORA76	SNORD115-13	SNORD117	SNORD45A	SNORD99
SCARNA21	SNORA7A	SNORD115-14	SNORD118	SNORD45B	
SCARNA22	SNORA80D	SNORD115-15	SNORD12	SNORD47	
SCARNA26A	SNORA81	SNORD115-17	SNORD123	SNORD48	

HLCs day 20 vs. Hepatocytes only					
snoID 0318	snoID 0392	snoID 0725	SNORA38	SNORD149	
snoID 0371	snoID 0409	snoID 0729	SNORA50	SNORD170	
snoID 0379	snoID 0709	SCARNA16	SNORA84	SNORD76	
snoID 0386	snoID 0714	SNORA101B	SNORD115-31	SNORD88B	
HLCs day 24 vs. Hepatocytes only					
SCARNA1	SNORA38B	SNORA63D	SNORD17		
SNORA23	SNORA61	SNORD169	SNORD63B		
HLCs day 20 vs HLCs day 24					
snoID_0681	SNORD113-5	SNORD113-7	SNORD114-3	SNORD114-14	SNORA101B
SNORD114-12	SNORD113-8	SNORD148	SNORD114-22	SNORD113-6	SNORD114-26
snoID_0381	snoID_0409	SNORD114-20	SNORD114-9	SNORD113-9	SNORA38B
snoID_0714	snoID_0388	SNORD114-28	SNORD114-25	SNORA38	SNORD114-17
SNORD160	SNORD114-1	SNORD170	SNORD114-21	SNORD123	

Erklärung über die eigenständige Abfassung der Arbeit

Hiermit erkläre ich, dass ich die vorliegende Arbeit selbstständig und ohne unzulässige Hilfe oder Benutzung anderer als der angegebenen Hilfsmittel angefertigt habe. Ich versichere, dass Dritte von mir weder unmittelbar noch mittelbar eine Vergütung oder geldwerte Leistungen für Arbeiten erhalten haben, die im Zusammenhang mit dem Inhalt der vorgelegten Dissertation stehen, und dass die vorgelegte Arbeit weder im Inland noch im Ausland in gleicher oder ähnlicher Form einer anderen Prüfungsbehörde zum Zweck einer Promotion oder eines anderen Prüfungsverfahrens vorgelegt wurde. Alles aus anderen Quellen und von anderen Personen übernommene Material, das in der Arbeit verwendet wurde oder auf das direkt Bezug genommen wird, wurde als solches kenntlich gemacht. Insbesondere wurden alle Personen genannt die direkt an der Entstehung der vorliegenden Arbeit beteiligt waren. Die aktuellen gesetzlichen Vorgaben in Bezug auf die Zulassung der klinischen Studien, die Bestimmungen des Tierschutzgesetzes, die Bestimmungen des Gentechnikgesetzes und die allgemeinen Datenschutzbestimmungen wurden eingehalten. Ich versichere, dass ich die Regelungen der Satzung der Universität Leipzig zur Sicherung guter wissenschaftlicher Praxis kenne und eingehalten habe.

.....

Datum

.....

Unterschrift

Acknowledgements

This thesis was performed in the Cell Techniques and Applied Stem Cell Biology Department of Leipzig University, Germany during the years 2014-2017. This project was funded by the EU Marie Skłodowska-Curie Actions BIOART Project grant no.316690, EU-FP7-PEOPLE-ITN-2012

First of all, I would like to thank Professor Augustinus Bader for giving me the opportunity to do my PhD in his laboratory and for employment in the Bioart Project. His guidance and support during the past years have been invaluable for which I am especially grateful.

I am also sincerely thankful to my second supervisor Professor Peter Stadler who gave me the opportunity to explore bioinformatic during my PhD studies. He was giving me enormous patience, guidance and warm encouragement.

I am grateful to Dr. Shibashish Giri for his support. Without his help, it would not have been possible to be part of Bioart project without him.

I would like to acknowledge Ilona Krystel for being there for me through the whole time and for the helps she provided during these past years in the lab. Her good advice has always been helpful for the progress of this study.

This thesis would not have been possible without all my collaborators Dr. Stephanie Kehr and Dr. Stephan Bernhart which are thanked for their encouragement and guidance in bioinformatics. Other special thanks to Dr. Nico Scherf for his help with the image analyses. I would like to extend special thanks to Dr. Heidrun Holland for her kindness and help with karyotyping and scientific discussions.

Last, but by no means least, I want to profoundly thank my family and friends for their continuous support, love, and belief in me.